Neuromagnetic approaches to measuring auditory brain function in cochlear implant recipients: MEG markers of speech processing and evaluation of a prototype MEG system

by

Qingqing Meng

MACQUARIE University

KIT-Macquarie Brain Research Laboratory

Department Cognitive Science

Faculty of Human Sciences

Macquarie University, Sydney, Australia

A thesis submitted in fulfilment of the requirements for the

degree of Doctor of Philosophy

May 2018

Statement from Author

This work has not previously been submitted for a degree or diploma in any university. To the best of my knowledge and belief, the thesis contains no material previously published or written by another person except where due reference is made in the thesis itself.

(Signed)   Date: 21/052018

Candidate's name: Qingqing Meng

Ethical review, guidance and approval have been obtained from:

Macquarie University Ethics Review Committee (Human Research). *"MEG, EEG and fMRI Studies of adult cognition"* (Ref: 5201300054.)

Acknowledgments

I would like to express my deepest gratitude to my principle supervisor Associate Professor Blake Johnson, associate supervisor Professor Catherine McMahon and Dr. Yiwen Li for their guidance, advices and encouragements at every stage of my research work. They introduced me the proper manner and essential attitude to conduct a research work with their own behaviours. They also helped me on various annoying troubles with great patience. Without their support this PhD work would not be completed.

I would also like to thank Dr. Isabelle Boisvert (HEARing CRC research program coordinator) for her supreme support and guidance during this research work. Dr. Masanori Higuchi (Kanazawa Institute of Technology) and Dr. Brett Swanson (Cochlear Ltd) for their expert guidance and support on the technical aspects of MEG system and cochlear implant system.

I would like to express my sincere gratitude to my friends and members of the HEARing Cooperative Research Centre (HEARing CRC); KIT-Macquarie Brain Research Laboratory; ARC Centre of Excellence in Cognition and its Disorders (CCD); Department of Cognitive Science; Department of Linguistics and the Audiology and Hearing Research Group (AHRG) for their kind help in various forms. Special thanks go to: Associate Professor Paul Sowman, Dr. Ronny Ibrahim, Dr. Yanan Sun, Associate Professor Peng Zhou, Dr. Huizhen (Joann) Tang, Dr. Yi (Valarie) Pu, Dr. Xuejing Lv, Dr. Na Gao, Ms. Rebecca Gelding, Ms. Amanda Fullerton and Mr. Robert Seymour for their invaluable advices and companion during this PhD journey.

Last but not the least, I would like to dedicate this thesis to my wife Linlin (Maggie) Wu, my daughter Grace Meng, my parents and parents-in-law for their non-stop support, encouragement and unconditional love.

Abstract

There is substantial variability in the speech perception performance achieved by different cochlear implant (CI) recipients, for reasons that are poorly understood but that may be attributable to changes in the way that the brain functions after auditory deprivation. Objective measures of speech processing in the brains of CI recipients would be valuable for identifying the central sources of performance variability and provide potential targets for intervention. Within an adult population, the specific objectives of the present thesis were to: (1) evaluate the effects of intelligibility on a reported novel MEG brain response that tracks hierarchical linguistic structures in connected speech; (2) evaluate the effects of prior perceptual experience on the MEG response, which reflects increased intelligibility of the degraded speech signal; (3) evaluate the capabilities of a novel, prototype MEG system designed to measure auditory brain function in cochlear implant recipients. Noise vocoding was employed to degrade the speech signal to a level that approximates the signal produced by a cochlear implant. Results showed that responses to sentence- and phrase-level structures were systematically reduced with reduced intelligibility of the speech signal; and that cortical sources coherent with intelligible phrase and sentence-level structures were left lateralized. Responses to sentence-level structure were slightly but significantly enhanced by prior experience; and this enhancement was associated with greater coherence in the right cerebral hemisphere (STG). Our evaluation of the prototype MEG system showed that CI artefacts from an emulator device were strongly attenuated. However, cochlear implant recipients still showed substantial levels of noise that preclude reliable measurements of auditory evoked brain activity. We conclude that further improvements will be required before the prototype MEG system is capable of routine measurements with CI recipients. Dissociated from artefacts at stimulus presentation frequency, this brain response to spoken language may serve as a sensitive markers of speech processing in CI recipients.

Chapter 1: Hearing deprivation and cochlear implant performance: a perspective from the brain

Qingqing Meng[1,2,4]
Yiwen Li Hegner[1,2]
Catherine McMahon[1,3,4,5]
Blake W Johnson[1,2,4]

[1]HEARing Co-operative Research Centre, Melbourne, Victoria, Australia
[2]Macquarie University, Department of Cognitive Science, Sydney, New South Wales, Australia
[3]Macquarie University, Department of Linguistics, Sydney, New South Wales, Australia
[4]ARC Centre of Excellence in Cognition and its Disorders, Macquarie University, Sydney, New South Wales, Australia
[5]Centre for Implementation of Hearing Research, Macquarie University, New South Wales, Australia

1 Scope and motivation

Profound deafness alters the functioning of the central auditory system - and higher cognitive and linguistic centers of the brain - in ways that are not currently understood and in ways that are not necessarily reversed even if hearing can be restored. These alterations have important implications for both clinical and experimental science. From a clinical point of view, it is increasingly clear that these alterations in the brain are crucial determinants of the success of cochlear implants. From a basic science point of view, cochlear implants represent a powerful natural experiment on the human brain. By providing input into a system that has experienced profound sensory deprivation, cochlear implants provide us with a unique opportunity to evaluate the effects of cortical reorganization and plasticity.

To date there has been a paucity of study of these effects in the human brain. The present thesis addresses this gap by using magnetoencephalography (MEG) to investigate neuromagnetic markers of brain processes that may reflect the ultimate goal to be achieved by cochlear implants – the achievement or re-establishment of effective speech perception in the deafened brain.

Such neural markers of brain function will provide objective targets for audiological remediation and training strategies that seek to develop patterns of acoustic stimulation that can more effectively engage the processing pathways within the brain. They will also provide powerful and unique insights into the plastic capabilities and limitations of the human brain.

Another motivation of the present thesis was to assess a novel prototype MEG system that has been engineered to cope with the electromagnetic artefacts of the cochlear implant. This new MEG instrument was the result of a collaboration with engineers at the Applied Electronics Laboratory at the Kanazawa Institute of Technology, Japan. The first phase of the project was funded by the HEARingCRC Project 4.7.2b, "Cortical Evaluation of Implant Performance". The

second phase of development, and the present thesis, was supported by the HearingCRC Project XR1.1.3 "Brain processes after implantation".

2 Background

Modern cochlear implants (CIs) are multiple-electrode arrays implanted into the cochlea. These arrays bypass the non-functional sensory cells of the cochlea by directly stimulating the surviving fibres of the acoustic nerve. CIs are at the forefront of research on neural prostheses and are considered a model of how such devices can restore function to patients with profound sensory impairments. In their modern incarnations, CIs have achieved unambiguous success in restoring communication function in adults and in older patients who have been deafened after the acquisition of language ("post-lingual deafness"), and in enabling development of language when implanted early in children born with bilateral deafness ("pre-lingual deafness") (Cosetti & Waltzman, 2011). An impressive level of restored functioning can be achieved in these populations, with a median score of 72% accuracy on tests of sentence intelligibility with no background noise (Gifford, Shallop, & Peterson, 2008). Many CI patients are able to converse on the telephone in quiet conditions (Spahr & Dorman, 2004). Finally, CIs provide unique and valuable scientific opportunities for basic research into the effects of deafness and restoration of hearing on the central auditory system (Lazard, Giraud, Gnansia, Meyer, & Sterkers, 2012; Middlebrooks, Bierer, & Snyder, 2005).

Modern CI devices incorporate the cutting edge of technology, processing capabilities, and surgical techniques. While the technological advances have provided unequivocal improvement of function in the majority of conventional recipients, there remain three vexing issues that are not completely understood and for which there do not seem to be clear-cut technical solutions:

Variability in hearing performance among apparently similar implant recipients.

Variability in language comprehension and development of language among apparently similar implant recipients.

Difficulties in hearing and understanding speech in noisy or multi-talker environments, even for implant recipients who have excellent comprehension in quiet situations.

Converging research over the last several decades now points to a major source of these problems within the brains of implant patients, rather than in the implants themselves.

CI technology has reached the point where it restores a remarkable level of speech comprehension to many deaf children and adults. Approximately 400 Australians receive a CI each year (Economics, 2007). CI research continues apace and will deliver further improvements in the encoding and delivery of acoustic information to the central auditory system (Wilson & Dorman, 2008). However, improvements in performance of CIs are limited by our inability to answer fundamental questions about how the central auditory system deciphers patterns of input from both artificial and natural stimulation. Understandably, the main work in CI research to date has been directed at replicating the function of the cochlea, a 'bottom-up' approach. As the technological capacity to bypass the cochlea has increased, it has become increasingly clear that implant performance depends not only on the quality and clarity of the input signal, but also on the ability of the brain to interpret the information in that signal.

A review by Wilson and Dorman (Wilson & Dorman, 2008) concludes that "A fundamentally new approach may be needed to help those patients presently at the low end of the performance spectrum … They may have compromised "auditory brains" as suggested by … many recent findings." (p. 18). An emerging theme in present research (Cosetti & Waltzman, 2011; Lazard et al., 2012; Moore & Shannon, 2009; Wilson & Dorman, 2008) indicates a pressing need to incorporate a 'top-down', cognitive neuroscience-based approach to better understand how the

CI and the human brain interact. Deafness does not simply remove the auditory input: deafness has a fundamental impact on cognitive processes such as phonological processing (Lazard et al., 2010; Mortensen, Mirz, & Gjedde, 2006) and results in functional brain reorganization at cortical levels far removed from the auditory periphery (Robertson & Irvine, 1989). Even with early bilateral cochlear implantation, deficits in cortical processing of binaural cue (interaural time differences) were still reported for children aged between 5 and 7 (Easwar, Yamazaki, Deighton, Papsin, & Gordon, 2017). Therefore, taking a more comprehensive approach to CI research has important implications for both clinical rehabilitation and basic cognitive science, and is highly likely to have translational benefits for other disorders of language, reading, and cognition.

In particular, this approach asks what the brain needs for effective input, given the neurophysiological changes in the brain that are caused by lack of natural auditory input. Such patterns of stimulation are likely to be much different from those specified only by a conventional focus on replicating the signals generated from the normally functioning auditory nerve (Wilson & Dorman, 2008). Effective rehabilitation strategies for people with deafness/hearing difficulties will increasingly rely on research that disentangles the relative roles of the sensory periphery and the higher-level perceptual and cognitive functions of the cerebral cortex. Increased understanding of the central processes involved will enable the development of auditory training programs and possibly drug therapies, which would aim to develop these processes following implantation.

A fundamental barrier to a top-down approach to CI research has been a paucity of methods for measuring brain function in CI recipients. The reason is that the ferromagnetic materials and electronic components in most commercial CIs are incompatible with neuroimaging methods like functional magnetic resonance imaging (fMRI) and MEG.

MEG is short for "magnetoencephalography," which is a method for measuring magnetic fields produced by neurons in the human brain (Ioannides, 2006) using sensors called "superconducting quantum interference devices" (SQUIDs) (Fagaly, 2006). The SQUIDs are maintained at superconducting temperatures in a bath of liquid helium within a vacuum-insulated cylinder (termed a "dewar"). The neuromagnetic fields measured by MEG are extremely small compared to fields generated by the urban environment (on the order of femtoTesla – i.e. 10-15 Tesla -- as compared to the microTesla magnitude of the Earth's magnetic field, and the milliTesla strength of many electronic appliances). Accordingly, conventional MEG instruments can only be operated in a heavily shielded room in the absence of ferromagnetic materials and electronics that generate electromagnetic fields.

MEG has proven to be an important advance in the study of human auditory brain function, for several reasons. First, in contrast to fMRI, the MEG instrument itself is completely silent and does not introduce any acoustic artefacts during brain measurements. Second, MEG has excellent temporal resolution, tracking neural activity on a millisecond-by-millisecond basis. Third, in contrast to electroencephalography (EEG), MEG provides excellent spatial resolution in measuring brain activity in the auditory cortex (particularly in the superior temporal plane) as various tissues of the brain and head that strongly affect volume-conducted electrical fields are essentially transparent to magnetic fields. It is capable, for example, of resolving the functional tonotopic map of the auditory cortex (Elbert et al., 2002; Fujioka et al., 2003) and the functional asymmetries in the two cerebral hemispheres (Reite, Zimmerman, & Zimmerman, 1981).

For these reasons MEG is an extremely attractive candidate for imaging auditory cortical function in cochlear implant patients. However, the CI device itself is highly incompatible with conventional MEG instruments due to the large magnetic fields produced by the permanent magnet and by the electronics of the CI (milliTesla magnitude, orders of magnitude larger than

the femtoTesla scale brain fields). In the last ten years only one study has carried out MEG recordings, and this was a study of two adult CI recipients with (very rare) magnet-free implants (Pantev, Dinnesen, Ross, Wollbrink, & Knief, 2006).

3 Objectives and Overview

There were three specific objectives of the present thesis:

Objective 1: Evaluate the effect of intelligibility of the brain response to different levels of hierarchical linguistic structures.

Objective 2: Evaluate plastic changes in these markers driven by previous experience with acoustic and linguistic information and associated with increased intelligibility of degraded speech.

Objective 3: Evaluate the capability of a prototype MEG system designed to cope with the electromagnetic artefact from cochlear implants.

4 Overview of the current work

The rest this thesis is organized as follow:

Chapter 2: A general review on the history and development of MEG instrumentation is first provided. Applications of MEG in measuring the auditory brain function of normal and pathological hearing population are then discussed in more details.

Chapter 3: brain responses were measured from nineteen normal hearing participants using MEG. Listeners were presented with isochronous four-word sentences (adjective/pronoun-noun-verb-noun) containing syllable-level, phrase-level and sentence level linguistic structures (stimulus materials adapted from the study of Ding et al. (Ding, Melloni, Zhang, Tian, & Poeppel,

2016)). Intelligibility of the sentences was parametrically manipulated with noise-vocoding (natural, 16-channel, and 8-channel). Finally, in a control condition speech was presented with random ordering of short frames of natural speech ("shuffled speech"). Results showed (1) distinct MEG following responses to all three linguistic structures; (2) MEG responses to sentence and phrase-level structures were systematically reduced with reduced intelligibility of the speech signal; (3) Cortical sources coherent with phrase and sentence structure were left lateralized, whereas brain activity coherent to syllable/word structure was bilateral. The enhancement of coherence to intelligible compared to unintelligible speech was also left lateralized and localized to the parasylvian cortex.

Chapter 4: The same experimental paradigm was used to investigate the effect of perceptual experience on comprehension of degraded speech. Increased comprehension of vocoded sentences was induced by first exposing listeners to the non-degraded speech. Results showed that (1) the MEG response coherent to sentence-level structure was slightly but significantly enhanced; (2) No significant effects of prior experience were observed at the phrase and syllable level response; (3) The enhancement by prior experience was associated with greater coherence in the right cerebral hemisphere

Chapter 5: In a third set of investigations, we evaluated a prototype MEG system that was custom-engineered for use with cochlear implant recipients. The prototype incorporates two main innovations: (1) a set of reference sensors for noise cancellation; and (2) a novel "irregular baseline" gradiometer configuration with (a) null or low sensitivity to magnetic fields at a distance corresponding to the location of a unilateral cochlear implant; and (b) maximal sensitivity to near magnetic fields at distances corresponding to the contralateral auditory cortex. Using a cochlear implant emulator device, we show that these engineering innovations strongly attenuate the noise generated by the implant magnet and electronics. However, tests with four

cochlear implant recipients showed substantial levels of noise that still preclude measurements of brain activity. Further system-level improvements will be required before the system is capable of routine measurements with CI recipients.

Chapter 6: Results of empirical studies and evaluation of the prototype MEG system are summarized and their significances are discussed. Suggestions for future work are also proposed. Finally result of a preliminary sentence intelligibility test with CI recipients using EEG is presented.

5 Author Contributions

Q.M. and B.J. conceived and wrote the paper. All of the authors discussed the contents and edited the manuscript.

References

Cosetti, M. K., & Waltzman, S. B. (2011). Cochlear implants: current status and future potential. *Expert Review of Medical Devices*, *8*(3), 389–401. https://doi.org/10.1586/erd.11.12

Ding, N., Melloni, L., Zhang, H., Tian, X., & Poeppel, D. (2016). Cortical tracking of hierarchical linguistic structures in connected speech. *Nature Neuroscience*, *19*(1), 158. https://doi.org/10.1038/nn.4186

Easwar, V., Yamazaki, H., Deighton, M., Papsin, B., & Gordon, K. (2017). Cortical Representation of Interaural Time Difference Is Impaired by Deafness in Development: Evidence from Children with Early Long-term Access to Sound through Bilateral Cochlear Implants Provided Simultaneously. *Journal of Neuroscience*, *37*(9), 2349–2361. https://doi.org/10.1523/JNEUROSCI.2538-16.2017

Economics, D. A. (2007, August 24). Listen hear! the economic impact and cost of hearing loss in Australia [Text]. Retrieved May 14, 2018, from http://apo.org.au/node/2755

Elbert, T., Sterr, A., Rockstroh, B., Pantev, C., Müller, M. M., & Taub, E. (2002). Expansion of the Tonotopic Area in the Auditory Cortex of the Blind. *Journal of Neuroscience*, *22*(22), 9941–9944. https://doi.org/10.1523/JNEUROSCI.22-22-09941.2002

Fagaly, R. (2006). Superconducting quantum interference device instruments and applications. *Review of Scientific Instruments*, *77*(10), 101101.

Fujioka, T., Ross, B., Okamoto, H., Takeshima, Y., Kakigi, R., & Pantev, C. (2003). Tonotopic representation of missing fundamental complex sounds in the human auditory cortex. *European Journal of Neuroscience*, *18*(2), 432–440. https://doi.org/10.1046/j.1460-9568.2003.02769.x

Gifford, R. H., Shallop, J. K., & Peterson, A. M. (2008). Speech Recognition Materials and Ceiling Effects: Considerations for Cochlear Implant Programs. *Audiology and Neurotology*, *13*(3), 193–205. https://doi.org/10.1159/000113510

Ioannides, A. A. (2006). Magnetoencephalography as a Research Tool in Neuroscience: State of the Art. *The Neuroscientist*, *12*(6), 524–544. https://doi.org/10.1177/1073858406293696

Lazard, D. S., Giraud, A.-L, Gnansia, D., Meyer, B., & Sterkers, O. (2012). Understanding the deafened brain: Implications for cochlear implant rehabilitation. *European Annals of Otorhinolaryngology, Head and Neck Diseases*, *129*(2), 98–103. https://doi.org/10.1016/j.anorl.2011.06.001

Lazard, D. S., Lee, H. J., Gaebler, M., Kell, C. A., Truy, E., & Giraud, A. L. (2010). Phonological processing in post-lingual deafness and cochlear implant outcome. *NeuroImage*, *49*(4), 3443–3451. https://doi.org/10.1016/j.neuroimage.2009.11.013

Middlebrooks, J. C., Bierer, J. A., & Snyder, R. L. (2005). Cochlear implants: the view from the brain. *Current Opinion in Neurobiology*, *15*(4), 488–493. https://doi.org/10.1016/j.conb.2005.06.004

Moore, D. R., & Shannon, R. V. (2009). Beyond cochlear implants: awakening the deafened brain. *Nature Neuroscience*, *12*(6), 686–691. https://doi.org/10.1038/nn.2326

Mortensen, M. V., Mirz, F., & Gjedde, A. (2006). Restored speech comprehension linked to activity in left inferior prefrontal and right temporal cortices in postlingual deafness. *NeuroImage*, *31*(2), 842–852. https://doi.org/10.1016/j.neuroimage.2005.12.020

Pantev, C., Dinnesen, A., Ross, B., Wollbrink, A., & Knief, A. (2006). Dynamics of auditory

   plasticity after cochlear implantation: a longitudinal study. *Cerebral Cortex*, *16*(1), 31–

   36.

Reite, M., Zimmerman, J. T., & Zimmerman, J. E. (1981). Magnetic auditory evoked fields:

   Interhemispheric asymmetry. *Electroencephalography and Clinical Neurophysiology*,

   51(4), 388–392. https://doi.org/10.1016/0013-4694(81)90102-4

Robertson, D., & Irvine, D. R. F. (1989). Plasticity of frequency organization in auditory cortex of

   guinea pigs with partial unilateral deafness. *Journal of Comparative Neurology*, *282*(3),

   456–471. https://doi.org/10.1002/cne.902820311

Spahr, A. J., & Dorman, M. F. (2004). Performance of Subjects Fit With the Advanced Bionics CII

   and Nucleus 3G Cochlear Implant Devices. *Archives of Otolaryngology–Head & Neck

   Surgery*, *130*(5), 624–628. https://doi.org/10.1001/archotol.130.5.624

Wilson, B. S., & Dorman, M. F. (2008). Cochlear implants: a remarkable past and a brilliant

   future. *Hearing Research*, *242*(1), 3–21.

Chapter 2: Magnetoencephalography (MEG): A review of methods and applications for investigating normal and impaired auditory brain function

Qingqing Meng[1,2,4]
Yiwen Li Hegner[1,2]
Catherine McMahon[1,3,4,5]
Blake W Johnson[1,2,4,]

[1]HEARing Co-operative Research Centre, Melbourne, Victoria, Australia
[2]Macquarie University, Department of Cognitive Science, Sydney, New South Wales, Australia
[3]Macquarie University, Department of Linguistics, Sydney, New South Wales, Australia
[4]ARC Centre of Excellence in Cognition and its Disorders, Macquarie University, Sydney, New South Wales, Australia
[5]Centre for Implementation of Hearing Research, Macquarie University, New South Wales, Australia

Abstract

Owing to its excellent temporal and spatial resolution, MEG has long been an important tool of human auditory neuroscience. In recent years this neuroimaging technique has achieved new prominence due to a surge of neuroscientific interest in the perceptual and cognitive roles of auditory brain rhythms, a fairly dramatic change of focus that has been characterized as a paradigm shift. In the context of this rapidly evolving theoretical and empirical landscape, the present review provides an overview of current MEG applications and future directions for study of normal and pathological function of the human auditory system.

1 Introduction

Magnetoencephalography (MEG) is a method for measuring magnetic fields produced by working neurons in the human brain. In the last several decades MEG has evolved into an important human neuroimaging technique with many well-defined applications in basic research and clinical medicine. Since the original description of MEG auditory responses (Reite, Edrich, Zimmerman, & Zimmerman, 1978), a number of important advantages to this technique have become apparent in the auditory context. Signals from the major auditory fields of the superior temporal lobe are readily accessible to MEG measurements; and like the electroencephalogram (EEG), the high temporal resolution of MEG (on the order of milliseconds) is appropriate to the time-scales of acoustic signals, however, MEG has higher spatial resolution and is particularly well-suited for studying lateralised functions that are more difficult to parse with EEG measurements (Nagarajan, Gabriel, & Herman, 2012). On a practical level, MEG is fundamentally safe for use with children and adults, and typically has an easier and faster set-up than EEG. MEG is also noiseless and so avoids the problem of acoustic artifacts introduced by gradient switching in functional magnetic resonance imaging (fMRI). For these reasons, MEG is often considered a method of choice for investigating central auditory function in the human brain.

In recent years this technique has achieved new prominence in the context of hearing research. This greater prominence is attributable to two important neuroscientific developments. First, hearing researchers and clinicians have generally shifted from a focus on the auditory periphery to a greater interest and appreciation of the role of higher-level brain functions in hearing (Wilson & Dorman, 2008; Peelle, Troiani, Grossman, & Wingfield, 2011; Peelle & Wingfield, 2016). Second, recent decades have seen a veritable paradigm shift in neuroscience, from an emphasis on "evoked" or "event-related" brain responses to well-defined experimental manipulations, towards a view that encompasses the importance of ongoing, intrinsic brain activity (Raichle,

2009). Intrinsic brain rhythms or oscillations are now considered to play an important, even central, role in audition (Arnal, Poeppel, & Giraud, 2015) and language perception (Gross, Hoogenboom, et al., 2013; Poeppel, Emmorey, Hickok, & Pylkkänen, 2012; Giraud & Poeppel, 2012). Compared to other techniques, MEG is particularly efficacious for measuring these electromagnetic brain oscillations.

However, for a number of reasons, MEG systems are presently much less common in research and clinical settings than alternative techniques. Hence many auditory researchers and clinicians may have little or no familiarity with the technique. The purpose of the present review is to provide a concise description of MEG principles, methods and instrumentation, geared to hearing researchers and clinicians who may have little or no exposure to this technique. An appreciation of the underlying principles of the MEG is important for understanding the unique strengths and weaknesses of the technique. These features have shaped the technical and commercial evolution of MEG and also largely explain the current role of MEG and its perceived importance relative to better-known techniques including EEG and fMRI.

This review is intended to be an introduction to the use of MEG for studies of auditory function and auditory impairment and is meant to be accessible to broad readership. For those who wish to pursue the topic in more depth the following references provide a guide to recent reviews and standard reference works in the field. Recent general reviews of the MEG as a technique are provided in (Baillet, 2017; Cheyne & Papanicolaou, 2017; Proudfoot, Woolrich, Nobre, & Turner, 2014) and (Riitta Hari & Salmelin, 2012) provide a review and historical overview of the field. Three recent MEG textbooks are important current reference works: MEG-EEG Primer (Riitta Hari & Puce, 2017), Magnetoencephalography: From Signals to Dynamic Cortical Networks (Supek & Aine, 2014), MEG: An Introduction to Methods (Hansen, Kringelbach, & Salmelin, 2010). Important reviews of the neurophysiological basis of EEG/MEG include: (M. X. Cohen, 2017;

Schomer & Da Silva, 2012a). The physical and mathematical bases of the MEG inverse problem are presented in (Baillet, Mosher, & Leahy, 2001; Vrba & Robinson, 2001; Hämäläinen, Hari, Ilmoniemi, Knuutila, & Lounasmaa, 1993; Sarvas, 1987). SQUID sensors are reviewed in (Fagaly, 2006). Publication guidelines for conducting and reporting MEG research are provided in (Keil et al., 2014; Gross, Baillet, et al., 2013). Finally, reviews of basic auditory neuroscience studies using MEG have been provided in several book chapters: (Poeppel & Hickok, 2015; Gutschalk, 2014; Nagarajan, Gabriel, & Herman, 2012; Lütkenhöner & Poeppel, 2011; Brignell, Hall, & Witton, 2008).

2 Background

2.1 History of MEG and Hardware Development

The pioneering MEG measurement, of the human alpha rhythm (D. Cohen, 1968), was carried out by David Cohen using an elaborate million turn copper induction coil and a magnetically shielded room. The advent of superconducting quantum interference devices (SQUIDs) developed by James Zimmerman (Zimmerman, Thiene, & Harding, 1970), allowed the measurement of MEG brain signals of a quality that approached that of EEG signals (Cohen, 1972) and laid the foundation for modern MEG.

MEG measurements were initially carried out by brain researchers using "single channel" instruments capable of measuring signals from only a single position over the head. In order to obtain a topographic map of a brain magnetic field researchers had to make repeated sequential measurement of brain response at different head positions, an arduous process that could stretch over several days of recordings and pushed the limits of endurance of experimental subjects. By the mid-1980s MEG instruments had evolved into multi-channel systems of seven- and then 37-channel configurations that could map most of a hemisphere with one recording, and dual 37-channel configurations could finally map both the activity from regions of both

hemispheres simultaneously. A decade later, the mid-1990's saw the advent of modern whole head, or full-cortex systems that can effectively measure activity from the entire brain. Such systems contain well over a hundred to several hundred SQUID sensors (**Figure 1**).

Figure 1: MEG systems at the KIT-Macquarie Brain Research Laboratory located at the Australian Hearing Hub, Macquarie University. Top left. Adult (right) and child (left) MEG systems are located side by side within a single magnetically-shielded room. The adult MEG has 160 SQUID sensors, the child system has 125. Both systems are designed for supine positioning of participants. The child system is sized for preschool children aged 3-5 years. Right. MEG simulator for training of child participants. Bottom left. Prototype MEG system engineered for use with unilateral cochlear implant recipients.

MEG brain signals are exceedingly small – on the order of tens to hundreds of femtoTesla (fT; a fT is 10^{-15}T) – relative to ambient sources of magnetic fields. To provide some perspective, the neuromagnetic signals of the muscles and heart are much larger (10^{-10} T); electronic devices, automobiles, and trains produce fields on the order of 10^{-7} to 10^{-2} T; the Earth itself has a magnetic field on the order of 10^{-5}T; a horseshoe magnet has a field of 10^{-3} T; and MRI scanners produce fields of 1.5 T or greater. Measurement of the infinitesimally tiny brain signals therefore

requires both highly sensitive sensors; and some method of suppressing magnetic field contributions from noise sources.

SQUID sensors, usually composed of pure niobium, can enormously amplify these tiny brain signals by inductively coupling them to an electronic circuit that generates measurable voltage changes as a function of applied magnetic-flux (Fagaly, 2006). A SQUID consists of a superconducting loop interrupted by two non-superconducting Josephson junctions (weak links), required to generate a measurable resistance across the SQUID circuit. The SQUID itself consists of a thin film of niobium with a diameter of less than 1 mm. The small surface area of the SQUID provides only a limited capability to couple to external magnetic fields. This coupling is enhanced with a pickup coil a loop of niobium with an outer diameter of approximately 1 cm. The pickup coil is inductively coupled to the SQUID via an "input coil". The combination of pickup coil and input coil is referred to as a "flux transformer" and provides the required combination of high sensitivity and high magnetic coupling required for MEG measurements.

Niobium has a superconducting transition temperature (the temperature at which a material abruptly loses all electrical resistance) of 9.2 K. To achieve superconductivity the niobium SQUIDS are bathed in liquid helium, which has a boiling point of 4.2°K. This requirement for a liquid helium bath determines the basic configuration of all modern MEG systems, which is essentially a large vacuum insulated cylinder (termed a dewar) with a head shaped cavity at the bottom which is lined with the SQUID sensors and into which a participant's head is inserted for brain measurements. Since the MEG sensors are in permanently fixed positions the dewar head cavity must be engineered accordingly to satisfy opposing requirements: to bring the sensors as close as possible to the head (because magnetic fields fall off sharply with distance); and to accommodate as many heads as possible. Given the variability in human head size and shape the

result is inevitably a compromise but most MEG systems are able to accommodate 95% to 99% of adult heads (**Figure 2A**).
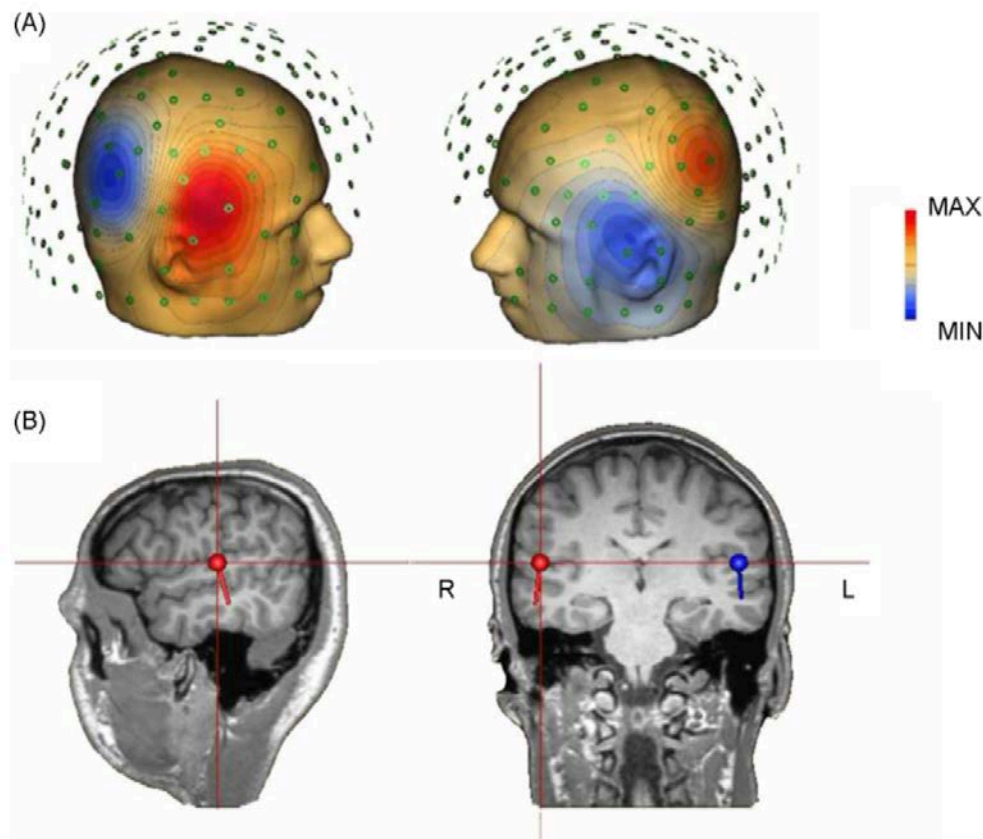
Figure 2: Auditory evoked magnetic fields elicited by onset of 500 ms of white noise delivered binaurally at 70 dB SPL. The latency of this response is about 100 ms after sound onset (see time series waveform in Figure 3). (A) Head shape is derived from magnetic resonance images of an adult participant. The 160 MEG sensors are shown with respect to the surface of the head. Colors show magnetic fields resulting from activation of auditory cortex in the superior temporal plane. Red represents magnetic flux leaving the head, blue show magnetic flux re-entering the head. The source of the magnetic field is ionic current flow in the pyramidal cells of the auditory cortex, located approximately midway between the maxima and minima of the surface magnetic fields. (B) Locations of the sources of the surface fields are represented by balls, the orientations of the sources are indicated by sticks, showing the direction of positive current flow is downward. The field maps at (A) can be predicted by the right-hand rule of electromagnetism, which states that if you point the right thumb in the direction of current flow, then magnetic fields will follow the direction of your curved fingers. Electrical fields are perpendicular to the magnetic fields. In this case negative current flow is pointed up, so the electroencephalogram would record a negativity at the top surface of the head (the N100 event-related potential) and reversed-polarity version of this response at recording locations inferior to the mid-temporal lobe. Figure adapted with permission from (Johnson & Hautus, 2010).

Noise suppression is another important requirement for most MEG measurements in an urban environment. Passive shielding is achieved by placing the MEG instrument in a multi-tonne magnetically-shielded room (MSR), usually constructed of 2-3 layers of aluminum and mu-metal. Active shielding systems typically combine a lighter passively shielded MSR with flux-gate (non-superconducting) magnetometers and electronics for active cancellation of ambient fields. With

20

effective shielding SQUID-based MEG systems have a noise floor of about 2-4 fT/Hz$^{1/2}$. Further noise suppression is achieved by configuring the flux transformer of the MEG sensors into a "gradiometer". A simple flux transformer, consisting of a pickup coil and input coil (for coupling to the SQUID), is referred to as a magnetometer.

The capital cost of a modern MEG system with MSR is similar to a clinical MRI scanner. Operating costs are largely from liquid helium which boils off at a rate of approximately 70-100 L per week. Rising international costs of helium are increasing interest in recovery and re-liquefication systems, although few MEG installations have these at present. At present, there are approximately 150 "whole-head" MEG systems (multichannel instruments that can measure activity from the entire brain simultaneously) in the world. These are concentrated in Europe (particularly Germany and Great Britain), the United States and Canada, and Japan, with more recent appearances also in South Korea, Taiwan, Israel and Australia (http://megcommunity.org/index.php?option=com_content&view=article&id=9&Itemid=31).

While the current generation of MEG systems are based on conventional SQUIDs, MEG sensor technology is undergoing a rapid evolution at the present time. One new commercial system (http://www.york-instruments.co.uk/technology/#sensor) uses a hybrid SQUID (termed "HyQuid™") sensor that does not require liquid helium. Many also anticipate that room temperature sensors based on optically pumped magnetometers (OPMs; Knappe, Sander, & Trahms, 2014) may be available in commercial MEG systems in the relatively near future. This next generation of helium-free systems are likely to have significantly lower capital and running costs, facilitating their penetration into biomedical and research facilities.

2.2 MEG in the Context of Other Imaging Techniques

Neuromagnetic fields are generated by ionic current flows in active neurons. As with EEG signals, MEG signals primarily involve postsynaptic potentials in the cortical pyramidal cells. To generate a measurable extracerebral signal requires the summated activity of a large number of neurons within a patch of cortex at least several square cm in extent. While post-synaptic potentials are much smaller signals than action potentials, their longer duration provides a much larger temporal window for summation; consequently, MEG signals are largely generated from postsynaptic potentials. The physical geometry and orientation of neurons is another crucial factor in effective summation of neuromagnetic fields. The parallel orientation of the cortical pyramidal cells allows for effective spatial summation and these are known as "open-field" generators. In contrast, the relatively random orientations of neurons such as cortical stellate cells contribute to self-cancelling of fields and these are referred to as "closed-field" generators. Unlike the EEG which measures signals from both sulci and gyri (Jackson & Bolger, 2014), the MEG is relatively less sensitive to signals generated in the gyri of the cerebral cortex. The reason is that because magnetic fields circle the longitudinal axis of a neuron, the field generated by a purely radial neuron do not exit the head. In practice, relatively few neurons are purely radial, so that MEG has some sensitivity to most of the cortex except for neurons at the very crests of the gyri (Hillebrand & Barnes, 2002).

Since MEG is a direct measure of ionic current flow in neurons, it can sample neural activity with an almost unlimited time resolution, or more accurately, a time resolution that is limited largely by the sampling capabilities of the equipment's analogue-to-digital converter. In practice, this is of the order of a millisecond or less. Put another way, MEG directly measures the fundamental currency of neuronal signals. This confers upon the technique the crucial advantage that it has the same time scaling as neuronal events. Pitted against this advantage is the fact that magnetic

fields sum algebraically (see section on the inverse problem, below), making it difficult to resolve closely spaced events that also overlap in time. In other words, the same properties that confer excellent temporal resolution to MEG detract from its spatial resolution (Baillet, 2017). Having said this, the spatial resolution of the MEG is generally considered superior to that of the EEG, because volume-conducted electrical fields are strongly affected by conductive inhomogeneities and anisotropies of the cerebral and extracerebral tissues (Schomer & Da Silva, 2012a) and these must be factored into the volume conduction model during brain source localization (Haueisen, Ramon, Czapski, & Eiselt, 1995; Oostendorp & van Oosterom, 1991). In contrast, the various tissues of the brain and head are essentially transparent to magnetic fields and can be effectively modeled without knowledge of their resistive properties (Baillet et al., 2001). This dramatic reduction in computational complexity is a fundamental advantage of MEG over EEG. See **Table 1** for a detailed comparison of EEG and MEG techniques.

Table 1: A comparison of EEG and MEG

	EEG	MEG
Referential measurement	Yes	No
Fields generated from	Volume currents	Primary currents
Sensors	In contact with scalp	Not in contact with scalp
Electromagnetic shielding	Usually not required	Usually required
Capital Costs	Low	High
Operational Costs	Low	High
Biophysical modelling	Complex	Simple
Localization of generators	Optional	Usually directed to localization

Instead of measuring the magnetic force field that is directly instantiated by ionic current flow in neurons, neuroimaging techniques such as fMRI and positron emission tomography (PET) index the *consequences* of neural activity (changes in regional cerebral blood oxygenation levels and/or cerebral metabolism). This fundamental difference confers unique advantages and disadvantages to each technique. MEG can track neural activity on a millisecond by millisecond basis because it measures the fundamental currency of this activity. The temporal resolution of

fMRI/PET is inherently less (hundreds of milliseconds to many seconds) because the metabolic and regional cerebral blood-oxygenation-level-dependent consequences of neuronal activity are temporally sluggish and follow with a lag. On the other hand, PET and fMRI have very accurate spatial resolution because location is directly encoded in their signals and tomographic imaging is straightforward (Narayana, Saboury, Newberg, Papanicolaou, & Alavi, n.d.; Bailey, Townsend, Valk, & Maisey, 2005; Stamatakis, Orfanidou, & Papanicolaou, 2017; Singleton, 2009). The derivation of location from MEG signals is a more complicated matter, largely because electromagnetic fields exhibit linear superposition, that is they sum algebraically. The consequence of this property is that, while it is straightforward to compute external magnetic fields given a known configuration of brain sources, it is not possible to directly compute brain sources given only information about external fields. Since numbers also exhibit algebraic summation, this problem is readily understood by realising that one can easily compute a unique solution for the result of 2 + 3; however, if one is given only the result of 5, it is not possible to compute a single configuration of numerical sources (there are in fact an infinite number of solutions).

The lack of a unique inverse places the bioelectromagnetic inverse problem in the class of mathematical problems termed "ill-posed" problems. In effect, these problems cannot be solved without information drawn from outside the strict logic of the problem. In general MEG brain source "imaging" or "localization" approaches condition the inverse problem to reduce the set of possible solutions to a finite set; construct forward models of the sources; and then probe the set of forward models for a match to the data. Three classes of inverse solutions in common use include dipole modeling, minimum norm estimation, and spatial filtering (beamforming). Dipole modeling is a highly constrained, "overdetermined" (because the number of sources is much smaller than the number of MEG sensors) solution which reduces the number of possible MEG

generators to a small set (most frequently, 1 or 2) of active brain sources, which can be physically modelled as "equivalent current dipoles" whose forward solutions can be readily calculated and whose positions can be parametrically changed and fit to measured fields in a least squares sense. Dipole modelling is a well-understood approach that has been well-validated for situations involving one or a few highly focal brain sources, such as some classes of epileptic foci, and early components of sensory evoked responses. In contrast, minimum norm estimation and beamforming analyses are "distributed source models" which calculate the dipole moments of thousands of (stationary) dipoles distributed in a grid over the brain volume. The distributed source models are important advances, dispensing with the need to specify, a priori, the number of independent sources (as in dipole modelling); and extending the domain of source analysis far beyond the limited realm of simple focal source modeling to much more complicated (and realistic) situations involving extensive and temporally overlapping regions of the brain.

3 MEG signals and Auditory Responses

It is useful to conceive of two broad classes of MEG signals, termed event-related (or evoked) responses and intrinsic brain oscillations (or, interchangeably intrinsic brain rhythms). Event-related responses are considered to be brain responses that are elicited by and time-locked to, some temporally well-defined sensory, motor, or even cognitive "event". Depending on whether the 'event' is transient in time or steady-state, event-related responses can be further classified into transient event-related fields (ERFs) and evoked steady-state responses (SSRs). ERFs are conceived of and analysed in the time domain as a fairly stereotyped series of MEG amplitude fluctuations locked to the evoking event (**Figure 3**). In contrast SSRs are usually analysed in the frequency domain as periodic brain responses imposed by periodic (spectrally well-defined) stimuli (**Figure 4**).
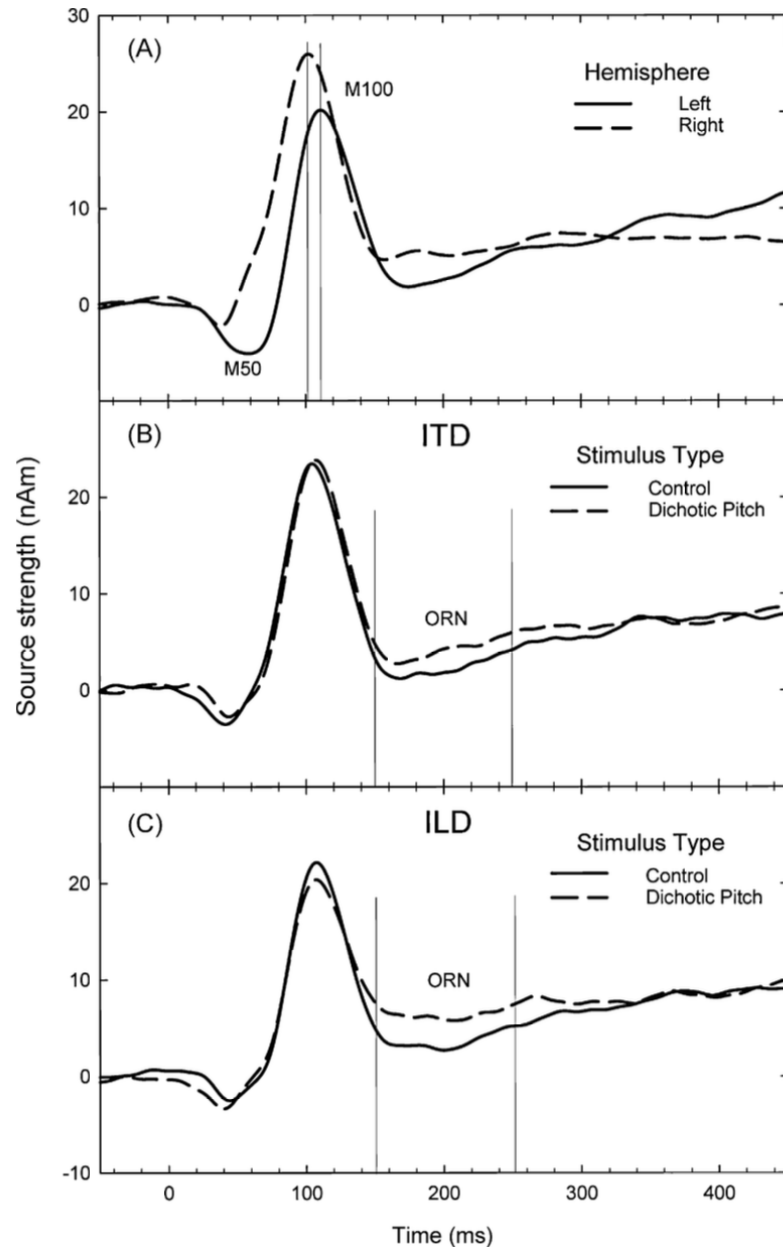
Figure 3: Auditory cortex source waveforms show time resolution of MEG responses to 500 ms of binaural white noise. Waveforms are grand averages of responses from 12 normal hearing participants. (A) M50 and M100 responses are robustly elicited by sound onsets. These correspond to the P50 and N100 responses of the auditory event-related potential recorded with the electroencephalogram. Peaks latencies are slightly earlier in the right hemisphere than the left hemisphere. (B) Object-related negativity (ORN) response is elicited at a latency of 150-250 ms when an interaural time delay is introduced to a narrow band of frequencies in the white noise stimulus, resulting in the perception of a "dichotic pitch" in addition to the background noise. (C) ORN amplitude is increased when dichotic pitch is produced with an interaural level difference, which has greater perceptual salience than the pitch produced by an interaural time delay. Figure adapted with permission from (Johnson & Hautus, 2010).

26
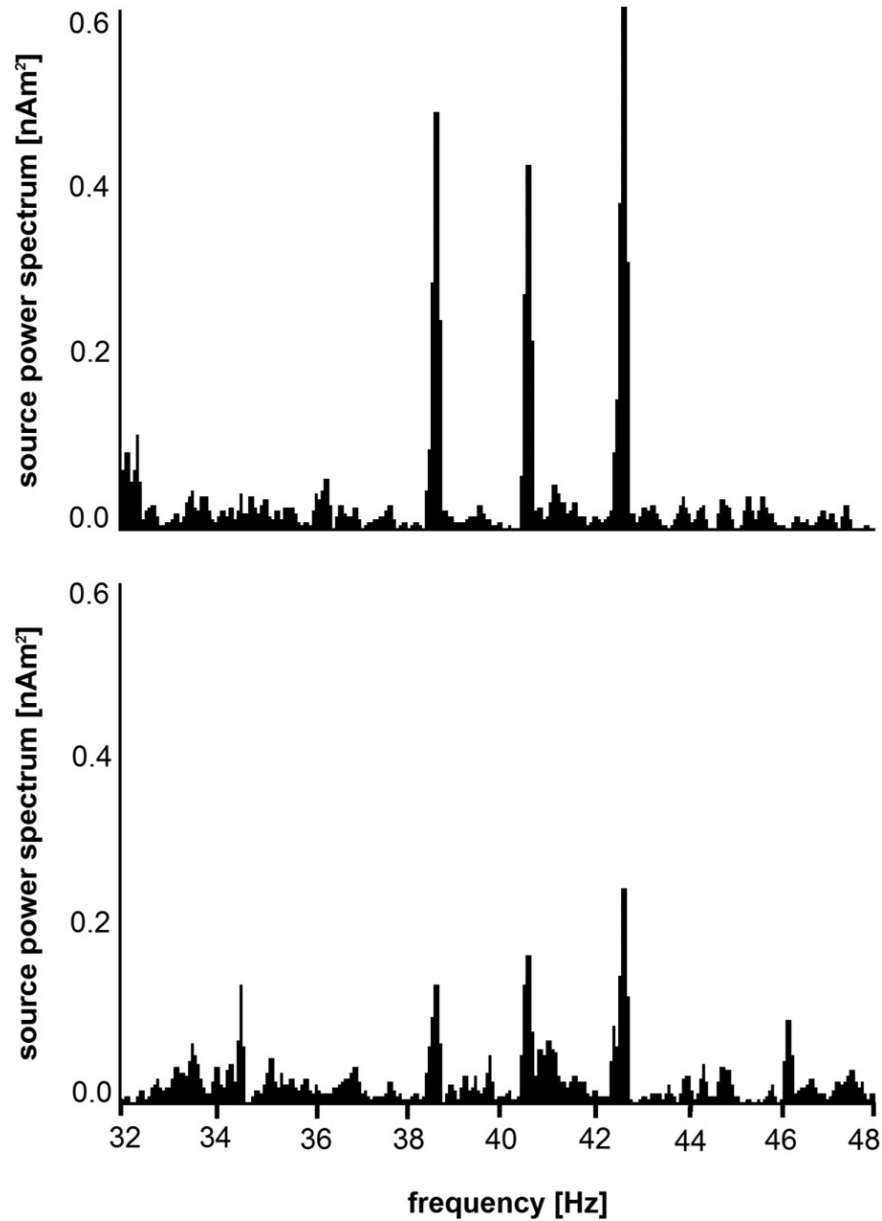
Figure 4: Auditory steady state response evoked by three superimposed amplitude modulated sine tones from a representative participant using monaural stimulation. The modulation depth is 100% and duration is 8192 ms with 20ms onset and offset cosine ramps. The carrier frequencies matched the audiometric edge frequency (edge condition: E, which was defined as that location on the frequency axis at which the hearing loss function exhibited its largest slope), the tinnitus frequency in patients and the "surrogate tinnitus frequency" 1½ octaves above the audiometric edge frequency in controls (tinnitus condition: T), and a frequency 1½ octaves below the audiometric edge (sub-edge condition: S). The modulation frequencies were set to 38.6, 40.6, and 42.6 Hz (conditions 38, 40, and 42). Composite tones consisted of linear superposition of the single tones and all combinations of carrier and modulation frequencies occurred at equal probabilities (S38+E40+T42, S40+E42+T38, S42+E38+T40). Top: Hemisphere contralateral to the ear of stimulation. Bottom: Hemisphere ipsilateral to the ear of stimulation. Figure adapted with permission from (E Diesch, Andermann, Flor, & Rupp, 2010)

Intrinsic brain oscillations, on the other hand, are ongoing oscillatory brain activities (or rhythms) that can be measured either in the absence of external stimuli (spontaneous responses) or as event-related modulations of these rhythms (induced rhythms). Both types of activity are manifest in the form of large-scale oscillations with either simple or complex profiles over both

time and frequency domains, and normally combined "time-frequency" analysis is employed to evaluate both temporal and spectral characteristics **(Figure 5)**. Induced brain responses are usually referred to as event-related spectral perturbations (ERSPs; Pfurtscheller & Lopes da Silva, 1999a). ERSPs can in turn be categorized into two types: event-related synchronisations (ERS), referring to an increase in amplitude of a particular frequency band; and event-related desynchronizations (ERD), referring to decrease in amplitude. Some theorists (e.g. Mazaheri & Jensen, 2008) hold that the distinction between evoked and induced MEG signals may be partly or wholly an artificial one, but in practice the distinction is useful and widespread.
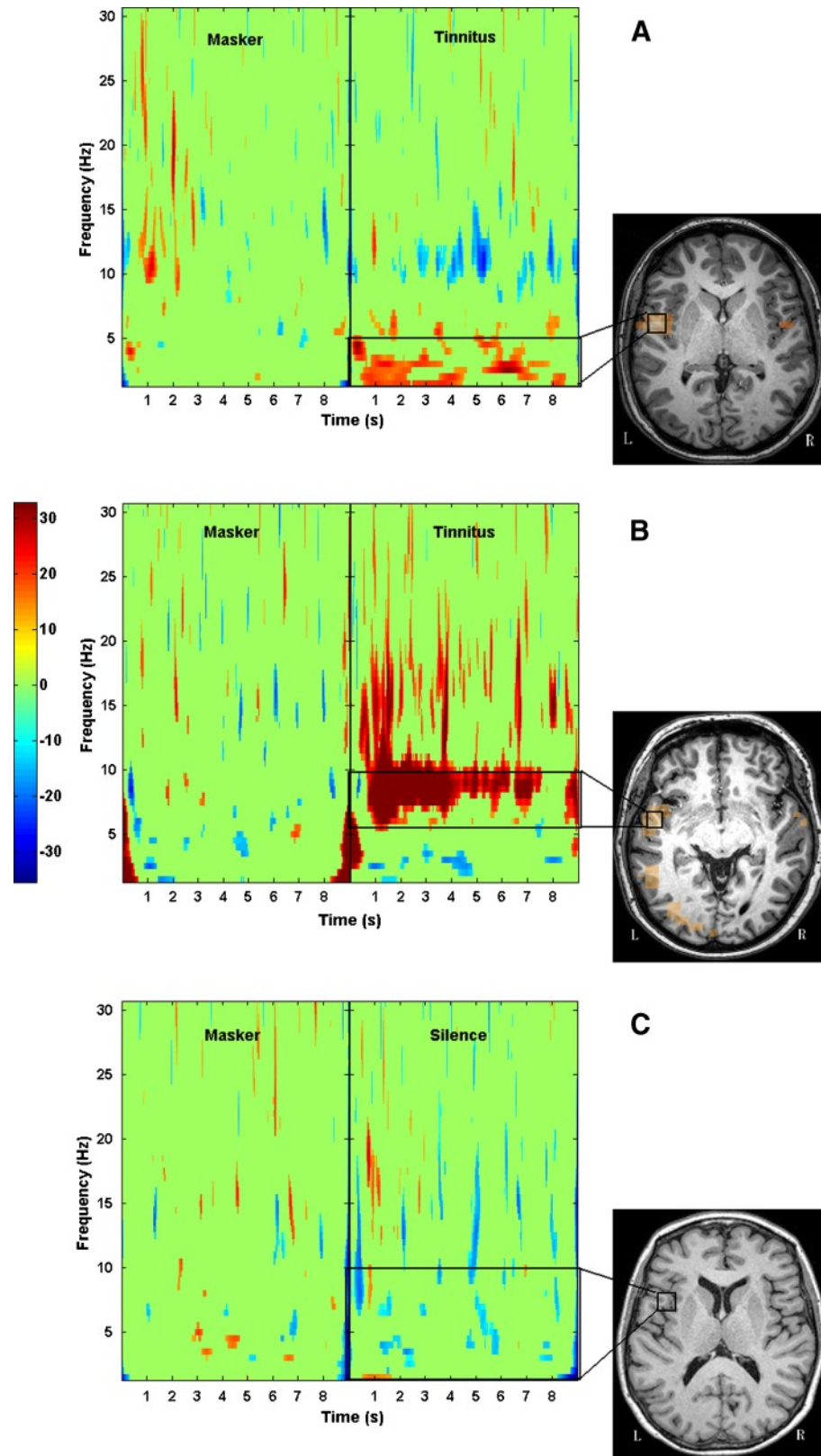
Figure 5: Time–frequency spectrogram for the" masker period" (10 seconds, 0.1-12 kHz noise masker presented binaurally at 50 dB SPL) and "silence period" (10 seconds) from two participants with tinnitus and hearing loss who experienced reduction of their tinnitus with masking, and a participant with no tinnitus and clinically normal hearing. Plot A: Enhanced low frequency (1-4 Hz) activity appearing with the onset of tinnitus percept. Plot B: Onset of low frequency (5-8 Hz) activity following the masker in another tinnitus patient. Plot C: Same analysis in a participant with no tinnitus and clinically normal hearing. Source locations were identified in the plot A and plot B using beamformer in the silence period when tinnitus percept was present. Figure adapted with permission from (Adjamian, Sereda, Zobay, Hall, & Palmer, 2012)

3.1 Auditory Evoked (Event-Related) Fields

In the auditory domain, event-related responses are generally evoked by various kinds of acoustic stimuli. These auditory evoked fields (AEFs) encompass a large and (steadily increasing) number of time-locked responses used by researchers as neurophysiological markers of auditory processing in the brain. A comprehensive survey of these markers is beyond the scope of the present review, the interested reader is referred to (Gutschalk, 2014; Lütkenhöner & Poeppel, 2011) for more detailed treatments of these responses. In general any acoustic change from silence to sound to silence will elicit a transient cortical on-response to the sound onset, an off-response to sound offset, and a sustained field which decays (defined by a time-constant) in amplitude between onset and offset (Lammertmann & Lütkenhöner, 2001). The transient on-response is the most prominent of these and in practice is the dominant or only observable response in most acoustic experiments. The MEG on-response to a simple acoustic event (500 ms of white noise) is illustrated in **Figure 3** and is characterized by fairly well-defined peaks at latencies of about 50 ms (M50 response) and 100 ms (M100) after the noise onset, and followed by a broader, less well-delineated peak at latencies between about 150-250 ms (M200). MEG's capability for assessing lateralization of auditory processing is shown in **Figure 3(A)**, which shows clear hemispheric differences in latency and amplitude of the M50 and M100 responses to these diotically-presented noise stimuli. While event-related (EEG) potentials measure comparable peaks (termed P50, N100, and P200, respectively), hemispheric differences are more difficult to discern in auditory ERPs (Nagarajan et al., 2012), which are maximal at the vertex and containing contributions from both hemispheres.

 Figure 3(B) and **Figure 3(C)** further illustrate how the AEF can be leveraged to provide strong inferences about the timing of neurophysiological mechanisms for important classes of auditory processing events. In these plots, the diotic noise stimulus used in **Figure 3(A)** was modified to

introduce a dichotic time (B) or level (C) difference for a narrow frequency band (300-700 Hz) within the noise. The result is that listeners now "hear out" a lateralized pitch in addition to central noise, a perceptual illusion referred to as "dichotic pitch". The ERF plots of **Figure 3(B)** show that the dichotic pitch ERF shows an increased amplitude (object-related negativity; ORN) relative to the diotic noise ERF during a time interval of about 150-250 ms after sound onsets. Since the two types of stimuli were monaurally identical, the contrast between diotic and dichotic pitch ERFs provides a strong temporal constraint on the cortical processing of the binaural cue to dichotic pitch. **Figure 3(C)** shows a similar ORN response for the binaural level cue.

Auditory steady-state responses (ASSRs) are neural responses evoked by rapid periodic acoustic stimulation whose frequency components exhibit constant phase and amplitude (Picton, John, Dimitrijevic, & Purcell, 2003a). The most prominent ASSRs can be acquired when the stimulation frequency is around 40 Hz in awake human subjects (Galambos, Makeig, & Talmachoff, 1981). Although likely containing contributions from multiple regions of the auditory nervous system, ASSRs at frequencies below 50 Hz have been associated with cortical regions rather than subcortical areas (Mauer, 1999; Herdman et al., 2002; Draganova, Ross, Wollbrink, & Pantev, 2008). The MEG measured ASSRs from a representative participant (modulation frequencies were set to 38.6, 40.6, and 42.6 Hz; carrier frequencies were individually determined relative to the audiometric edge of the participant) is shown in **Figure 4**. This spectral plot showed three distinct components at frequencies corresponding to the modulation rates as well as a difference between the hemisphere contralateral and ipsilateral to the ear of stimulation. With custom designed stimuli, the magnitude of components of the composite response can be utilized to provide evaluation of auditory function from a frequency specific point of view. As the responses evoked by rapidly presented stimuli are less affected by state of consciousness or levels of arousal, ASSRs have been employed to assess hearing thresholds clinically in new-borns (Tanaka,

Kuriki, Nemoto, & Uchikawa, 2013). A detailed introduction of human auditory steady-state response is given in Picton et al. (Picton, John, Dimitrijevic, & Purcell, 2003b).

3.2 Intrinsic Brain Oscillations

The intrinsic rhythms of the human brain have been studied since the original description of the alpha rhythm by Berger prior to WWII (Schomer & Da Silva, 2012a). The waking human brain is characterized by five prominent rhythms: the aforementioned alpha rhythm (8-12 Hz); beta (13-30 Hz); and gamma (35-80 Hz or higher); theta (3-7 Hz); delta (2 Hz or lower) (Pfurtscheller & Lopes da Silva, 1999b; R Hari, Salmelin, Mäkelä, Salenius, & Helle, 1997). The alpha "band" actually comprises several physiologically distinct rhythms. The occipital-parietal alpha rhythm is particularly prominent when subjects close their eyes (Jasper & Shagass, 1941). The mu rhythm (7.5-12.5 Hz) has been described as an "idling" rhythm of the resting peri-rolandic cortices and exhibits a striking desynchronization during movement, and often a strong "rebound" synchronization when movement ceases (Cheyne, 2013). A small amplitude "tau" (6.5-9.5 Hz) rhythm generated from auditory cortices can be detected with MEG (Tiihonen et al., 1991) but with EEG only in cases where the bones of the temporal skull have been compromised (thus it is referred to as a "breach" rhythm) (Schomer & Da Silva, 2012b). Beta rhythms are generated in a variety of brain structures but are most prominently associated with MEG measurements of the resting primary motor cortex (Cheyne, 2013; Engel & Fries, 2010). Gamma rhythms are also generated in a variety of regions but are prominently associated with MEG measurements of activation of visual (Muthukumaraswamy & Singh, 2008), motor (Cheyne, 2013) and auditory cortex (Pantev et al., 1991).

An example of time-frequency spectrogram showing the intrinsic brain oscillatory activity during listening to a masker noise and silence is given in **Figure 5**. The enhanced delta/theta band activities following the noise masker are evidenced as reliable neural correlates of tinnitus

percept compared to normal hearing participant. The peak response locations identified with beamforming further illustrate the capability of MEG localizing underlying generators of cortical oscillations.

Acoustic signals such as speech, music and other environmental sounds unfold over time, and different kinds of information are conveyed at quite different time scales. For example, in speech, syllable rate periodicities occur at rates of approximately 4 - 7 per second, while much higher modulation rates (~50-500 Hz) are important for perception of voiced speech sounds and periodicity pitch. Intrinsic brain oscillations at different frequency scales have been proposed as putative mechanisms for encoding the corresponding time scales in speech (Giraud & Poeppel, 2012), thus providing a natural form of temporal "multiplexing" in order to encode the full dynamic range of temporal modulations in sounds (Gross, Hoogenboom, et al., 2013). This process is an important problem in auditory neurophysiology and is also a central issue for recent neurobiological models of language processing. One such model posits that slow (theta-band/delta-bad) and fast (gamma-band) intrinsic brain oscillations in auditory cortex become synchronized to slow (syllable rate) and fast (phoneme rate) periodicities in the speech stream to facilitate the speech perception process (Poeppel, 2003).

4. MEG in Listeners with Auditory Impairments

Auditory impairments such as hearing loss, tinnitus and auditory processing disorders (APD) are typical issues reported by patients in audiology clinics. As indicated in Diges et al. (Diges, Simón, & Cobo, 2017), these impairments can be concomitant or mutually exclusive and may affect one or several parts of the ascending auditory pathway from the periphery to the auditory cortex and cortical networks. Equipped with excellent temporal and spatial resolution, MEG serves as an ideal tool and has been employed to investigate corresponding impairments on auditory brain function. Early MEG studies investigating auditory pathologies mainly focused on AEFs elicited

with transient acoustic stimuli. There is now growing interest in investigating intrinsic brain oscillatory activities and patterns of connectivity across different brain regions. A summary of MEG investigations of auditory impairments is listed in **Table 2** with comparison to MEG measurements from normal hearing participants.

4.1 An overview of the common auditory impairments

Hearing loss, or hearing impairment, is defined as a partial or total inability to hear. Sensorineural hearing loss, as a result of disruption to the cochlea/auditory nerve is often investigated in the literature of neuroimaging studies. Age-related hearing loss (or presbyacusis) is the most common type of sensorineural hearing loss. It occurs gradually in most people as a result of normal ageing of the auditory system and has been reported to affect approximately 1/3 of adults aged 65 years and over (World Health Organization, 2017). Over and above the attenuation of perceived sound level, it causes difficulty in speech comprehension, especially when there are concurrent speakers or environmental sounds present in the background. Interventions for hearing loss include amplification devices (hearing aids) and in the case of severe-profound hearing loss, cochlear implants. Although to some extent the elevated hearing thresholds can be addressed with hearing aids and hearing ability can be restored to the profoundly deaf with cochlear implants, speech recognition performance varies considerably among individual listeners when there is concurrent noise present in the background (Kochkin, 2005; Tremblay & Miller, 2014). While high performing cochlear implant recipients can often understand speech in quiet environments, the poorest performers obtain little or no sensation of sound from the implant (Tyler, Lowder, Parkinson, Woodworth, & Gantz, 1995).

Impacts of age-related hearing loss are actually derived from two sources: indirect effects from cognitive declines associated with ageing; and directly through various disruptions along the auditory pathway. A discussion of the contributions from each factor as well as their interplay to

34

the changes in structure and function of cortical auditory regions is given in Cardin (2016). Results from a series of studies and reviews (F. Lin et al., 2014; F. R. Lin et al., 2011; Peelle & Wingfield, 2016; Pichora-Fuller & Levitt, 2012; Wayne & Johnsrude, 2015; Wingfield & Peelle, 2015) have suggested independent contributions from hearing loss to atrophy in the human auditory cortex and cognitive decline among older adults, which in turns exacerbates the effects of physiological ageing. These changes in central auditory system are regarded as an important factor distinct from the well-studied peripheral deficits in recent research work on hearing loss (Humes et al., 2012). As the restoration of auditory sensation via cochlear implantation is accomplished with impoverished sound signals, this may result in changes to the cognitive side of hearing: e.g. taxing cognitive function and/or changes in cognitive strategies or processes. EEG, fMRI and MEG studies have examined this effect with normal hearing participants using spectrally degraded speech signals to mimic implant recipients (Wöstmann, Herrmann, Wilsch, & Obleser, 2015; Wilsch, Henry, Herrmann, Maess, & Obleser, 2015; Erb, Henry, Eisner, & Obleser, 2013; Obleser, Wöstmann, Hellbernd, Wilsch, & Maess, 2012; Obleser & Kotz, 2011) and auditory cortical alpha oscillation has been proposed to be an index of changes in memory load during listening (Strauß, Wöstmann, & Obleser, 2014; Weisz, Hartmann, Müller, Lorenz, & Obleser, 2011). It is thus of critical interest to examine brain functioning in hearing impaired listeners under intervention to assess potential causes of the variability in performance.

Tinnitus refers to the perception of an auditory sensation (hissing, ringing sound or sometimes even voices and music) in the absence of a corresponding stimulus (Baguley, McFerran, & Hall, 2013). It affects 10%-20% of the world population (Shargorodsky, Curhan, & Farwell, 2010). A good review on the current knowledge of tinnitus as well as established and emerging treatment approaches is outlined in (Baguley et al., 2013). Mostly subjective and triggered by cochlear injury which leads to sensory deprivation, tinnitus is often accompanied by an audiometrically-

measurable hearing loss and was traditionally viewed as an inner-ear problem (Weisz, Wienbruch, Dohrmann, & Elbert, 2005). Although the precise neural mechanisms are unknown, current views regard the subjective sensation of tinnitus to result from functional changes in the central auditory system (increased spontaneous activity and/or synchrony) and abnormalities at various stages of the auditory pathway (Adjamian, 2014). Moreover, evidence from animal models and human brain-imaging studies have suggested that widely distributed non-auditory areas of the brain are also involved, associated with tinnitus distress and also participating in the generation of the phantom sound (De Ridder, Elgoyhen, Romo, & Langguth, 2011; Rauschecker, Leaver, & Mühlau, 2010).

In contrast to the specific auditory impairments described above, auditory processing disorder (APD) encompasses a variety of disorders that result from a deficiency in the central auditory nervous system. APD results in an impairment of the ability of the auditory pathway to appropriately integrate sound information for normal sound perception (Moore, Rosen, Bamiou, Campbell, & Sirimanna, 2013). According to the position statement from British Society of Audiology (BSA), APD can be categorized into developmental, acquired, and secondary forms. The exact definition of APD is still under debate, but a consensus holds that APD affects one or more of the following skills: sound localization and lateralization; auditory discrimination; auditory pattern recognition; temporal aspects of audition; or performance with competing acoustic signals and with degraded acoustic signals (Bamiou, Musiek, & Luxon, 2001). As reviewed in (Micallef, 2015a), conventional psychoacoustic tests are not considered to be sensitive to APD and there is an urgent need for neuroimaging techniques to contribute to the assessment of deficits associated with APD.

4.2 MEG in Hearing Loss, Intervention and Cognitive Listening Effort

4.2.1 MEG Studies on Hearing Loss

To date, MEG experiments in hearing loss patients have mainly measured AEFs using either simple or complex tones (Alain, Roye, & Salloum, 2014; Dietrich, Nieschalk, Stoll, Rajan, & Pantev, 2001). In addition to sensor level activity being normally assessed with EEG (Paulraj, Subramaniam, Yaccob, Adom, & Hema, 2015), equivalent current dipoles were used in these studies to model auditory cortical sources and results illustrated the fact that the cortical map can reorganize in hearing loss patients so that neurons deprived of their usual most sensitive afferent input changes their response frequencies.

Motivated by results from animal studies, auditory evoked fields were measured by Dietrich et al. to investigate the effects of steep high frequency hearing loss on functional reorganization of human auditory cortex (Dietrich et al., 2001). Specifically, the neurons that are usually responsive to the lost frequencies were speculated to start responding to adjacent tone frequencies (lesion edge frequencies). M100 magnetic fields evoked by tone burst with lesion edge frequency and two pre-lesion frequencies were recorded. Cortical activity evoked by the lesion edge frequency was shown to be significantly larger compared to those evoked by pre-lesion frequencies. This result was suggested to be due to an expanded representation of the lesion edge frequency, leading to a reorganization of the tonotopic map in auditory cortex. However, tinnitus was also present in this hearing loss group and this could also have contributed to the observed effects on AEFs. Another MEG study examined the difference in auditory evoked fields between older adults with mild hearing loss (age-related) and with normal hearing using a series of complex tones (Alain et al., 2014). The complex tones were constructed to have all harmonics in tune or with a mistuned third harmonic and were presented with different levels of background noise. AEFs showed enhanced M100 amplitude in the hearing-impaired group. The difference between

waveforms evoked by tuned and mistuned tones (object related negativity, or ORN) was also larger compared with that from normal listeners. This result was attributed to a reduction of inhibitory control in primary and associative auditory cortices for participants with age-related hearing loss and evidence for an independent contribution from hearing loss.

Contributions from hearing threshold differences were also reported in MEG studies examining auditory brain oscillations. Designed to investigate how ageing affects cortical encoding of speech, possible effects of hearing loss were reported on brain oscillations tracking the acoustic envelope of perceived speech sentences (Presacco, Simon, & Anderson, 2016a, 2016b). Compared with young adults, older adults exhibited significantly higher hearing thresholds and showed exaggerated speech entrainment activity in both quiet and noisy conditions. The reduction in speech tracking activity was also larger for the older adults group when background noise was introduced in the form of a single competing talker. When a meaningless background noise (an unfamiliar foreign language) was used, enhanced cortical speech tracking activity was observed with older adults but not the young adults. These results were attributed to an imbalance between inhibitory and excitatory processes or diminished efficiency of network connectivity caused by natural aging, whereas hearing loss could also be a possible contributor.

4.2.2 MEG Studies on Hearing Loss Intervention

For patients with hearing intervention devices, routine MEG measurement is generally not possible due to the inherent interference to MEG sensors caused by electronic and magnetic components from hearing aid/cochlear implant system. The few MEG studies of cochlear implant recipients have measured auditory evoked fields under unique laboratory set-ups. The first such observations were reported by Pelizzone et al. with a cochlear implant recipient who performed poorly in understanding free running speech without lip-reading after implantation (Pelizzone, Hari, Mäkelä, Kaukoranta, & Montandon, 1986). By using direct stimulation of short tone bursts

into the implant's processor of a cochlear implant in the congenitally deaf right ear, auditory evoked fields were measured with a 3-channel MEG instrument. Repetitive measurements were carried out to yield an adequate coverage over the entire brain and for comparison, a concurrent EEG recording was also conducted. Latency of the M100 peak was reported to be earlier than for normal hearing participants, due to the unnatural stimulation by the implanted prosthesis. The evoked magnetic fields measured from right hemisphere (ipsilateral to stimulation) were shown to be coincident with the auditory event-related potential (AEP) from the concurrent EEG recordings. The location and direction of equivalent current dipoles were both consistent with results obtained from normal hearing participants evoked by various kinds of different sound stimuli. However, only small responses could be observed from the left hemisphere (contralateral to stimulation) and the morphology of the AEF was different than that of the EEG ERP. This contradictory result, compared to observations from normal hearing people, was attributed to early childhood hearing loss, which presumably modifies the central auditory pathway. In a subsequent study, a post-lingually deaf cochlear implant recipient was recruited and tested with different kinds of auditory stimuli (Hari, Pelizzone, Mäkelä, Huttunen, & Kuuutila, 1988). In this patient, M100 AEF to short tone bursts, noise, frequency modulations of a continuous tone and noise/square-wave transitions were typical in latency and the corresponding patterns of magnetic field closely resembled those measured from participants with normal hearing. This result was speculated to be associated with the good speech recognition performance of the patient. Following the two successful case studies, another MEG experiment measured AEFs from a post-lingual deaf cochlear implant recipient who was using a device with extracochlear electrodes (Manfried Hoke, Pantev, Lütkenhöner, Lehnertz, & Sürth, 1989). In this case, M100 and M200 AEFs evoked by a 1000 Hz tone were delayed by around 40 ms, whereas the location and direction of M100 agreed with the data of normal hearing people.

The dipole moment of the M100 was significantly diminished though, possibly due to different placement of electrodes.

Measurement of AEFs were also used as an index of auditory plasticity by Pantev et al. in a longitudinal study of cochlear implant recipients (Pantev, Dinnesen, Ross, Wollbrink, & Knief, 2006). Two post-lingually deaf patients wearing unilateral magnet-free cochlear implant (Clarion 1.2 and Clarion CII, Advanced Bionics Corp., Sylmar, CA) were measured over a 2-year period. The M50 and M100 responses of both participants evoked by a continuous tone with a sudden frequency shifts were examined in 10 consecutive measurements. Almost normal component configuration was reported by the end of the study and the auditory evoked brain activities were successfully localized in the auditory cortex.

4.2.3 MEG Studies on Cognitive Effort in Adverse Listening Conditions

Cognitive effort or the listening demand increases in difficult listening conditions. This experience is quite evident with hearing aid users and cochlear implant recipients as a result of sound processing distortion from those devices and the incapability of current technology to efficiently suppress the background noise. As reviewed above, routine MEG measurements with hearing impaired people who wear these devices are not possible at this stage. However, studies with normal hearing participants and processed sound (spectral degradation or adding background noise) to mimic the listening experiences of hearing aid users or cochlear implant recipients have been carried out.

Obleser and colleagues have demonstrated that acoustic degradation to spoken digits resulted in an increased cortical alpha oscillation during stimulus-free retention period immediately after hearing those digits in their MEG study (Obleser et al., 2012). The acoustical adversity has been reported to drive an oscillatory network (source localized to right parietal, cingulate,

supramarginal, and superior temporal cortex) which also exhibits enhanced alpha activity when memory load increases. In another MEG study by Wilsch et al. (Wilsch et al., 2015), alpha oscillations were evaluated when syllables were presented in speech-shaped background noise and different temporal expectation benefits were facilitated by visual cues. From this study, concomitantly reduced cognitive load and alpha power were reported during the retention period of the first perceived syllable in a syllable pair matching task and the alpha activity was localized to the right insula. Results from these studies suggested intrinsic alpha oscillation as putative neural markers of cognitive load and set the stage for future studies on the impact of cognitive function of hearing loss patients, hearing aid users and cochlear implant recipients, as a consequence of chronic acoustic degradations from sensory input.

4.3 MEG in Tinnitus and Tinnitus Network

4.3.1 MEG Studies on Tinnitus: responses from sensors and auditory cortex

Numerous MEG studies have measured either AEFs or ASSRs in tinnitus patients. The amplitude ratio of auditory evoked fields (M100/M200) was first examined by Hoke et al. in an investigation of tinnitus patients (M Hoke et al., 1989). A significantly enhanced M100 component evoked by 1 kHz tone was reported for the tinnitus group together with a delayed and poorly developed M200 response compared to that of the normal-hearing controls. This study has initiated a series of subsequent experiments employing similar paradigms to measure changes in amplitude and latency of auditory evoked fields in tinnitus populations (Pantev, Hoke, Lütkenhöner, Lehnertz, & Kumpf, 1989; Jacobson et al., 1991; Colding-Jørgensen, Lauritzen, Johnsen, Mikkelsen, & Saermark, 1992; E. S. Hoke, Mühlnickel, Ross, & Hoke, 1998; Sereda, Adjamian, Edmondson-Jones, Palmer, & Hall, 2013). Source localization of evoked responses using equivalent current dipoles was also performed with an aim to reveal the underlying neural generators of tinnitus perception (Mühlnickel, Elbert, Taub, & Flor, 1998; Dietrich et al., 2001; McMahon, Ibrahim, &

Mathur, 2016). However, findings from these studies have been contradictory. Possible reasons for the discrepancies were discussed in (Adjamian, 2014) and include: the inadequacy of M100 or M100/M200 AEF to serve as a measure of tinnitus-related cortical change; and the oversimplified source model provided by equivalent current dipoles (ECD).

ASSRs acquired by MEG using a series of 40 Hz amplitude modulated tones were first used by Diesch et al. to investigate relationships between MEG responses and subjective ratings of tinnitus (Eugen Diesch et al., 2004). When the carrier frequency matched to the pitch of tinnitus perception, a positive correlation was reported between the intrusiveness of tinnitus and the amplitude of ASSR. In two follow up studies, Diesch et al. have confirmed this relationship using closely matched non-tinnitus controls group in terms of hearing threshold and age (E Diesch et al., 2010; Eugen Diesch, Andermann, Flor, & Rupp, 2010). Another MEG study used 40 Hz amplitude modulated tones with eight different carrier frequencies between 384 Hz and 6561 Hz to compare tonotopic frequency representations between tinnitus patients and normal healthy controls (Wienbruch, Paul, Weisz, Elbert, & Roberts, 2006). A bilateral ASSR frequency gradient shift was shown together with an increase in the strength of dipole moment in the primary auditory region for the tinnitus group. This was interpreted as a result of reduced inhibition in deafferented regions of the primary auditory cortex; however, hearing threshold differences were not controlled in this study.

As tinnitus perception is ongoing, spontaneous brain activity has been a useful index and used by many investigators to reveal differences in time-frequency profiles of the MEG signals between tinnitus patients and controls. Weisz and colleagues reported a marked decrease in alpha (8-12 Hz) power and an enhancement in delta power (1.5-4 Hz) compared to a normal hearing control group (Weisz, Moratti, Meinzer, Dohrmann, & Elbert, 2005). Significant correlations were also found between both abnormal spontaneous activities and tinnitus related

distress, with the strongest association observed in right temporal and left frontal regions. This result has been linked to reduced lateral inhibition (Llinás, Ribary, Jeanmonod, Kronberg, & Mitra, 1999), however this correlation has not been found across all studies as it could also be confounded by hearing-loss related disinhibition.

A subsequent MEG study examined gamma band oscillations, and a power increase, particularly between 50-60 Hz, was reported (Weisz, Dohrmann, & Elbert, 2007). Moreover, activity around 55 Hz was shown to determine the laterality of tinnitus perception. Patients with unilateral or unilaterally dominant tinnitus showed stronger contralateral activity at 55 Hz, whereas no such lateralization was observed for subjects with equally strong tinnitus on both sides. MEG measurements of spontaneous brain oscillations have also been used to evaluate the effect of residual inhibition (RI) and masking, two strategies commonly employed to suppress the tinnitus percept. By comparing the spontaneous brain activities, a significant reduction of power in delta band during RI but not periods of tinnitus was found in the temporal regions in (Kahlbrock & Weisz, 2008). Also with MEG, both RI and residual excitation (RE) were observed in a group of chronic tinnitus patients in (Sedley et al., 2012). Positive correlations between tinnitus intensity and both delta/theta and gamma band oscillations in a subgroup of the patients who reported RI were found in the auditory cortex. In contrast, the RE experience subgroup exhibited an inverse correlation between tinnitus percept and auditory cortical gamma oscillations.

When white noise was used to mask the experience of tinnitus, group level differences in delta band between tinnitus patients (with and without hearing loss) and normal hearing controls were shown in (Adjamian et al., 2012). While significantly higher in the tinnitus group, delta band activity showed a reduction during masking period for those patients who reported an experience of inhibition.

The measurement of a close resemblance to induced oscillatory brain activities in tinnitus was obtained by Ortmann et al. investigating a group of musicians who reported no chronic tinnitus but transient perception immediately after band practice (Ortmann, Müller, Schlee, & Weisz, 2011). A temporary tinnitus experience was created by exposing the group of musicians to loud music and MEG measurements were acquired both with and without previous exposure to loud music. Compared with resting-state spontaneous oscillations, a rapid increase in gamma band power was reported in the right auditory cortex for most of the participants.

4.3.2 MEG Studies on Tinnitus: a network beyond auditory cortex

Evidenced by the involvement of both auditory and non-auditory cortical structures there has been an emerging agreement of a distributed network in tinnitus disorder. Pioneered by Schlee et al. in an attempt to characterise a "tinnitus network", ASSRs evoked by amplitude-modulated tones at tinnitus frequency and 1.1, 2.2 octaves below have been investigated in their MEG study (Schlee, Weisz, Bertrand, Hartmann, & Elbert, 2008). The results showed a phase synchrony between the anterior cingulum, the right frontal lobe, and the right parietal lobe. This long-range brain connectivity was also demonstrated to be strongly correlated with the individual tinnitus distress ratings. However, the phase synchrony effect could be due to hearing loss alone, as this factor was not segregated out from tinnitus.

Intrinsic brain oscillation based connectivity has also been evaluated. To examine the difference in activation of distributed cortical networks, phase synchrony was calculated on resting state MEG recordings and compared between chronic tinnitus patients and healthy control participants by Schlee et al. (Schlee, Hartmann, Langguth, & Weisz, 2009). Inter-areal coupling indexed by phase synchrony in the alpha band was significantly reduced while a marked increase in gamma band was seen for tinnitus patients. Brain network coupling in alpha and gamma bands was negatively correlated across all subjects. Also, the distribution of gamma network was also

shown to be more widespread in patients with tinnitus duration longer than 4 years. In another study to further explore the long-range information flow between auditory and non-auditory brain regions among tinnitus patients, Schlee et al. applied a beamforming technique to reconstruct brain activity at source level (Schlee, Mueller, et al., 2009a). A global network including core structures such as the prefrontal cortex, the orbitofrontal cortex and the parieto-occipital region was identified together with a positive correlation between the information flow from this global network to temporal cortex and tinnitus distress.

4.4 MEG in Auditory Processing Disorders (APD)

To our knowledge, MEG has not been used to examine the cortical processing involved in APD, perhaps partly due to its often being concomitant with other learning and language disorders; and also, in part because the research focus has been predominantly on sub-cortical processing in APD (Larson & Lee, 2014). Some neuroimaging data has been acquired from the APD patients, using PET (Ruytjens, Willemsen, Van Dijk, Wit, & Albers, 2006), diffusion tensor imaging (Owen et al., 2013) and fMRI (Pluta et al., 2014). Results from these studies have suggested both regional abnormal brain activities (bilateral auditory cortex, posterior cingulate gyrus) and abnormal brain structural connectivity (frontally distributed atypical white matter microstructure). Unfortunately, these resting state abnormalities and structural changes do not reflect deficits in specific brain function. With its strengths of measuring neural activity directly and non-invasively at millisecond scale, it is promising that MEG will find applications in APD research. Recent reviews (Larson & Lee, 2014; Micallef, 2015b) have suggested that MEG, combined with improved source localization and connectivity measures, may be applied to assist APD diagnosis and assessment of intervention strategies.

5 Summary and Future Directions in Hearing Research

MEG has long been a valuable tool for the study of central auditory and speech processing with normal hearing population. It has much higher temporal resolution than hemodynamic techniques such as fMRI, and in practice has better spatial resolution than the EEG. It is well suited for studying the developing brain, particularly of preschool children aged 3-5 years. In recent years, interest in the MEG for auditory/linguistic neuroimaging has been strongly stimulated by the increasing appreciation and understanding of the role of neuronal oscillations in auditory temporal processing and language perception. This neuroscientific paradigm shift coincides with a shift in the focus of hearing researchers and clinicians toward a greater appreciation of the role of cognitive factors in hearing and communication. Taken together these two trends are driving demand for functional imaging tools that can index higher levels of the auditory and linguistic systems of the brain. In many respects, MEG is the method of choice for such purposes.

In the context of auditory MEG measurements, it should be noted that a characteristic of beamformer approaches is that their performance degrades sharply for spatially separated but highly synchronous sources (Cheyne & Papanicolaou, 2017). As a consequence, it is commonly believed that beamformer methods will have difficulty in resolving the two auditory cortices since these tend to be activated bilaterally by sounds. However, even with diotic stimulation, there are typically measurable hemispheric differences in terms of the latencies, magnitudes and morphologies of auditory cortical MEG waveforms. In practice, beamformers and dipole models provide comparable resolution of event-related responses in auditory cortical sources (Gascoyne, Furlong, Hillebrand, Worthen, & Witton, 2016). Also, in the context of auditory research, an important advantage of MEG is that the scanning equipment is entirely silent during

its operation. Further, the scanning equipment is relatively open and few if any participants report any issues with claustrophobia during MEG scans.

In the context of evaluating impaired auditory brain function and effects of hearing loss interventions, MEG currently has found very limited applications except for tinnitus. This is largely due to the fact that peripheral hearing deficits and the resulting pathological auditory brain function interact with each other and complicate the measurement result. Results from the example MEG studies evaluating pathological auditory brain function suggested that auditory evoked responses can only give a limited depiction with regards to the impairments on central nervous system and results are to some extent controversial. On the other hand, intrinsic oscillations from a distributed brain network other than specific brain regions are better suited as neural markers of impact from different auditory impairments. As the results from MEG studies by Schlee et al. (Schlee, Hartmann, et al., 2009; Schlee, Mueller, et al., 2009b) demonstrated, subjective tinnitus may be better characterised with distributed brain networks instead of restricting the examinations of activities in auditory cortex. Intrinsic cortical oscillations just serve as an effective tool to facilitate these inter-network/inter-area communications through various kinds of power, phase or frequency-based couplings. With tailored oscillation-based source space analysis techniques, MEG could potentially be used to better understand and evaluate these pathologies, either acquired after maturation or manifest during the development of the central auditory pathway.

Another obvious factor that impedes MEG research in hearing loss intervention area is the fact that its superconducting sensors are highly sensitive to interference from the electronic and magnetic components of hearing aids and cochlear implants (these devices produce magnetic fields in the mT range). It would be highly useful to deploy MEG to study the effects of hearing loss, and remediation of hearing loss, on higher-level auditory and linguistic brain processes, but

47

advances in instrumentation are required in order for MEG to be used in conjunction with cochlear implants (see Chapter 5).

6 Author Contributions

Q.M., Y.L.H., C.M and B.J. conceived and wrote the paper. All of the authors discussed the contents and edited the manuscript.

Tables

Table 1: A comparison of EEG and MEG

	EEG	MEG
Referential	Yes	No
Fields generated from	Volume currents	Primary currents
Sensors	In contact with scalp	Not in contact with scalp
Electromagnetic shielding	Usually not required	Usually required
Capital Costs	Low	High
Operational Costs	Low	High
Biophysical modelling	Complex	Simple
Localization of generators	Optional	Usually directed to localization

Table 2: MEG studies in Listeners with Auditory Impairments

Study	Type of Auditory Impairment	MEG Measurements	Results
Dietrich et al., 2001	Hearing loss (HL)	AEFs evoked by tones at both lesion edge and prelesion frequencies	Enhanced M100 response at lesion edge frequency
Alain et al., 2014	Hearing loss (HL)	AEFs evoked by complex tones both in tune and mistuned; The difference between this two (ORN)	Enhanced M100 and ORN
Presacco et al., 2016 a.	Hearing loss (HL)	Intrinsic brain oscillations entrained to speech envelope in meaningful and meaningless background noise	Enhanced entrainment activity under meaningful background noise condition
Presacco et al., 2016 b	Hearing loss (HL)	Intrinsic brain oscillations entrained to speech envelope in quiet and in meaningful background noise	Enhanced entrainment activity under both quiet and noisy condition
Hoke et al., 1989a	Tinnitus	AEFs evoked by 1 kHz tone	Enhanced M100 and reduced M200
Pantev et al., 1989	Tinnitus	AEFs evoked by 1 kHz tone (longitudinal study for a patient suffered from acoustic trauma)	Gradual recovery of M100 and M200 to normal levels over 6 months
Jacobson et al., 1991	Tinnitus	AEFs evoked by 1 kHz tone	No significant differences in either amplitude or latency of M100 and M200
Colding- Jørgensen et al., 1992	Tinnitus	AEFs evoked by 1 kHz tone	No significant differences in either amplitude or latency of M100 and M200
Muhlnickel et al., 1998	Tinnitus	AEFs evoked by 1 kHz, 2 kHz, 8 kHz tones and tone at tinnitus frequency	Equivalent current dipole location of M100 to the tinnitus frequency shifted away from tonotopic map
Hoke et al. 1998	Tinnitus	AEFs evoked by a tinnitus frequency tone and either a 1kHz or a 4kHz tone whichever is farther away from tinnitus frequency	Enhanced M100 and reduced M200

Sereda et al. 2013	Tinnitus	AEFs evoked by an audiometric edge frequency tone, a tinnitus frequency tone, a tone within hearing loss range and a tone in normal hearing range	No significant differences in amplitude of M100
McMahon et al., 2016	Tinnitus	AEFs evoked by 0.5 kHz, 1 kHz, 2 kHz and 4kHz tones (longitudinal study during a 30-week tinnitus treatment)	Equivalent current dipole source power of M100 to 0.5 kHz and 1 kHz tones were larger and more anteriorly located. Source power remained during the treatment while source locations shifted towards the direction recorded from control group
Diesch et al. 2004	Tinnitus	40 Hz ASSRs with carrier frequencies equal to tinnitus frequency, audiometric edge, two frequencies below audiometric edge and two frequencies between audiometric edge and tinnitus frequency	A positive correlation between subjective tinnitus ratings and the amplitude of ASSR when carrier frequency matched tinnitus frequency
Weisz et al. 2005a	Tinnitus	spontaneous brain oscillations	Alpha (8-12 Hz) power decrease and delta (1.5-4 Hz) power increase.
Wienbruch et al. 2006.	Tinnitus	40 Hz ASSRs with carrier frequencies equal to eight different frequencies (384, 576, 864, 1296, 1944, 2916, 4374, or 6561 Hz)	Bilateral ASSR frequency gradients shift and an increase in the strength of dipole moment in the primary auditory region
Weisz et al. 2007	Tinnitus	Spontaneous brain oscillations	Gamma (50-60 Hz) power increase, activity around 55Hz determined laterality of tinnitus perception

Kahlbrock and Weisz 2008	Tinnitus	Spontaneous brain oscillations	Delta power decrease during residual inhibition
Schlee et al. 2008	Tinnitus	37.1 Hz ASSRs with carrier frequencies equal to tinnitus frequency, 1.1 and 2.2 octaves below tinnitus frequency	A phase synchrony between the anterior cingulum, the right frontal lobe, and the right parietal lobe.
Schlee et al. 2009a	Tinnitus	Spontaneous brain oscillations	Deceased alpha phase synchrony and increased gamma phase synchrony
Schlee et al. 2009b	Tinnitus	Spontaneous brain oscillations	A positive correlation between the information flow from a global network (prefrontal cortex, orbitofrontal cortex and the parieto-occipital region) to temporal cortex and tinnitus distress
Diesch et al. 2010a	Tinnitus	39.1 Hz and 41.1 Hz ASSRs with carrier frequency equals to tinnitus frequency, audiometric edge and a frequency 1.5 octaves below audiometric edge (1.5 octaves above audiometric edge for controls)	Positive correlation between subjective tinnitus ratings and the amplitude of ASSR when carrier frequency matched tinnitus frequency
Diesch et al. 2010b	Tinnitus	38.6 Hz, 40.6 Hz and 42.6 Hz ASSRs with carrier frequency equals to tinnitus frequency, audiometric edge and a frequency 1.5 octaves below audiometric edge (1.5 octaves above audiometric edge for controls)	Positive correlation between subjective tinnitus ratings and the amplitude of ASSR when carrier frequency matched tinnitus frequency
Ortmann et al. 2011	Tinnitus	Induced brain oscillations	Increased gamma band oscillation in the right auditory cortex
Sedley et al. 2012	Tinnitus	Spontaneous brain oscillations	Residual inhibition group: positive correlations between tinnitus percept and

| | | | auditory cortex delta/theta, gamma band oscillations

Residual excitation group: negative correlation between tinnitus percept and auditory cortex gamma oscillations. |
|---|---|---|---|
| Adjamian et al. 2012 | Tinnitus | Spontaneous brain oscillations | Increased delta band activity with a reduction during masking period for patients experienced inhibition. |
| Pelizzone et al. 1986 | Cochlear Implant | AEFs evoked by 1 kHz tones | A reduced contralateral AEF and a normal ipsilateral AEF due to early childhood hearing loss. |
| Hari et al. 1988 | Cochlear Implant | AEFs evoked by 1 kHz tones, square wave after a noise burst and frequency modulations of a continuous 1 kHz tone | AEFs closely resemble AEFs evoked by same acoustic stimuli in normal hearing participants (result of post-lingual deafness). |
| Hoke et al. 1989b | Cochlear Implant | AEFs evoked by 1 kHz tones | Delayed M100, M200 components and diminished M100 due to extra-cochlear electrode placement. |
| Pantev et al. 2006 | Cochlear Implant | AEFs evoked by frequency modulations of a continuous 1 kHz tone | Gradual recovery of M50 and M100 components for two post-lingual deaf recipients over 2 years. |
| Larson and Lee 2014 | Auditory Processing Disorder (APD) | N/A | Source level analysis with the minimum-norm estimate (MNE) method was recommended for potential measurement with APD patients. |

References

Adjamian, P. (2014). The application of electro- and magneto-encephalography in tinnitus

    research - methods and interpretations. *Frontiers in Neurology*, *5*, 228.

    https://doi.org/10.3389/fneur.2014.00228

Adjamian, P., Sereda, M., Zobay, O., Hall, D. A., & Palmer, A. R. (2012). Neuromagnetic

    indicators of tinnitus and tinnitus masking in patients with and without hearing loss.

    Journal of the Association for Research in Otolaryngology, *13*(5), 715–731.

Alain, C., Roye, A., & Salloum, C. (2014). Effects of age-related hearing loss and background

    noise on neuromagnetic activity from auditory cortex.

Arnal, L. H., Poeppel, D., & Giraud, A. (2015). Temporal coding in the auditory cortex. *Handb

    Clin Neurol*, *129*, 85–98.

Baguley, D., McFerran, D., & Hall, D. (2013). Tinnitus. *The Lancet*, *382*(9904), 1600–1607.

    https://doi.org/10.1016/S0140-6736(13)60142-7

Bailey, D. L., Townsend, D. W., Valk, P. E., & Maisey, M. N. (2005). *Positron emission

    tomography*. Springer.

Baillet, S. (2017). Magnetoencephalography for brain electrophysiology and imaging. *Nature

    Neuroscience*, *20*(3), 327–339.

Baillet, S., Mosher, J. C., & Leahy, R. M. (2001). Electromagnetic brain mapping. *IEEE Signal

    Processing Magazine*, *18*(6), 14–30.

Bamiou, D., Musiek, F., & Luxon, L. (2001). Aetiology and clinical presentations of auditory

    processing disorders—a review. *Archives of Disease in Childhood*, *85*(5), 361–365.

Brignell, C. J., Hall, D. A., & Witton, C. (2008). Mapping the auditory brain using

magnetoencephalography (MEG). In *Brain Mapping Research Developments* (p. 13).

Nova Publishers.

Cardin, V. (2016). Effects of aging and adult-onset hearing loss on cortical auditory regions.

Frontiers in Neuroscience, *10*.

Cheyne, D. O. (2013). MEG studies of sensorimotor rhythms: A review. *Experimental Neurology*,

245, 27–39. https://doi.org/10.1016/j.expneurol.2012.08.030

Cheyne, D. O., & Papanicolaou, A. C. (2017). Magnetoencephalography and magnetic source

imaging. *Oxford Handb. Funct. Brain Imaging Neuropsychol. Cogn. Neurosci.*, 13–42.

Cohen, D. (1968). Magnetoencephalography: evidence of magnetic fields produced by alpha-

rhythm currents. *Science (New York, N.Y.)*, *161*(3843), 784–786.

Cohen, D. (1972). Magnetoencephalography: detection of the brain's electrical activity with a

superconducting magnetometer. *Science (New York, N.Y.)*, *175*(4022), 664–666.

Cohen, M. X. (2017). Where Does EEG Come From and What Does It Mean? *Trends in

Neurosciences*, *40*(4), 208–218. https://doi.org/10.1016/j.tins.2017.02.004

Colding-Jørgensen, E., Lauritzen, M., Johnsen, N., Mikkelsen, K., & Saermark, K. (1992). On the

evidence of auditory evoked magnetic fields as an objective measure of tinnitus.

Electroencephalography and Clinical Neurophysiology, *83*(5), 322–327.

De Ridder, D., Elgoyhen, A. B., Romo, R., & Langguth, B. (2011). Phantom percepts: tinnitus and

pain as persisting aversive memory networks. *Proceedings of the National Academy of*

Sciences of the United States of America, *108*(20), 8075–8080.
https://doi.org/10.1073/pnas.1018466108

Diesch, E, Andermann, M., Flor, H., & Rupp, A. (2010). Interaction among the components of
multiple auditory steady-state responses: enhancement in tinnitus patients, inhibition in
controls. *Neuroscience*, *167*(2), 540–553.

Diesch, Eugen, Andermann, M., Flor, H., & Rupp, A. (2010). Functional and structural aspects of
tinnitus-related enhancement and suppression of auditory cortex activity. *Neuroimage*,
50(4), 1545–1559.

Diesch, Eugen, Struve, M., Rupp, A., Ritter, S., Hülse, M., & Flor, H. (2004). Enhancement of
steady-state auditory evoked magnetic fields in tinnitus. *European Journal of
Neuroscience*, *19*(4), 1093–1104.

Dietrich, V., Nieschalk, M., Stoll, W., Rajan, R., & Pantev, C. (2001). Cortical reorganization in
patients with high frequency cochlear hearing loss. *Hearing Research*, *158*(1–2), 95–101.

Diges, I., Simón, F., & Cobo, P. (2017). Assessing Auditory Processing Deficits in Tinnitus and
Hearing Impaired Patients with the Auditory Behavior Questionnaire. *Frontiers in
Neuroscience*, *11*, 187. https://doi.org/10.3389/fnins.2017.00187

Draganova, R., Ross, B., Wollbrink, A., & Pantev, C. (2008). Cortical Steady-State Responses to
Central and Peripheral Auditory Beats. *Cerebral Cortex*, *18*(5), 1193–1200.
https://doi.org/10.1093/cercor/bhm153

Engel, A. K., & Fries, P. (2010). Beta-band oscillations--signalling the status quo? *Current
Opinion in Neurobiology*, *20*(2), 156–165. https://doi.org/10.1016/j.conb.2010.02.015

Erb, J., Henry, M. J., Eisner, F., & Obleser, J. (2013). The Brain Dynamics of Rapid Perceptual

    Adaptation to Adverse Listening Conditions. *Journal of Neuroscience*, *33*(26), 10688–

    10697. https://doi.org/10.1523/JNEUROSCI.4596-12.2013

Fagaly, R. (2006). Superconducting quantum interference device instruments and applications.

    Review of Scientific Instruments, *77*(10), 101101.

Galambos, R., Makeig, S., & Talmachoff, P. J. (1981). A 40-Hz auditory potential recorded from

    the human scalp. *Proceedings of the National Academy of Sciences of the United States

    of America*, *78*(4), 2643–2647.

Giraud, A.-L., & Poeppel, D. (2012). Cortical oscillations and speech processing: emerging

    computational principles and operations. *Nature Neuroscience*, *15*(4), 511–517.

Gross, J., Baillet, S., Barnes, G. R., Henson, R. N., Hillebrand, A., Jensen, O., … others. (2013).

    Good practice for conducting and reporting MEG research. *Neuroimage*, *65*, 349–363.

Gross, J., Hoogenboom, N., Thut, G., Schyns, P., Panzeri, S., Belin, P., & Garrod, S. (2013).

    Speech rhythms and multiplexed oscillatory sensory coding in the human brain. *PLoS

    Biology*, *11*(12).

Gutschalk, A. (2014). MEG Auditory Research. In *Magnetoencephalography* (pp. 679–711).

    Springer.

Hämäläinen, M., Hari, R., Ilmoniemi, R. J., Knuutila, J., & Lounasmaa, O. V. (1993).

    Magnetoencephalography—theory, instrumentation, and applications to noninvasive

    studies of the working human brain. *Reviews of Modern Physics*, *65*(2), 413.

Hansen, P., Kringelbach, M., & Salmelin, R. (2010). *MEG: An introduction to methods*. Oxford university press.

Hari, R, Pelizzone, M., Mäkelä, J., Huttunen, J., & Kuuutila, J. (1988). Neuromagnetic Responses from a Deaf Subject to Stimuli Presented through a Multichannel Cochlear Prosthesis*. *Ear and Hearing*, *9*(3), 148–152.

Hari, R, Salmelin, R., Mäkelä, J. P., Salenius, S., & Helle, M. (1997). Magnetoencephalographic cortical rhythms. *International Journal of Psychophysiology*, *26*(1), 51–62. https://doi.org/10.1016/S0167-8760(97)00755-1

Hari, Riitta, & Puce, A. (2017). *MEG-EEG Primer*. Oxford University Press.

Hari, Riitta, & Salmelin, R. (2012). Magnetoencephalography: from SQUIDs to neuroscience: Neuroimage 20th anniversary special edition. *Neuroimage*, *61*(2), 386–396.

Haueisen, J., Ramon, C., Czapski, P., & Eiselt, M. (1995). On the influence of volume currents and extended sources on neuromagnetic fields: A simulation study. *Annals of Biomedical Engineering*, *23*(6), 728–739. https://doi.org/10.1007/BF02584472

Herdman, A. T., Lins, O., Van Roon, P., Stapells, D. R., Scherg, M., & Picton, T. W. (2002). Intracerebral sources of human auditory steady-state responses. *Brain Topography*, *15*(2), 69–86.

Hillebrand, A., & Barnes, G. R. (2002). A quantitative assessment of the sensitivity of whole-head MEG to activity in the adult human cortex. *NeuroImage*, *16*(3 Pt 1), 638–650.

Hoke, E. S., Mühlnickel, W., Ross, B., & Hoke, M. (1998). Tinnitus and event-related activity of the auditory cortex. *Audiology and Neurotology*, *3*(5), 300–331.

Hoke, M, Feldmann, H., Pantev, C., Lütkenhöner, B., Lehnertz, K., & Kumpf, W. (1989). Objective

evidence of tinnitus in auditory evoked magnetic fields. In *Advances in Biomagnetism*

(pp. 319–322). Springer.

Hoke, Manfried, Pantev, C., Lütkenhöner, B., Lehnertz, K., & Sürth, W. (1989). Magnetic fields

from the auditory cortex of a deaf human individual occurring spontaneously or evoked

by stimulation through a cochlear prosthesis. *Audiology*, *28*(3), 152–170.

Humes, L. E., Dubno, J. R., Gordon-Salant, S., Lister, J. J., Cacace, A. T., Cruickshanks, K. J., …

Wingfield, A. (2012). Central presbycusis: a review and evaluation of the evidence.

Journal of the American Academy of Audiology, *23*(8), 635–666.

https://doi.org/10.3766/jaaa.23.8.5

Jackson, A. F., & Bolger, D. J. (2014). The neurophysiological bases of EEG and EEG

measurement: A review for the rest of us. *Psychophysiology*, *51*(11), 1061–1071.

https://doi.org/10.1111/psyp.12283

Jacobson, G. P., Ahmad, B., Moran, J., Newman, C. W., Tepley, N., & Wharton, J. (1991).

Auditory evoked cortical magnetic field (M 100—M 200) measurements in tinnitus and

normal groups. *Hearing Research*, *56*(1), 44–52.

Jasper, H., & Shagass, C. (1941). Conditioning of the occipital alpha rhythm in man. *Journal of

Experimental Psychology*, *28*(5), 373–388. https://doi.org/10.1037/h0056139

Johnson, B. W., & Hautus, M. J. (2010). Processing of binaural spatial information in human

auditory cortex: neuromagnetic responses to interaural timing and level differences.

Neuropsychologia, *48*(9), 2610–2619.

https://doi.org/10.1016/j.neuropsychologia.2010.05.008

Kahlbrock, N., & Weisz, N. (2008). Transient reduction of tinnitus intensity is marked by

concomitant reductions of delta band power. *BMC Biology*, *6*, 4.

https://doi.org/10.1186/1741-7007-6-4

Keil, A., Debener, S., Gratton, G., Junghöfer, M., Kappenman, E. S., Luck, S. J., … Yee, C. M.

(2014). Committee report: publication guidelines and recommendations for studies

using electroencephalography and magnetoencephalography. *Psychophysiology*, *51*(1),

1–21.

Knappe, S., Sander, T., & Trahms, L. (2014). Optically-pumped magnetometers for MEG. In

Magnetoencephalography (pp. 993–999). Springer.

Kochkin, S. (2005). MarkeTrak VII: Customer satisfaction with hearing instruments in the digital

age. *The Hearing Journal*, *58*(9), 30.

https://doi.org/10.1097/01.HJ.0000286545.33961.e7

Lammertmann, C., & Lütkenhöner, B. (2001). Near-DC magnetic fields following a periodic

presentation of long-duration tonebursts. *Clinical Neurophysiology : Official Journal of

the International Federation of Clinical Neurophysiology*, *112*(3), 499–513.

Larson, E., & Lee, A. K. (2014). Potential use of MEG to understand abnormalities in auditory

function in clinical populations.

Lin, F., Ferrucci, L., An, Y., Goh, J., Doshi, J., Metter, E., … Resnick, S. M. (2014). Association of

hearing impairment with brain volume changes in older adults. *Neuroimage*, *90*, 84–92.

Lin, F. R., Metter, E. J., O'Brien, R. J., Resnick, S. M., Zonderman, A. B., & Ferrucci, L. (2011).

Hearing loss and incident dementia. *Archives of Neurology*, *68*(2), 214–220.

Llinás, R. R., Ribary, U., Jeanmonod, D., Kronberg, E., & Mitra, P. P. (1999). Thalamocortical dysrhythmia: a neurological and neuropsychiatric syndrome characterized by magnetoencephalography. *Proceedings of the National Academy of Sciences*, *96*(26), 15222–15227.

Lütkenhöner, B., & Poeppel, D. (2011). From tones to speech: magnetoencephalographic studies. In *The Auditory Cortex* (pp. 597–615). Springer.

Mauer, G. (1999). Generators of amplitude modulation following response (AMFR). *Paper Presented at 16^<th> Meeting of the Evoked Response Audiometry Study Group, Tromso, Norway, Jun, 1999*. Retrieved from http://ci.nii.ac.jp/naid/10018018445/

Mazaheri, A., & Jensen, O. (2008). Asymmetric amplitude modulations of brain oscillations generate slow evoked responses. *The Journal of Neuroscience : The Official Journal of the Society for Neuroscience*, *28*(31), 7781–7787. https://doi.org/10.1523/JNEUROSCI.1631-08.2008

McMahon, C. M., Ibrahim, R. K., & Mathur, A. (2016). Cortical Reorganisation during a 30-Week Tinnitus Treatment Program. *PloS One*, *11*(2), e0148828. https://doi.org/10.1371/journal.pone.0148828

Micallef, L. A. (2015a). Auditory Processing Disorder (APD): Progress in Diagnostics So Far. A Mini-Review on Imaging Techniques. *The Journal of International Advanced Otology*, *11*(3), 257–261.

Micallef, L. A. (2015b). Auditory Processing Disorder (APD): Progress in Diagnostics So Far. A Mini-Review on Imaging Techniques. *The Journal of International Advanced Otology*, *11*(3), 257–261.

Moore, D. R., Rosen, S., Bamiou, D.-E., Campbell, N. G., & Sirimanna, T. (2013). Evolving concepts of developmental auditory processing disorder (APD): a British Society of Audiology APD special interest group 'white paper.' *International Journal of Audiology*.

Mühlnickel, W., Elbert, T., Taub, E., & Flor, H. (1998). Reorganization of auditory cortex in tinnitus. *Proceedings of the National Academy of Sciences of the United States of America*, *95*(17), 10340–10343.

Muthukumaraswamy, S. D., & Singh, K. D. (2008). Spatiotemporal frequency tuning of BOLD and gamma band MEG responses compared in primary visual cortex. *NeuroImage*, *40*(4), 1552–1560. https://doi.org/10.1016/j.neuroimage.2008.01.052

Nagarajan, S., Gabriel, R. A., & Herman, A. (2012). Magnetoencephalography. In *The Human Auditory Cortex* (pp. 97–128). Springer.

Narayana, S., Saboury, B., Newberg, A. B., Papanicolaou, A. C., & Alavi, A. (n.d.). Positron Emission Tomography. In *The Oxford Handbook of Functional Brain Imaging in Neuropsychology and Cognitive Neurosciences*.

Obleser, J., & Kotz, S. A. (2011). Multiple brain signatures of integration in the comprehension of degraded speech. *NeuroImage*, *55*(2), 713–723. https://doi.org/10.1016/j.neuroimage.2010.12.020

Obleser, J., Wöstmann, M., Hellbernd, N., Wilsch, A., & Maess, B. (2012). Adverse Listening Conditions and Memory Load Drive a Common Alpha Oscillatory Network. *Journal of Neuroscience*, *32*(36), 12376–12383. https://doi.org/10.1523/JNEUROSCI.4908-11.2012

Oostendorp, T., & van Oosterom, A. (1991). The potential distribution generated by surface electrodes in inhomogeneous volume conductors of arbitrary shape. *IEEE Transactions on Bio-Medical Engineering*, *38*(5), 409–417. https://doi.org/10.1109/10.81559

Ortmann, M., Müller, N., Schlee, W., & Weisz, N. (2011). Rapid increases of gamma power in the auditory cortex following noise trauma in humans. *European Journal of Neuroscience*, *33*(3), 568–575.

Pantev, C., Dinnesen, A., Ross, B., Wollbrink, A., & Knief, A. (2006). Dynamics of auditory plasticity after cochlear implantation: a longitudinal study. *Cerebral Cortex*, *16*(1), 31–36.

Pantev, C., Hoke, M., Lütkenhöner, B., Lehnertz, K., & Kumpf, W. (1989). Tinnitus remission objectified by neuromagnetic measurements. *Hearing Research*, *40*(3), 261–264.

Pantev, C., Makeig, S., Hoke, M., Galambos, R., Hampson, S., & Gallen, C. (1991). Human auditory evoked gamma-band magnetic fields. *Proceedings of the National Academy of Sciences of the United States of America*, *88*(20), 8996–9000.

Paulraj, M. P., Subramaniam, K., Yaccob, S. B., Adom, A. H. B., & Hema, C. R. (2015). Auditory Evoked Potential Response and Hearing Loss: A Review. *The Open Biomedical Engineering Journal*, *9*, 17–24. https://doi.org/10.2174/1874120701509010017

Peelle, J. E., Troiani, V., Grossman, M., & Wingfield, A. (2011). Hearing Loss in Older Adults Affects Neural Systems Supporting Speech Comprehension. *Journal of Neuroscience*, *31*(35), 12638–12643. https://doi.org/10.1523/JNEUROSCI.2559-11.2011

Peelle, J. E., & Wingfield, A. (2016). The Neural Consequences of Age-Related Hearing Loss. *Trends in Neurosciences*.

Pelizzone, M., Hari, R., Mäkelä, J., Kaukoranta, E., & Montandon, P. (1986). Activation of the auditory cortex by cochlear stimulation in a deaf patient. *Neuroscience Letters*, *68*(2), 192–196.

Pfurtscheller, G., & Lopes da Silva, F. H. (1999a). Event-related EEG/MEG synchronization and desynchronization: basic principles. *Clinical Neurophysiology : Official Journal of the International Federation of Clinical Neurophysiology*, *110*(11), 1842–1857.

Pfurtscheller, G., & Lopes da Silva, F. H. (1999b). Event-related EEG/MEG synchronization and desynchronization: basic principles. *Clinical Neurophysiology : Official Journal of the International Federation of Clinical Neurophysiology*, *110*(11), 1842–1857.

Pichora-Fuller, M. K., & Levitt, H. (2012). Speech comprehension training and auditory and cognitive processing in older adults. *American Journal of Audiology*, *21*(2), 351–357.

Picton, T. W., John, M. S., Dimitrijevic, A., & Purcell, D. (2003a). Human auditory steady-state responses: Respuestas auditivas de estado estable en humanos. *International Journal of Audiology*, *42*(4), 177–219.

Picton, T. W., John, M. S., Dimitrijevic, A., & Purcell, D. (2003b). Human auditory steady-state responses: Respuestas auditivas de estado estable en humanos. *International Journal of Audiology*, *42*(4), 177–219.

Poeppel, D. (2003). The analysis of speech in different temporal integration windows: cerebral lateralization as 'asymmetric sampling in time.' *Speech Communication*, *41*(1), 245–255.

Poeppel, D., Emmorey, K., Hickok, G., & Pylkkänen, L. (2012). Towards a new neurobiology of language. *Journal of Neuroscience*, *32*(41), 14125–14131.

Poeppel, D., & Hickok, G. (2015). Electromagnetic recording of the auditory system. *Handbook of Clinical Neurology*, *129*, 245–255. https://doi.org/10.1016/B978-0-444-62630-1.00014-7

Proudfoot, M., Woolrich, M. W., Nobre, A. C., & Turner, M. R. (2014). Magnetoencephalography. *Practical Neurology*, practneurol–2013.

Raichle, M. E. (2009). A paradigm shift in functional brain imaging. *Journal of Neuroscience*, *29*(41), 12729–12734.

Rauschecker, J. P., Leaver, A. M., & Mühlau, M. (2010). Tuning out the noise: limbic-auditory interactions in tinnitus. *Neuron*, *66*(6), 819–826. https://doi.org/10.1016/j.neuron.2010.04.032

Reite, M., Edrich, J., Zimmerman, J., & Zimmerman, J. (1978). Human magnetic auditory evoked fields. *Electroencephalography and Clinical Neurophysiology*, *45*(1), 114–117.

Sarvas, J. (1987). Basic mathematical and electromagnetic concepts of the biomagnetic inverse problem. *Physics in Medicine and Biology*, *32*(1), 11.

Schlee, W., Hartmann, T., Langguth, B., & Weisz, N. (2009). Abnormal resting-state cortical coupling in chronic tinnitus. *BMC Neuroscience*, *10*, 11. https://doi.org/10.1186/1471-2202-10-11

Schlee, W., Mueller, N., Hartmann, T., Keil, J., Lorenz, I., & Weisz, N. (2009a). Mapping cortical hubs in tinnitus. *BMC Biology*, *7*, 80. https://doi.org/10.1186/1741-7007-7-80

Schlee, W., Mueller, N., Hartmann, T., Keil, J., Lorenz, I., & Weisz, N. (2009b). Mapping cortical hubs in tinnitus. *BMC Biology*, *7*, 80. https://doi.org/10.1186/1741-7007-7-80

Schlee, W., Weisz, N., Bertrand, O., Hartmann, T., & Elbert, T. (2008). Using auditory steady state responses to outline the functional connectivity in the tinnitus brain. *PloS One*, *3*(11), e3720. https://doi.org/10.1371/journal.pone.0003720

Schomer, D. L., & Da Silva, F. L. (2012a). *Niedermeyer's electroencephalography: basic principles, clinical applications, and related fields*. Lippincott Williams & Wilkins.

Schomer, D. L., & Da Silva, F. L. (2012b). *Niedermeyer's electroencephalography: basic principles, clinical applications, and related fields*. Lippincott Williams & Wilkins.

Sedley, W., Teki, S., Kumar, S., Barnes, G. R., Bamiou, D.-E., & Griffiths, T. D. (2012). Single-subject oscillatory γ responses in tinnitus. *Brain : A Journal of Neurology*, *135*(Pt 10), 3089–3100. https://doi.org/10.1093/brain/aws220

Sereda, M., Adjamian, P., Edmondson-Jones, M., Palmer, A. R., & Hall, D. A. (2013). Auditory evoked magnetic fields in individuals with tinnitus. *Hearing Research*, *302*, 50–59.

Shargorodsky, J., Curhan, G. C., & Farwell, W. R. (2010). Prevalence and characteristics of tinnitus among US adults. *The American Journal of Medicine*, *123*(8), 711–718. https://doi.org/10.1016/j.amjmed.2010.02.015

Singleton, M. J. (2009). Functional Magnetic Resonance Imaging. *The Yale Journal of Biology and Medicine*, *82*(4), 233.

Stamatakis, E. A., Orfanidou, E., & Papanicolaou, A. C. (2017). Functional Magnetic Resonance Imaging. *The Oxford Handbook of Functional Brain Imaging in Neuropsychology and Cognitive Neurosciences*, 43.

Strauß, A., Wöstmann, M., & Obleser, J. (2014). Cortical alpha oscillations as a tool for auditory selective inhibition. *Frontiers in Human Neuroscience*, *8*. https://doi.org/10.3389/fnhum.2014.00350

Supek, S., & Aine, C. J. (2014). *Magnetoencephalography: From Signals to Dynamic Cortical Networks*. Springer Berlin Heidelberg. Retrieved from https://books.google.com.au/books?id=tz6DMAEACAAJ

Tanaka, K., Kuriki, S., Nemoto, I., & Uchikawa, Y. (2013). Auditory Steady-State Responses in Magnetoencephalogram and Electroencephalogram: Phenomena, Mechanisms, and Applications. *Advanced Biomedical Engineering*, *2*, 55–62.

Tiihonen, J., Hari, R., Kajola, M., Karhu, J., Ahlfors, S., & Tissari, S. (1991). Magnetoencephalographic 10-Hz rhythm from the human auditory cortex. *Neuroscience Letters*, *129*(2), 303–305.

Tremblay, K. L., & Miller, C. W. (2014). How Neuroscience Relates to Hearing Aid Amplification. *International Journal of Otolaryngology*, *2014*. https://doi.org/10.1155/2014/641652

Tyler, R., Lowder, M. W., Parkinson, A. J., Woodworth, G. G., & Gantz, B. J. (1995). Performance of adult ineraid and nucleus cochlear implant patients after 3.5 years of use. *Audiology*, *34*(3), 135–144.

Vrba, J., & Robinson, S. E. (2001). Signal processing in magnetoencephalography. *Methods (San Diego, Calif.)*, *25*(2), 249–271. https://doi.org/10.1006/meth.2001.1238

Wayne, R. V., & Johnsrude, I. S. (2015). A review of causal mechanisms underlying the link between age-related hearing loss and cognitive decline. *Ageing Research Reviews*, *23*, 154–166.

Weisz, N., Dohrmann, K., & Elbert, T. (2007). The relevance of spontaneous activity for the coding of the tinnitus sensation. *Progress in Brain Research*, *166*, 61–70. https://doi.org/10.1016/S0079-6123(07)66006-3

Weisz, N., Hartmann, T., Müller, N., Lorenz, I., & Obleser, J. (2011). Alpha rhythms in audition: cognitive and clinical perspectives. *Frontiers in Psychology*, *2*, 73. https://doi.org/10.3389/fpsyg.2011.00073

Weisz, N., Moratti, S., Meinzer, M., Dohrmann, K., & Elbert, T. (2005). Tinnitus perception and distress is related to abnormal spontaneous brain activity as measured by magnetoencephalography. *PLoS Medicine*, *2*(6), e153.

Weisz, N., Wienbruch, C., Dohrmann, K., & Elbert, T. (2005). Neuromagnetic indicators of auditory cortical reorganization of tinnitus. *Brain : A Journal of Neurology*, *128*(Pt 11), 2722–2731. https://doi.org/10.1093/brain/awh588

Wienbruch, C., Paul, I., Weisz, N., Elbert, T., & Roberts, L. E. (2006). Frequency organization of the 40-Hz auditory steady-state response in normal hearing and in tinnitus. *NeuroImage*, *33*(1), 180–194. https://doi.org/10.1016/j.neuroimage.2006.06.023

Wilsch, A., Henry, M. J., Herrmann, B., Maess, B., & Obleser, J. (2015). Alpha Oscillatory Dynamics Index Temporal Expectation Benefits in Working Memory. *Cerebral Cortex*, *25*(7), 1938–1946. https://doi.org/10.1093/cercor/bhu004

Wilson, B. S., & Dorman, M. F. (2008). Cochlear implants: a remarkable past and a brilliant future. *Hearing Research*, *242*(1), 3–21.

Wingfield, A., & Peelle, J. E. (2015). The effects of hearing loss on neural processing and plasticity. *Frontiers in Systems Neuroscience*, *9*.

World Health Organization. (2017, February). WHO | Deafness and hearing loss. Retrieved

February 14, 2018, from http://www.who.int/mediacentre/factsheets/fs300/en/

Wöstmann, M., Herrmann, B., Wilsch, A., & Obleser, J. (2015). Neural Alpha Dynamics in

Younger and Older Listeners Reflect Acoustic Challenges and Predictive Benefits. *Journal*

of Neuroscience, *35*(4), 1458–1467. https://doi.org/10.1523/JNEUROSCI.3250-14.2015

Zimmerman, J., Thiene, P., & Harding, J. (1970). Design and Operation of Stable rf-Biased

Superconducting Point-Contact Quantum Devices, and a Note on the Properties of

Perfectly Clean Metal Contacts. *Journal of Applied Physics*, *41*(4), 1572–1580.

Chapter 3: Effects of Intelligibility on Cortical Responses to Speech

Qingqing Meng[1,2,4]
Yiwen Li Hegner[1,2]
Iain Giblin[3,4]
Catherine McMahon[1,3,4,5]
Blake W Johnson[1,2,4]

[1]HEARing Co-operative Research Centre, Melbourne, Victoria, Australia
[2]Macquarie University, Department of Cognitive Science, Sydney, New South Wales, Australia
[3]Macquarie University, Department of Linguistics, Sydney, New South Wales, Australia
[4]ARC Centre of Excellence in Cognition and its Disorders, Macquarie University, Sydney, New South Wales, Australia
[5]Centre for Implementation of Hearing Research, Macquarie University, New South Wales, Australia

Abstract

Cortical activity has been shown to track different levels of linguistic structure in connected speech (syllables, phrases and sentences), independent of the physical regularities of the acoustic stimulus. In the current study, we investigated the effect of speech intelligibility on this brain activity as well as the underlying neural sources. Using magnetoencephalography (MEG), brain responses to speech and spectrally degraded speech in nineteen normal hearing participants were measured. Noise-vocoding was used to spectrally-degrade the speech stimuli. Results showed that the cortical MEG coherence to linguistic structure changed parametrically with the intelligibility of the speech signal. Cortical responses coherent with phrase and sentence structures were left-hemisphere lateralized, whereas responses coherent to syllable/word structure were bilateral. The enhancement of coherence to intelligible compared to unintelligible speech was also left lateralized and localized to the left parasylvian cortex. These results demonstrated that cortical responses to higher level linguistics structures (phrase and sentence level) are highly sensitive to speech intelligibility. Since the noise vocoded sentences mimic (to some extent) the auditory input provided by a cochlear implant, these objective neurophysiological measures have potential clinical utility for assessment of cochlear implant performance.

1 Introduction

Neural oscillations in the delta, theta and gamma frequency bands have been hypothesized as important mechanisms for speech perception. Recent neurolinguistic models (Giraud & Poeppel, 2012; Hickok & Poeppel, 2007) have proposed that these brain rhythms serve to segregate and package linguistic units at different time scales (corresponding to the prosodic, syllabic and phonemic time scales in speech) for further processing. A number of studies have reported that the auditory cortex exhibits activity that becomes phase-synchronized to the speech temporal envelope (Ahissar et al., 2001; Lakatos et al., 2005; Luo & Poeppel, 2007; Peelle, Gross, & Davis, 2013; Zion Golumbic et al., 2013). Prominent quasi-periodic cues occur at the syllabic rate of speech (corresponding to the speech envelope), which has a rate of about 4-7 Hz in natural speaking (Chandrasekaran, Trubanova, Stillittano, Caplier, & Ghazanfar, 2009; MacNeilage, 1998). Psychophysical studies (Drullman, Festen, & Plomp, 1994; Shannon, Zeng, Kamath, Wygonski, & Ekelid, 1995) have demonstrated that the speech envelope is a powerful cue for speech perception and is critically important for comprehension of speech processed by cochlear implants (Shannon, Fu, Galvin, & Friesen, 2004). Often described as "cortical entrainment" (Ding & Simon, 2014), neural phase-locking to syllable rate modulations of the speech envelope has been suggested to serve as a mechanism for the perceptual segmentation of the continuous speech stream into meaningful chunks, a parsing that facilitates extraction of linguistic information (Luo & Poeppel, 2007).

An important line of evidence for this proposition comes from studies showing that cortical phase-locking is significantly attenuated when speech intelligibility is degraded by destroying fine-structure while preserving the overall speech envelope (Peelle et al., 2013; Ding, Chatterjee, & Simon, 2014; Rimmele, Zion Golumbic, Schröger, & Poeppel, 2015). This line of reasoning is contentious, however. Other researchers have argued that the speech entrainment

phenomenon is largely or entirely determined by the acoustic, rather than linguistic, features of speech signal (Howard & Poeppel, 2010; Doelling, Arnal, Ghitza, & Poeppel, 2014; Millman, Johnson, & Prendergast, 2015). As discussed in several reviews (Peelle & Davis, 2012; Ding & Simon, 2014; Zoefel & VanRullen, 2015), this debate has arisen largely because it is difficult to unambiguously disentangle speech intelligibility and speech acoustics in these experiments.

A recent magnetoencephalography (MEG) study provides an important methodological advance by demonstrating that activities from auditory cortex can track *abstract* linguistic structures, i.e., linguistic regularities that are embedded in connected speech but have no physical presence in the acoustic properties of the signal (Ding, Melloni, Zhang, Tian, & Poeppel, 2016). By presenting short sentences constructed with the same syntactic structure to participants in an isochronous manner, concurrent cortical tracking activity to syllable, phrase and sentence level linguistic structures was reported. Importantly, this neural tracking activity of the larger linguistic structures at phrase and sentence level is unambiguously dissociated from any acoustic cues to these units, as there were no physical phrase or sentence boundaries present in the isochronous speech signal. The authors concluded that a grammar-based internal construction process corresponding to the hierarchical linguistic structure must have been carried out (Ding, Melloni, Tian, & Poeppel, 2017).

In the current study we used the experimental paradigm of Ding et al. (2016) to investigate the issue of how speech intelligibility affects neural tracking of the speech stream, measured with MEG. Unlike previous studies, the Ding et al. (2016) paradigm permits an unambiguous separation of linguistic and acoustic cues; and further, permits the comparison of intelligibility effects on neural responses associated with distinct timescales (syllable, phrase and sentence) in connected speech. A parametric reduction in speech intelligibility was achieved using noise-vocoding (Shannon et al., 1995), which progressively reduces the amount of spectral detail

present in the speech signal (i.e. the number of frequency channels used in the vocoding) while closely preserving the temporal envelope.

2 Materials & Methods

2.1 Participants

Experiment participants were 19 native speakers of English aged between 18 to 38 years old (mean 25 years old; 12 female) with normal hearing and no history of neurological, psychiatric, or developmental disorders (self-reported). All participants were right-handed and gave written informed consent under the process approved by the Human Subjects Ethics Committee of Macquarie University. As reimbursement for their participation, subjects received either course credits or payment.

2.2 Stimuli

All speech materials were synthesized using the MacinTalk text to speech synthesizer (male voice Alex, Mac OS X 10.11.4). In total, 180 four-syllable (a monosyllabic word for each syllable) English sentences were generated to form a sentence list (**Appendix 1**). All sentences in the list followed the same syntactic structure: adjective/pronoun + noun + verb + noun. Each syllable was synthesized independently, and all the synthesized syllables (200 – 376 ms in duration) were adjusted to 320 ms by padding silence at the end or truncation. The offset of each syllable was smoothed by a 25-ms cosine window. As the length of each syllable is different, these operations do not introduce any prosodic cues.

From the 180 sentences in the total pool, 60 (first set) were randomly selected to be presented in the unprocessed form ("natural speech"). The same set of 60 sentences were used to generate "shuffled sentences." A second set of 60 sentences were randomly selected from the remaining

120 sentences for "16 channel noise vocoding", and the remaining set (third set) of 60 sentences were used for "8 channel noise vocoding".

Sentences were presented in a trial consisting of 12 sentences of the same type. From the sub pools of 60 sentences/condition, 12 sentences were randomly drawn from the pool of 60 for the first trial, another 12 randomly drawn from the remainder of 48, and so on to produce 5 trials of 12 sentences for each condition. This process was repeated six times to produce a total of 30 trials for each condition for the whole experiment. Over the 30 trials, each sentence was repeated six times. In each trial, 12 sentences were presented isochronously. The way of stimulus construction and presentation makes the noises vocoded speech much less intelligible than those natural speech being noise vocoded with same number of channels (Smith, Delgutte, & Oxenham, 2002; Ding et al., 2014).

In catch trials ("outlier" trial in the terminology from Ding et al., 2016), 3 consecutive words selected from a random position within a trial, were replaced by three random words to abolish any meaningful sentence structure. There were eight outlier trials for each condition.

 A schematic plot of the hierarchical linguistic structures embedded in the isochronously presented syllable streams is depicted in **Figure 1** below:

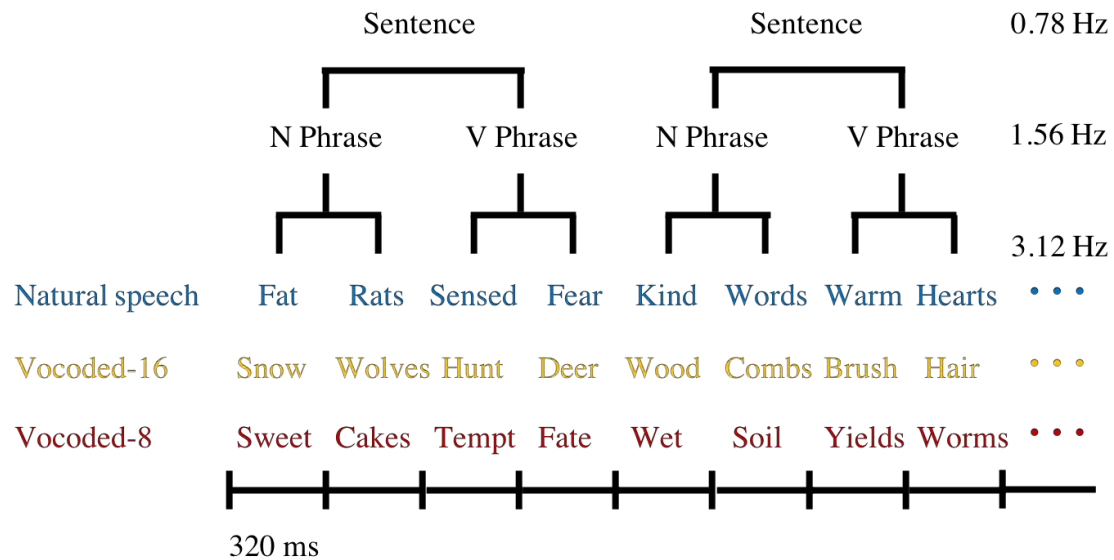|	Sentence				Sentence			0.78 Hz

Figure 6: Sequences of English monosyllabic words under different acoustic conditions were presented isochronously, forming phrases and sentences. N and V depict noun and verb, respectively.

2.2.1 Noise Vocoding

The remaining 120 four-syllable sentences from the sentence list were processed with noise vocoding to degrade intelligibility. Noise vocoding was performed using custom Matlab scripts (jessica.monaghan@mq.edu.au). The frequency range of 200 Hz to 22,050 Hz was divided into 16 or 8 logarithmically spaced channels using a 6th order Butterworth filter, the frequency span of each derived channel is shown in **Table 3**. Sixty randomly selected sentences were used to produce the 16-channel noise vocoded speech and the remaining sentences were used for the 8-channel noise vocoding. More spectral detail was preserved with higher number of frequency channels used in the vocoding. In each frequency channel, the envelope of the speech stimulus was extracted with full wave rectification and applying a low-pass filter below 300 Hz (2nd order Butterworth filter). This envelope was then used to amplitude modulate white noise filtered into the same frequency channel from which the envelope was extracted. These envelope-modulated noises were then recombined over frequency channels to yield the noise-vocoded speech segments. The root-mean-square (RMS) level of the noise-vocoded stimulus was normalized to match that of the original speech signal.

Table 3:Frequency range of individual channels derived in noise vocoding

Condition	Channel Number	Frequency Range (Hz)
16-Channel	1	100 - 234
	2	234 - 320
	3	320 - 438
	4	438 - 599
	5	599 - 820
	6	820 - 1122
	7	1122 - 1535
	8	1535 - 2100
	9	2100 - 2873
	10	2873 - 3931
	11	3931 - 5379
	12	5379 - 7359
	13	7359 - 10069
	14	10069 - 13777
	15	13777 - 18850
	16	18850 - 22040
8-Channel	1	100 - 280
	2	280 - 548
	3	548 - 1073
	4	1073 - 2100
	5	2100 - 4111
	6	4111 - 8049
	7	8049 - 15758
	8	15758 - 22040

2.2.2 Shuffled Speech

The same set of 60 four-syllable sentences used for the "natural speech" condition was employed again to produce shuffled sound streams as described in Ding et al. (2016). Each syllable in the original speech sentence was segmented into five overlapping slices of 72 ms in length and with 10 ms overlapping portions with neighbouring slices. The overlapped region for each slice was smoothed by a tapered cosine window, except for the first slice (onset) and the last slice (offset) for the sentence. As indicated by its name, a shuffled speech sentence was constructed by shuffling all slices at the same position across sentences so that the slices in a given sentence were all replaced by slices randomly chosen from different sentences at the corresponding position. In a shuffled speech trial, 12 different shuffled sentences were played sequentially and were the same length of the natural or noise-vocoded speech trials. In an outlier trial, four

consecutively shuffled syllables were replaced by four randomly chosen monosyllabic English

words from the sentence list of 60 that did not form a sentence (e.g. trim, fruit, tails, soap).

2.2.3 Stimulus Characterization

Acoustic properties of the speech stimuli used were characterized by the slow varying temporal

envelope which reflects the sound intensity fluctuations. The amplitude envelope for each

stimulus was extracted using half-wave rectification and the mean power spectrum shown in

Figure 7, was acquired by applying a Fast Fourier Transform (FFT) to individual amplitude

envelope and then averaging within each condition.
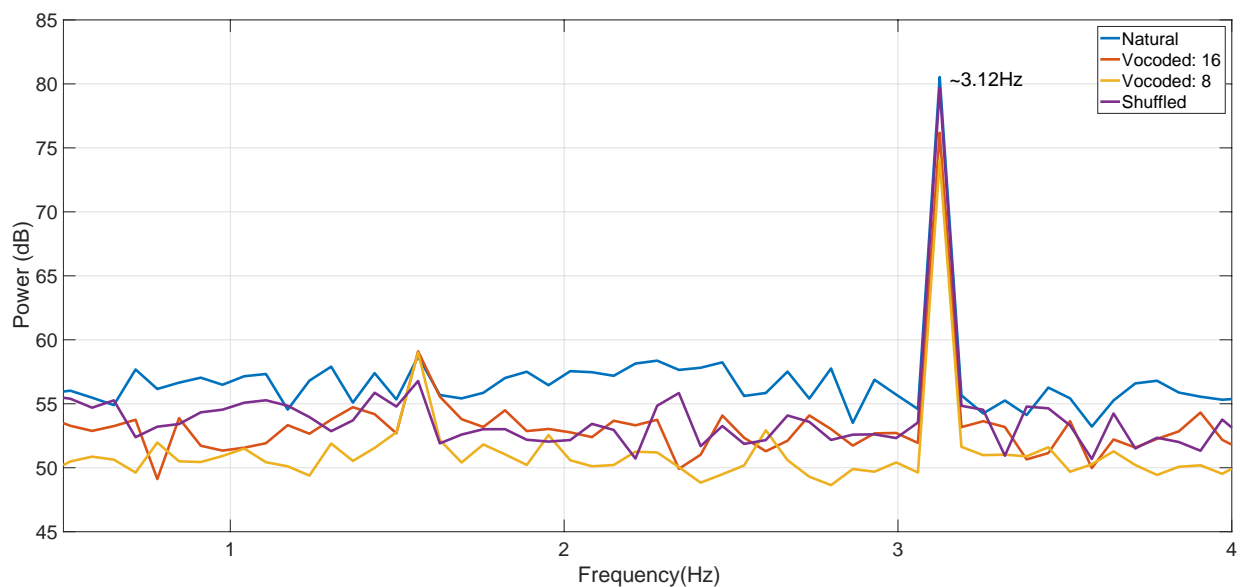
Figure 7: Power spectra of the different speech stimuli. Stimulus power was strongly modulated at word rate (~3.12 Hz) but not at phrase (~1.56 Hz) or sentence rates (~0.78 Hz) (see Figure 6).

2.3 Experimental Procedure

Example sentences from each condition were played to each participant prior to the experiment.

Natural four-syllable English sentences, noise vocoded four-syllable English sentences using 16

and 8 channels and shuffled sequences were presented in separate blocks at 75dB SPL using

insert earphones. The order to present all blocks was counterbalanced across participants.

Participants were instructed to fix their gaze on a frontal central cross projected to a ceiling

screen and indicate whether it was a normal trial or an outlier trial via button press at the end of each trial. The button press also initiates presentation of next trial with a randomized delay at either 1.2 s, 1.4s or 1.6 s. Each block had 22 normal trials and 8 outlier trials and the trials were presented in a random order.

2.4 MEG & MRI Data Acquisition

Prior to MEG recordings, marker coil positions and head shapes were measured with a pen digitizer (Polhemus Fastrack, Colchester, VT). Brain activities to speech streams under different intelligibility conditions were recorded continuously using the KIT-Macquarie MEG160 (Model PQ1160R-N2, KIT, Kanazawa, Japan), a whole-head MEG system consisting of 160 first-order axial gradiometers with a 50-mm baseline (Kado et al., 1999; Uehara et al., 2003). MEG data was acquired with the analog filter settings as 0.03 Hz high-pass, 200 Hz low-pass, power line noise pass through and A/D convertor settings as 1000 Hz sampling rate and 16-bit quantization precision. The measurements were carried out with participants in a supine position in a magnetically shielded room (Fujihara Co. Ltd., Tokyo, Japan). Marker coils positions were also measured before and after each recording block to quantify participants' head movement, the displacements were all below 5mm. The total duration of the experiment was about 45 minutes.

Magnetic resonance images (MRI) of the head were acquired for 19 participants at the Macquarie University Hospital, Sydney, using a 3 Tesla Siemens Magnetom Verio scanner with a 12-channel head coil. Images were acquired using an MP-RAGE sequence (208 axial slices, TR = 2000 ms, TE = 3.94 s, FOV = 240 mm, voxel size= 0.9 mm^3, TI = 900, flip angle = 9°).

2.5 Data Analysis

MEG data analysis was performed on normal trials only, using the opensource FieldTrip-20160515 toolbox (Oostenveld, Fries, Maris, & Schoffelen, 2011) and custom Matlab

(MathWorks) scripts. Offline MEG data were first filtered with a high-pass filter (0.1 Hz), a low-pass filters (30 Hz) and a notch filter (50 Hz, 100 Hz, 150 Hz) and then segmented into epochs according to trial definition. To avoid excessive stimulus-onset evoked responses, only the data between start of the second sentence (or the fifth syllable if the stimulus contained no sentential structure) and the end of each trial were analysed further. All data trials were down-sampled to 200 Hz prior to independent component analysis (ICA)(Makeig, Bell, Jung, & Sejnowski, 1996) to remove eye-blinks, eye-movements, heartbeat-related artefacts and magnetic jumps. Components corresponding to those artefacts were identified as by their spectral, topographical and time course characteristics. After ICA artefact rejection, all 22 normal trials of MEG data with an epoch length of 14.8-second were averaged in the time domain.

2.5.1 Sensor Level Analysis

Data analysis was carried out in the frequency domain to reveal brain activities tracking the different levels of linguistic units. Frequency spectra were calculated by applying FFT to the time-domain averaged MEG data (14.08 s) with a Hanning window, resulted in a frequency resolution of approximately 0.071 Hz.

A recent study by Zhang & Ding (2017) demonstrated that the tracking of hierarchical linguistic structures actually emerges at the beginning of the stimulus and are reflected by slow neural fluctuations, rather than a series of transient responses at boundaries (Zhang & Ding, 2017). Motivated by these time-domain characteristics, we also calculated the magnitude-squared coherences between the MEG recordings and a composite signal, which is comprised of sinewaves with zero initial phase and at frequencies correspond to the presentation rate of syllables/words, phrases and sentences respectively (**Figure 8**). The magnitude-squared coherence is a frequency-domain measure of phase consistency between two signals across multiple measurements, with a normalized value lies between 0 and 1 at distinct frequency

points. Therefore, phase relationship between these sinewaves in the composite signal can be arbitrary. All MEG data trials, as well as the composite signal, were segmented into short frames of 2.56-second in length and transformed into frequency domain via the FFT using a sliding Hanning window (50% overlap, 10 frames/trial, ~ 0.39Hz frequency resolution). Coherence was then calculated with the power spectral density at each MEG channel and the cross-spectral density between each MEG channel and the composite signal, estimated from the frequency transformed data frames.
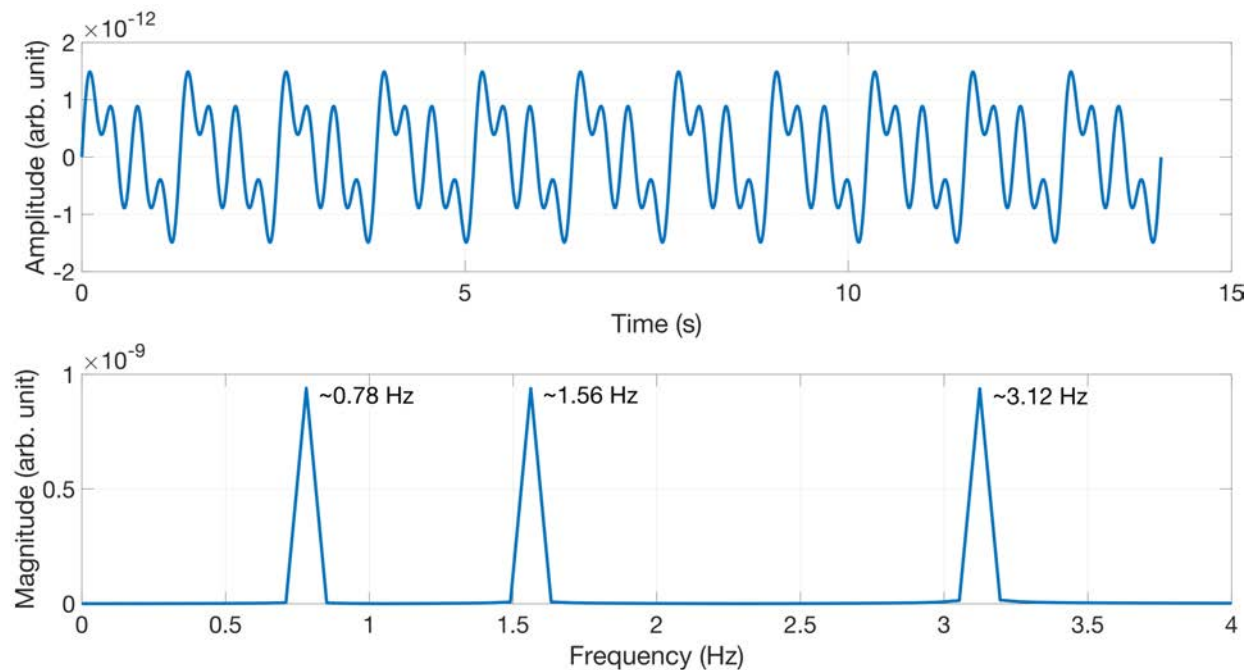
Figure 8: The composite signal used for coherence calculation. Top: time series of the composite signal with the duration equals to 11 short sentences. Bottom: Frequency domain representation of the composite signal exhibiting three distinct peaks at sentence rate (~0.78Hz), phrase rate (~1.56Hz) and syllable rate (~3.12Hz) respectively.

2.5.2 Source Level Analysis

To investigate the spatial distribution of cortical areas coherent to different levels of linguistic structure, we conducted a whole-brain beamforming analysis using Dynamic Imaging of Coherent Sources (DICS) (Gross et al., 2001) which is a frequency domain based linearly constrained minimum variance beamformer (Veen, Drongelen, Yuchtman, & Suzuki, 1997). Source models were constructed based on individual MRI for all participants. Cortical reconstruction (white-grey

matter boundary) and segmentation was performed with the Freesurfer image analysis suite (Fischl, 2012); http://surfer.nmr.mgh.harvard.edu/). Cortical mesh decimation (ld factor 10 resulting in 1002 vertices per hemisphere) and surface-based alignment was performed with SUMA - AFNI Surface Mapper (Saad & Reynolds, 2012). A single shell volume conduction model (Nolte, 2003) was adopted and the 2004 cortical surface vertices were used as MEG sources for the leadfield calculation. For more details of the source head modelling procedure, see (Li Hegner et al., 2018).

DICS was applied to the FFT transformed MEG data frames at the corresponding frequency of each linguistic unit across all intelligibility conditions, without trial rejection. Coefficients characterizing the beamformer were computed from the cross-spectral density matrix () and leadfield matrix at the dominant orientation. Source level coherence images were generated by calculating coherence values between neural activity at each vertex (source point) and the composite signal using the resulting beamformer coefficients. Random coherence images were generated as the average of 100 source space coherence values calculated using the same composite signal but were randomly shuffled at each time, similar to the implementation described in Peelle et al. (2013). Cortical level group analyses were performed using cluster-based permutation test to correct for multiple comparisons (Maris & Oostenveld, 2007) with a typical critical alpha value of 0.01 and 1000 random permutations. Each coherence image was contrasted with corresponding random coherence image to show its significance and the effect of speech intelligibility was evaluated by contrasting coherence images across experiment conditions.

3 Results

3.1 Behavioural results

Error rates and accuracies for the behavioural task (**orthogonal** design to ensure maintained vigilance) of the different experimental conditions are summarised in Table 2. Error rates/Accuracies were calculated by averaging the miss rate/hit rate for normal trials and the false alarm rate/hit rate for outlier trials under each intelligibility condition. Accuracy for the natural speech condition was significantly higher than that for the vocoded conditions (voc 16: p = 0.016, voc 8: p = 0.001) whereas the accuracy for the two vocoded conditions did not differ from each other (p = 0.96), assessed by paired two-sided t tests. As the experimental task for shuffled speech condition was different (detect consecutive monosyllabic English words embedded in shuffled syllable streams instead of detecting ungrammatical sentences), the behavioural performance was not statistically compared with the other conditions.

Table 2: Behavioural performance for all experimental conditions (upper: error rate mean $\pm$ SEM; lower: accuracy mean $\pm$ SEM)

Natural Speech	Vocoded Speech: 16	Vocoded Speech: 8	Shuffled Speech
36.8 $\pm$ 2.3%	45.6 $\pm$ 2.8%	45.7 $\pm$ 1.5%	18.3 $\pm$ 2.4%
63.2 $\pm$ 2.3%	54.4 $\pm$ 2.8%	54.3 $\pm$ 1.5%	81.7 $\pm$ 2.4%

3.2 Phase-Locked Responses to Hierarchical Linguistic Structures

Frequency response and coherence with the composite signal calculated under different intelligibility conditions were grand averaged across all participants as well as all MEG channels and plotted in **Figure** 9. Compared with the averaged power spectra of speech stimuli (**Figure 7**), it is evident that both frequency response and coherence plots show peaks corresponding to the phrase rate (~1.56 Hz), sentence rate (~0.78 Hz) and the syllable rate (~3.12 Hz). At the phrase and sentence levels, mean response magnitude and coherence both declined parametrically as

a function of decreasing speech intelligibility. In contrast, the mean syllable level response

magnitudes and coherence showed no systematic relationship to intelligibility levels.
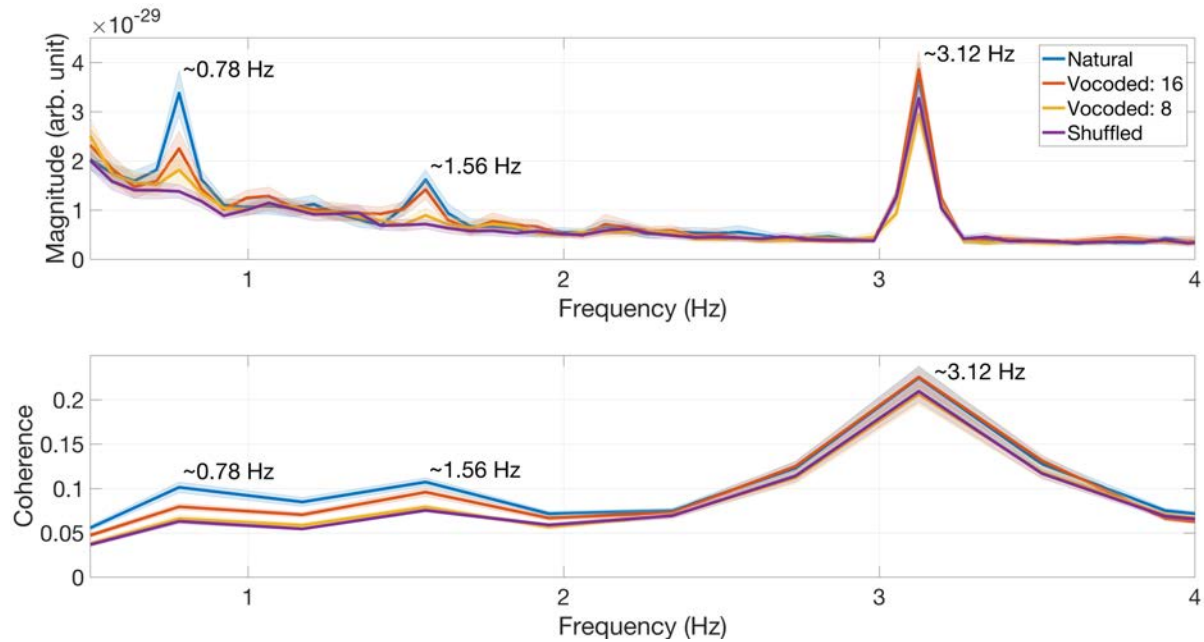

Figure 9: MEG tracking differs under different intelligibility conditions. Top: Averaged MEG sensor level frequency responses (160 channels)) exhibited different tracking activity to the hierarchical linguistic information (syllable, phrase and sentence). Bottom: Averaged MEG sensor level coherence between each MEG channel and the composite signal. The shaded area indicates 2 S.E.M.

3.3 Cortical Sources Coherent to Hierarchical Linguistic Structures

The DICS source localization results quantified as coherence values were overlaid on the cortical

mesh of each individual participant. For visualization purposes, source space results were grand

averaged and plotted on a common brain mesh generated using a template brain (an average of

40 brains and provided by FreeSurfer), segmented and processed following the same procedure

as described in the **Data Analysis** section.

Figure 10 shows grand mean source coherence results for each experimental condition and

linguistic unit. Compared to sensor level results, these source coherence values are smaller due

to the mapping from MEG sensors (160 channels) to cortical mesh (2004 vertices). Several

features are worth noting, prior to statistical analyses. First, mean coherence at the syllable level

was bilateral and similar in size, in both hemispheres, across all experimental conditions. Second,

mean coherence values at the phrase and sentence levels were larger in the left hemisphere, and

declined (in both hemispheres) as a function of decreasing intelligibility.
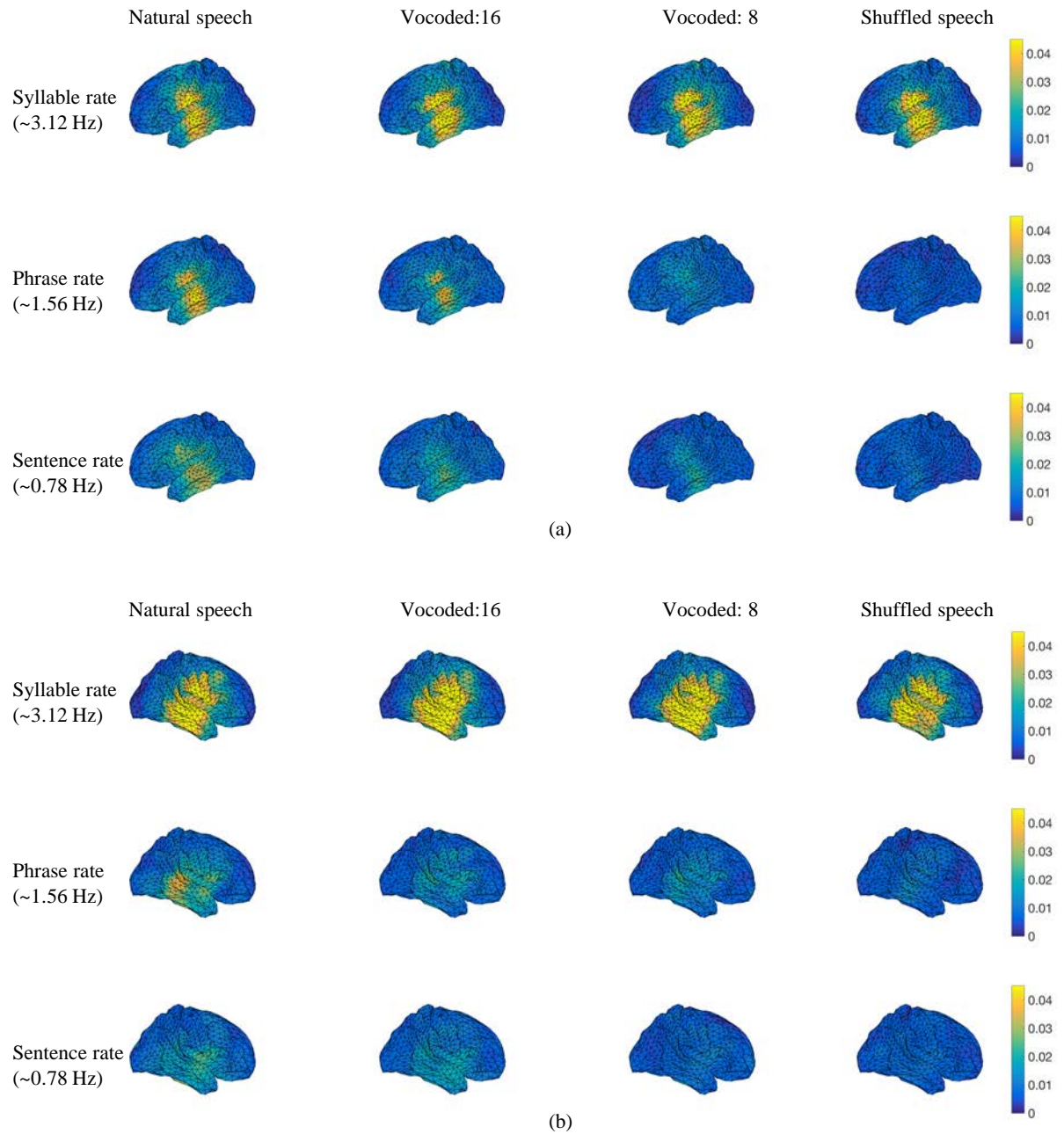
Figure 10: Source localization results grand averaged across all 19 participants and plotted on a template cortical mesh. (a): Left view of the grand averaged coherence values at frequencies corresponding to hierarchical linguistic structure and across all intelligibility conditions. (b): Right view of the grand averaged coherence values at frequencies corresponding to hierarchical linguistic structure and across all intelligibility conditions. Colour bars indicate coherence values.

3.2.1 Contrasts with random coherence

Whole-brain analyses contrasted coherence maps in each experimental condition against

"random" coherence maps (calculated using shuffled composite signals – see Methods section).

Results are shown in **Figure 11** using a sample-wise threshold of $p < 0.01$ and a $p < 0.01$ whole-brain cluster extent multiple comparison correction.

Figure 11: Contrasting source localized coherence tracking hierarchical linguistic structures under different intelligibility conditions with random coherence. (a) Cortical areas showing significant coherence under natural speech condition. (b) Cortical areas showing significant coherence under 16 channel vocoded speech condition. (c) Cortical areas showing significant coherence under 8 channel vocoded speech condition. (d) Cortical areas showing significant coherence under shuffled speech condition. Colour bars indicate t values without thresholding.

The results showed that natural speech elicited significant coherence in regions surrounding bilateral auditory cortices, for all three linguistic structures. Notably, there were no significant vertices at the phrase and sentence rates for the shuffled > random condition, as would be

expected since the shuffled condition was totally unintelligible and should therefore contain no information about phrase and sentence modulation. A third point to note is that the maps indicated greater coherence in the left hemisphere for the higher linguistic structures, especially at the lower intelligibility levels.

3.2.2 Contrasts against shuffled speech

The foregoing contrasts provided a picture of the overall extent to which our measured neuronal responses tracked each of the three rates in the composite signal. In the next step, we wished to isolate neuronal responses to the abstracted linguistic units (phrase and sentence units) with contrasts against shuffled speech (which purely retains the physical modulation at the syllable rate). In other words, the shuffled speech contrast allows us to remove the effect of any cues that are physically present in the speech stream.

As shown in **Figure 12**, significant clusters were found using a vertex-wise threshold of $p < 0.01$ and whole-brain cluster correction for multiple comparison at $p < 0.01$. No significant clusters were obtained for the syllable rate contrast (top row) or for the 8-channel contrast (not shown in the figure; presumably due to its low intelligibility). Notably, significant clusters for the sentence-level contrasts were restricted to the left hemisphere, as was the 16 channel phrase rate contrast.

Natural > Shuffled   16 ch > Shuffled

Syllable rate (~3.12 Hz)

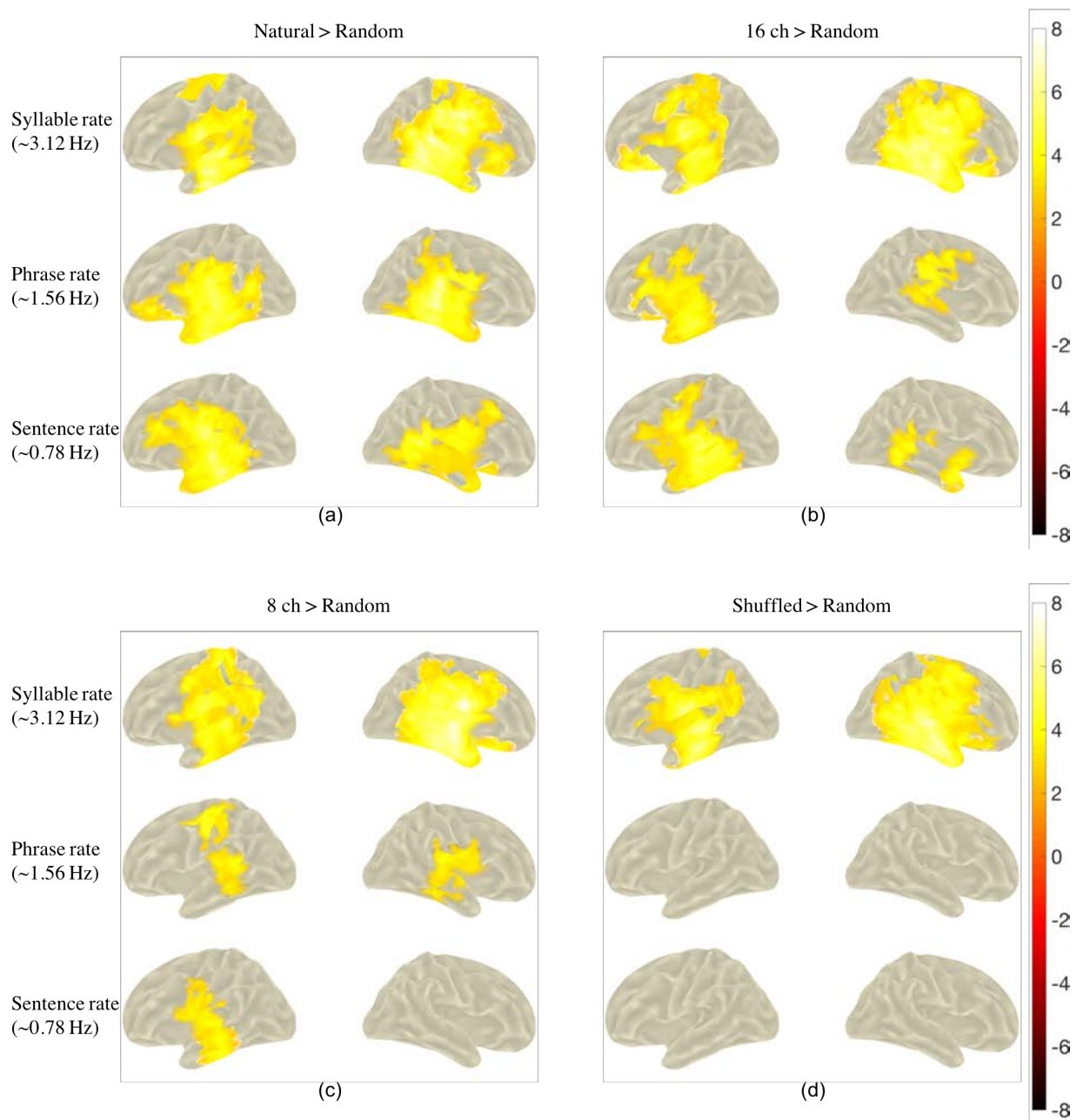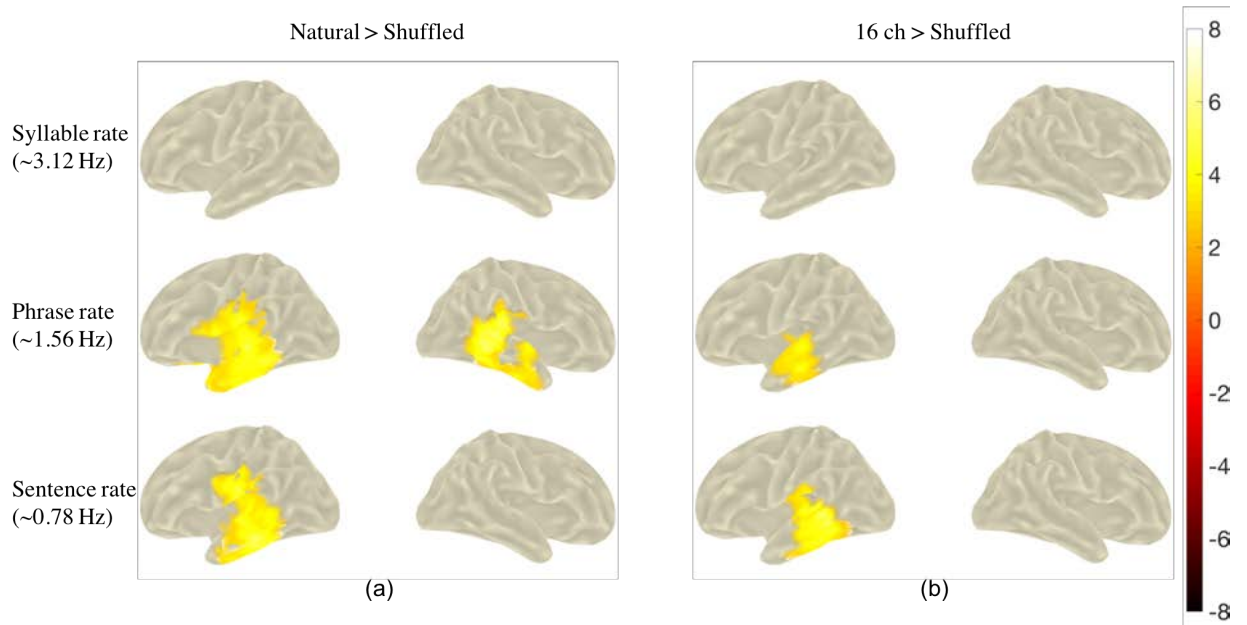Phrase rate (~1.56 Hz)

Sentence rate (~0.78 Hz)

(a)   (b)

Figure 12: Contrasting source localized coherence tracking hierarchical linguistic structures across different intelligibility conditions. (a) Cortical regions showing enhanced coherence under natural speech condition compared to the shuffled speech condition. (b) Cortical regions showing enhanced coherence under 16 channel vocoded speech condition compared to the shuffled speech condition. No significant clusters were found for the 8 channel vocoded speech condition. Colour bar indicates t values without thresholding.

4 Discussion

The results of this study replicated those of Ding et al. (2016) and confirmed that the human brain is sensitive to abstract linguistic structures that are unambiguously dissociated from any acoustic cues to these structures. To our knowledge, this is the first MEG replication of that study, although we note that the authors themselves have reported a replication using EEG measurements (Ding et al., 2017).

The novel contribution of the present study is to demonstrate that the MEG responses to abstract linguistic structures are sensitive to parametric manipulations of speech intelligibility. This sensitivity was manifest in the data as (1) reduced coherence of MEG responses to embedded linguistic structures (phrase and sentence rates) as a function of reduced intelligibility; and (2) coherent MEG responses to embedded linguistic structures became increasingly restricted to the

left cerebral hemisphere as a function of decreased intelligibility. This lateralisation is particularly apparent at the sentence level.

It is notable that intelligibility had little apparent effect on brain responses at the syllable level. The lack of effect on syllable level responses may be attributed to the fact that these are associated with responses evoked by the physical onsets of each syllable. The temporal envelope that reflects the energy fluctuation aligns with syllable rhythms in speech signals and were closely preserved across different intelligibility conditions with noise vocoding. This confound between acoustic and linguistic cues is inevitable in studies that employ naturalistic sentences for experimental stimuli (Zoefel & VanRullen, 2015). The results of the present experiment indicated that brain responses to mixed acoustic and linguistic cues may be largely driven by the acoustic cues and as such are relatively insensitive to manipulations of intelligibility. Such a lack of sensitivity make account for the mixed results reported in recent studies of cortical "entrainment" to the speech envelope (Ding et al., 2014; Ding & Simon, 2014; Howard & Poeppel, 2010; Millman et al., 2015; Peelle & Davis, 2012; Peelle et al., 2013; Zoefel & VanRullen, 2015). Importantly, and in contrast, our results indicated that unconfounded linguistic cues are clearly sensitive to intelligibility manipulations.

The lateralised results of our source analyses are striking. In his review of fMRI studies of speech comprehension, Peelle (Peelle, 2012) concluded that cortical lateralisation depends in a graded fashion on the level of acoustic and linguistic processing required. Processing related to non-speech signals (including amplitude modulated (AM) noise) is bilateral. As the requirements for linguistic analysis and integration increase (from AM sounds, through to phonemes, words, phrases and sentences), neural processing became increasingly left-lateralised. Our results are entirely consistent with these fMRI results.

The noise vocoding employed in the present study mimics the sound processing strategies employed by cochlear implant devices (Shannon et al., 2004). Achieving intelligible speech is the major objective of this intervention. As such, the present results, demonstrating that MEG brain responses are clearly sensitive to intelligibility manipulations are highly relevant to this application as they may potentially serve as highly useful and objective neural markers of speech perception in cochlear implant recipients.

5 Acknowledgements

We are grateful to Dr. Nai Ding for his helpful discussion during the design of this experiment, Mr. Craig Richardson and Dr. Jessica Monaghan for their help with speech material generation.

6 Author Contributions

Q.M., Y.L.H., I.G., C.M and B.J. conceived and designed the experiment. Q.M. performed the MEG experiments. QM, Y.L.H and B.J wrote the paper. All of the authors discussed the results and edited the manuscript.

References

Ahissar, E., Nagarajan, S., Ahissar, M., Protopapas, A., Mahncke, H., & Merzenich, M. M. (2001). Speech comprehension is correlated with temporal response patterns recorded from auditory cortex. *Proceedings of the National Academy of Sciences*, *98*(23), 13367–13372. https://doi.org/10.1073/pnas.201400998

Chandrasekaran, C., Trubanova, A., Stillittano, S., Caplier, A., & Ghazanfar, A. A. (2009). The Natural Statistics of Audiovisual Speech. *PLOS Computational Biology*, *5*(7), e1000436. https://doi.org/10.1371/journal.pcbi.1000436

Ding, N., Chatterjee, M., & Simon, J. Z. (2014). Robust cortical entrainment to the speech envelope relies on the spectro-temporal fine structure. *Neuroimage*, *88*, 41–46.

Ding, N., Melloni, L., Tian, X., & Poeppel, D. (2017). Rule-based and word-level statistics-based processing of language: insights from neuroscience. *Language, Cognition and Neuroscience*, *32*(5), 570–575. https://doi.org/10.1080/23273798.2016.1215477

Ding, N., Melloni, L., Zhang, H., Tian, X., & Poeppel, D. (2016). Cortical tracking of hierarchical linguistic structures in connected speech. *Nature Neuroscience*, *19*(1), 158. https://doi.org/10.1038/nn.4186

Ding, N., & Simon, J. Z. (2014). Cortical entrainment to continuous speech: functional roles and interpretations. *Frontiers in Human Neuroscience*, *8*. https://doi.org/10.3389/fnhum.2014.00311

Doelling, K. B., Arnal, L. H., Ghitza, O., & Poeppel, D. (2014). Acoustic landmarks drive delta– theta oscillations to enable speech comprehension by facilitating perceptual parsing. *NeuroImage*, *85*, 761–768. https://doi.org/10.1016/j.neuroimage.2013.06.035

Drullman, R., Festen, J. M., & Plomp, R. (1994). Effect of reducing slow temporal modulations on speech reception. *The Journal of the Acoustical Society of America*, *95*(5 Pt 1), 2670–2680.

Fischl, B. (2012). FreeSurfer. *NeuroImage*, *62*(2), 774–781. https://doi.org/10.1016/j.neuroimage.2012.01.021

Giraud, A.-L., & Poeppel, D. (2012). Cortical oscillations and speech processing: emerging computational principles and operations. *Nature Neuroscience*, *15*(4), 511–517.

Gross, J., Kujala, J., Hämäläinen, M., Timmermann, L., Schnitzler, A., & Salmelin, R. (2001). Dynamic imaging of coherent sources: Studying neural interactions in the human brain. *Proceedings of the National Academy of Sciences*, *98*(2), 694–699. https://doi.org/10.1073/pnas.98.2.694

Hegner, Y. L., Marquetand, J., Elshahabi, A., Klamer, S., Lerche, H., Braun, C., & Focke, N. K. (2018). Increased Functional MEG Connectivity as a Hallmark of MRI-Negative Focal and Generalized Epilepsy. *Brain Topography*, 1–12. https://doi.org/10.1007/s10548-018-0649-4

Hickok, G., & Poeppel, D. (2007). The cortical organization of speech processing. *Nature Reviews Neuroscience*, *8*(5), 393–402. https://doi.org/10.1038/nrn2113

Howard, M. F., & Poeppel, D. (2010). Discrimination of Speech Stimuli Based on Neuronal Response Phase Patterns Depends on Acoustics But Not Comprehension. *Journal of Neurophysiology*, *104*(5), 2500–2511. https://doi.org/10.1152/jn.00251.2010

Kado, H., Higuchi, M., Shimogawara, M., Haruta, Y., Adachi, Y., Kawai, J., … Uehara, G. (1999). Magnetoencephalogram systems developed at KIT. *IEEE Transactions on Applied Superconductivity*, *9*(2), 4057–4062. https://doi.org/10.1109/77.783918

Lakatos, P., Shah, A. S., Knuth, K. H., Ulbert, I., Karmos, G., & Schroeder, C. E. (2005). An Oscillatory Hierarchy Controlling Neuronal Excitability and Stimulus Processing in the Auditory Cortex. *Journal of Neurophysiology*, *94*(3), 1904–1911. https://doi.org/10.1152/jn.00263.2005

Luo, H., & Poeppel, D. (2007). Phase Patterns of Neuronal Responses Reliably Discriminate Speech in Human Auditory Cortex. *Neuron*, *54*(6), 1001–1010. https://doi.org/10.1016/j.neuron.2007.06.004

MacNeilage, P. F. (1998). The frame/content theory of evolution of speech production. *The Behavioral and Brain Sciences*, *21*(4), 499–511; discussion 511-546.

Makeig, S., Bell, A. J., Jung, T.-P., & Sejnowski, T. J. (1996). Independent Component Analysis of Electroencephalographic Data. In D. S. Touretzky, M. C. Mozer, & M. E. Hasselmo (Eds.), *Advances in Neural Information Processing Systems 8* (pp. 145–151). MIT Press. Retrieved from http://papers.nips.cc/paper/1091-independent-component-analysis-of-electroencephalographic-data.pdf

Maris, E., & Oostenveld, R. (2007). Nonparametric statistical testing of EEG- and MEG-data. *Journal of Neuroscience Methods*, *164*(1), 177–190. https://doi.org/10.1016/j.jneumeth.2007.03.024

Millman, R. E., Johnson, S. R., & Prendergast, G. (2015). The role of phase-locking to the temporal envelope of speech in auditory perception and speech intelligibility. *Journal of Cognitive Neuroscience*, *27*(3), 533–545. https://doi.org/10.1162/jocn_a_00719

Nolte, G. (2003). The magnetic lead field theorem in the quasi-static approximation and its use for magnetoencephalography forward calculation in realistic volume conductors. *Physics in Medicine and Biology*, *48*(22), 3637–3652.

Oostenveld, R., Fries, P., Maris, E., & Schoffelen, J.-M. (2011). FieldTrip: Open Source Software for Advanced Analysis of MEG, EEG, and Invasive Electrophysiological Data [Research article]. https://doi.org/10.1155/2011/156869

Peelle, J. E. (2012). The hemispheric lateralization of speech processing depends on what "speech" is: a hierarchical perspective. *Frontiers in Human Neuroscience*, *6*. https://doi.org/10.3389/fnhum.2012.00309

Peelle, J. E., & Davis, M. H. (2012). Neural Oscillations Carry Speech Rhythm through to Comprehension. *Frontiers in Psychology*, *3*. https://doi.org/10.3389/fpsyg.2012.00320

Peelle, J. E., Gross, J., & Davis, M. H. (2013). Phase-locked responses to speech in human auditory cortex are enhanced during comprehension. *Cerebral Cortex (New York, N.Y.: 1991)*, *23*(6), 1378–1387. https://doi.org/10.1093/cercor/bhs118

Rimmele, J. M., Zion Golumbic, E., Schröger, E., & Poeppel, D. (2015). The effects of selective attention and speech acoustics on neural speech-tracking in a multi-talker scene. *Cortex*, *68*, 144–154. https://doi.org/10.1016/j.cortex.2014.12.014

Saad, Z. S., & Reynolds, R. C. (2012). SUMA. *Neuroimage*, *62*(2), 768–773. https://doi.org/10.1016/j.neuroimage.2011.09.016

Shannon, R. V., Fu, Q.-J., Galvin, J., & Friesen, L. (2004). Speech Perception with Cochlear

> Implants. In *Cochlear Implants: Auditory Prostheses and Electric Hearing* (pp. 334–376).

> Springer, New York, NY. https://doi.org/10.1007/978-0-387-22585-2_8

Shannon, R. V., Zeng, F.-G., Kamath, V., Wygonski, J., & Ekelid, M. (1995). Speech Recognition

> with Primarily Temporal Cues. *Science*, *270*(5234), 303–304.

> https://doi.org/10.1126/science.270.5234.303

Uehara, G., Adachi, Y., Kawai, J., Shimogawara, M., Higuchi, M., Haruta, Y., … Kado, H. (2003).

> Multi-Channel SQUID Systems for Biomagnetic Measurement. *IEICE TRANSACTIONS on*

> *Electronics*, *E86-C*(1), 43–54.

Veen, B. D. V., Drongelen, W. V., Yuchtman, M., & Suzuki, A. (1997). Localization of brain

> electrical activity via linearly constrained minimum variance spatial filtering. *IEEE*

> *Transactions on Biomedical Engineering*, *44*(9), 867–880.

> https://doi.org/10.1109/10.623056

Zhang, W., & Ding, N. (2017). Time-domain analysis of neural tracking of hierarchical linguistic

> structures. *NeuroImage*, *146*, 333–340.

> https://doi.org/10.1016/j.neuroimage.2016.11.016

Zion Golumbic, E. M., Ding, N., Bickel, S., Lakatos, P., Schevon, C. A., McKhann, G. M., …

> Schroeder, C. E. (2013). Mechanisms Underlying Selective Neuronal Tracking of

> Attended Speech at a "Cocktail Party." *Neuron*, *77*(5), 980–991.

> https://doi.org/10.1016/j.neuron.2012.12.037

Zoefel, B., & VanRullen, R. (2015). The Role of High-Level Processes for Oscillatory Phase

    Entrainment to Speech Sound. *Frontiers in Human Neuroscience, 9*.

    https://doi.org/10.3389/fnhum.2015.00651

Appendix 1. Sentence stimuli

Fat rats sensed fear	Kind words warm hearts	Young kids close gates
Stacked shelves hold cans	Long fights cause hate	Flax threads hang plates
Big men drive trucks	Dead sharks spout blood	Their store sold jeeps
Bright flares shine light	Shrewd dogs dig holes	Wise cubs sip milk
Dry fur rubs skin	Lean girls like jeans	Four farms found cows
Sly fox stole eggs	Sick boys fail tests	Sharp knives cut cheese
Top chefs buy beef	Rear gates stop draughts	Soap suds cleanse toes
Our boss made deals	Firm palms make bread	Loud sounds scare moms
Two groups plant shrubs	Bad smells fill town	Weird clowns wear hats
All moms love kids	His aunt tied shoes	Her sons paint walls
New plans give hope	Quiet lambs graze grass	Giant bears walk trails
Large ants built nests	Soft forks spill rice	Drunk dudes sang tunes
Teen apes chase bugs	Tree frogs stalk flies	Small chicks catch grubs
Rude cats claw dogs	Black skies show stars	Brown bags take space
Rich cooks brew tea	Tall guys flee camp	Hot grills cook steaks
Fun games waste hours	Grey sheep seek hills	Big rocks clog roads

Pink toys please girls	Iced beer costs bucks	Storm floods ruin farms
Great waves wreck ships	Brave kings fight wars	Warm ground melts snow
Vain ears hear talk	Sore eyes shed tears	Keen blades slash tires
Close friends swap gifts	Harsh trails sprain joints	Posh wives pay bills
Horse hooves crush rocks	Mad dogs bite tails	Good shops pour drinks
Red lights stall cars	Fine gifts please hosts	Some pets climb trees
House maids scrub floors	Fierce flames sear steak	Snow limbs lift weights
Oil lamps start fires	Snow wolves hunt deer	Chrome tanks leak gas
Wood combs brush hair	Sheer noise hurts ears	Smart girls read books
Cold storms harm plants	John's wife bakes cakes	South lane leads home
Bowled balls strike pins	Blunt sticks smash glass	Parched fields need help
Three teams lost games	Smooth eggs hatch chicks	Steep hills slow bikes
Gas stoves heat pans	Cute birds build nests	Deep trust bonds friends
Cheap baits halt slugs	Sour food draws breath	Low planes dust crops
Weak sun heats rooms	Tight fists knock doors	Cruel hooks catch fish
Bee stings prick arms	Rough walks tax legs	Thick fog blocks views
Straw hats stop sun	Chopped logs choke creeks	Fire doors seal smoke

Farm aids swing bats	Tough spades crack slabs	Bald men ride trains
Old pumps lack grease	Spare keys lock halls	Plump wool coats sheep
Stretched arms seize balls	Iron spoon knocked floor	Wall clocks tell time
Round box stores coins	Bank clerks scan files	Square nets grab prawns
Dried fruit tastes good	Deep breaths save life	Mild rain wets ground
Gold rings cause fights	Small hands knead dough	Slim hips twirl hoops
Shoe tread stops slips	Thin ice risks lives	Brick walls guard homes
Fried chips burn tongues	Dark nights veil owls	Dear friends send mail
Open sports draw crowds	North winds bring joy	Sweet cakes tempt fate
Tall trees lose leaves	Lost goats scale cliffs	Grown men miss youth
Cracked plates spoil food	Wild pines drop cones	Spiked pins pierce rags
Chilled sheets help sleep	Bored dads drink beer	Wet soil yields worms
Bleak seas hide crabs	Bar soap cleans paws	Flat screws fix lights
Back teeth hurt jaws	Cool rooms keep meat	Calm swells raise yachts
Huge bull jumps fence	Bus tours tire guests	Tight belts hold pants
Race cars dodge oil	White sand covers boats	Road bikes skip holes
King crabs eat shrimp	Clay mugs store pens	Short talks blow minds

Wine grapes have seeds	Aged trains use coal	Hedge plants block paths
Quick gales break kites	Hard falls hurt knees	Spring buds prize soil
Rose tea stains pots	Used bricks fill yards	Toy spoons stir cups
Hot baths treat flu	Green plants feed birds	Bush snakes kill mice
Axe strokes trim rope	Strong light fades cloth	Wide trucks move trash
Nice guys give seats	Silk scarves ease throats	Eight ducks cross fields
Brass clips grip notes	Blue pens write words	Long waits bore boys
Salt lakes ooze slime	Trust funds hoard wealth	Stiff brooms sweep stones
Fresh staff like work	Flight crews serve lunch	Steel whisks whip cream
Sun glare burns eyes	Clear tape seals splits	High racks hold coats

Chapter 4: Effect of Perceptual Experience on Cortical Responses to Embedded Linguistic Structure

Qingqing Meng[1,2,4]
Yiwen Li Hegner[1,2]
Iain Giblin[3,4]
Catherine McMahon[1,3,4,5]
Blake W Johnson[1,2,4]

[1]HEARing Co-operative Research Centre, Melbourne, Victoria, Australia
[2]Macquarie University, Department of Cognitive Science, Sydney, New South Wales, Australia
[3]Macquarie University, Department of Linguistics, Sydney, New South Wales, Australia
[4]ARC Centre of Excellence in Cognition and its Disorders, Macquarie University, Sydney, New South Wales, Australia
[5]Centre for Implementation of Hearing Research, Macquarie University, New South Wales, Australia

Abstract

Neural activity has been demonstrated to track different levels of linguistic structure in connected speech (syllables, phrases and sentences), dissociated from the physical properties of the acoustic signal. In the current study, we investigated the effect of prior perceptual experience on this cortical tracking activity. In eighteen normal hearing participants, magnetoencephalography (MEG) was used to measure brain response to natural speech followed by either matching (the same) or mismatching (different) unintelligible speech. Noise-vocoding was used to generate the spectrally-degraded unintelligible speech stimuli from the natural speech material. Driven by the immediate previous experience with acoustic and linguistic information, coherence of MEG recordings to sentence level structure with matching speech was enhanced compared to that of the mismatching speech and its cortical source was localized to the right temporal cortex. When the prior perceptual experience was reversed by presenting the unintelligible speech before the natural speech, no difference in coherence was observed between the matching and the mismatching speech on all levels of linguistic structures. Thus, physically identical speech signals could either be or not be intelligible depending on the prior perceptual experience. This further demonstrated that using implicit cortical tracking of linguistic structure could be an objective (while this tracking is dissociated from the acoustic features) and sensitive (while the degree of tracking reflects perceptual learning) neural index of assessing speech intelligibility.

Keywords: Perceptual experience, Brain imaging, Magnetoencephalography (MEG)

1 Introduction

Psychophysical studies have shown that the slowly varying temporal envelope of speech signal contains major acoustic cues that are important for speech intelligibility (Drullman, Festen, & Plomp, 1994; Shannon, Zeng, Kamath, Wygonski, & Ekelid, 1995; Smith, Delgutte, & Oxenham, 2002). Electrophysiological studies have shown that the auditory cortex track the dynamics of speech envelope, approximately at the syllabic rate (Ahissar et al., 2001; Ding & Simon, 2012; Kayser, Ince, Gross, & Kayser, 2015; Lakatos et al., 2005; Luo & Poeppel, 2007; Rimmele, Zion Golumbic, Schröger, & Poeppel, 2015). This neural tracking activity, often referred to as "cortical entrainment" has been proposed as a putative neural mechanism underlying speech intelligibility. However, this functional role remains controversial (Ding & Simon, 2014; Peelle & Davis, 2012; Zoefel & VanRullen, 2015). Some authors maintain that cortical synchronization with the low-frequency speech envelope actively constrains the transfer of information from sensory to higher-order brain regions and this synchronization with the speech envelope is essential for speech comprehension (Ding, Chatterjee, & Simon, 2014; Peelle, Gross, & Davis, 2013; Zion Golumbic et al., 2013). Others have argued that the role of phase-locking brain responses may be restricted to encoding acoustic cues at the syllabic rhythm in speech (Nourski et al., 2009; Howard & Poeppel, 2010; Doelling, Arnal, Ghitza, & Poeppel, 2014), and that the cortical responses are mainly driven by the physical properties of the acoustic input. Due to the concomitant changes in speech intelligibility and speech acoustics, there has been a continuing debate about whether the brain envelope-following response mainly reflects processing of acoustic or linguistic information in speech.

A rapid and reliable enhancement in comprehension of degraded speech can be achieved with prior exposure to an intact speech signal (Davis, Johnsrude, Hervais-Adelman, Taylor, & McGettigan, 2005). This perceptual "pop-out" effect has associated with neurophysiological

changes in several neuroimaging studies (Dehaene-Lambertz et al., 2005; Giraud et al., 2004; Liebenthal, Binder, Piorkowski, & Remez, 2003; Sohoglu, Peelle, Carlyon, & Davis, 2012), and a recent intracranial study has reported a rapid automatic change in cortical tuning of stimulus features induced by perceptual experience (Holdgraf et al., 2016). Counter to expectations, however, neither the intracranial study of Holdgraf et al. (2016) nor a recent MEG study found any significant effects of prior perceptual experience on brain responses phase-locked to the temporal envelope of speech (Holdgraf et al., 2016; Millman, Johnson, & Prendergast, 2015).

A recent MEG study has demonstrated that activity from the auditory cortex can track *abstract* linguistic structure embedded in connected speech (Ding, Melloni, Zhang, Tian, & Poeppel, 2016). When short sentences were presented in an isochronous manner, concurrent cortical tracking activity to syllable/word, phrase and sentence level linguistic structure was reported. Importantly, this neural tracking activity of larger linguistic structure at phrase and sentence level was unambiguously dissociated from the cortical encoding of acoustic cues because there were no features/boundaries in the speech signal. Ding et al. (2016) concluded that an internal, grammar-based internal construction process must have been responsible for neural tracking of phrase and sentence structures independently of any acoustic features (Ding et al., 2016).

In the current study we adapted the experimental design of Ding et al. (2016) to investigate how prior perceptual experience would affect brain activity tracking hierarchical linguistic structure using magnetoencephalography (MEG). Compared with unintelligible speech with the same temporal envelope, previous studies have reported either enhanced cortical tracking to intelligible speech that contains more spectral detail (Ding et al., 2014; Peelle et al., 2013) or no difference for the entrainment to intelligible speech facilitated by perceptual experience (Holdgraf et al., 2016; Millman et al., 2015). We evaluated changes in brain response concurrently tracking three different levels of linguistic structure with different contextual information. Noise-

vocoding was used to render speech unintelligible while maintaining its temporal envelope (Shannon et al., 1995). Intelligibility of the degraded speech was manipulated by pre-exposing listeners to either matching or mismatching segments of intact speech.

2 Materials & Methods

2.1 Participants

18 native speakers of English aged between 18 to 39 years old (mean 26 years old; 13 females) participated in this experiment. All participants were right handed, with normal hearing and without any history of neurological, psychiatric, or developmental disorders (self-reported). Participants were either paid or received course credits for their participation and gave written informed consent under the process approved by the Human Subjects Ethics Committee of Macquarie University.

2.2 Stimuli

The speech materials were synthesized using the MacinTalk text to speech synthesizer (male voice Alex, Mac OS X 10.13.4). In total, 180 four-syllable (a monosyllabic word for each syllable) English sentences were generated to form a sentence list (**Appendix 1**). All sentences in the list followed the same syntactic structures: adjective/pronoun + noun + verb + noun. Each syllable was synthesized independently, and all the synthesized syllables (200 – 376 ms in duration) were adjusted to 320 ms by padding silence at the end or truncation. The offset of each syllable was smoothed by a 25-ms cosine window. 60 sentences were randomly selected to be presented without any further processing while the remaining 120 sentences were also processed with 8 channel noise vocoding to produce an unintelligible version of the sentence. The way of stimulus construction and presentation makes the noises vocoded speech much less intelligible than

natural speech being noise vocoded with same number of channels (Smith, Delgutte, & Oxenham, 2002; Ding et al., 2014).

2.2.1 Noise Vocoding

Noise vocoding was implemented using custom Matlab (MathWorks) scripts. The frequency range of 200Hz to 22,050Hz was divided into 8 logarithmically spaced channels (based on the task performance of a previous experiment, see Chapter 3) using a 6th order Butterworth filter. In each frequency channel, the envelope of the speech stimulus was extracted with full wave rectification and a low-pass filter at 300 Hz (2nd order Butterworth filter). This envelope was then used to amplitude-modulate white noise filtered into the same frequency band from which the envelope was extracted. These envelope-modulated noises were then recombined over frequency bands to yield the noise-vocoded speech segments. The root-mean-square (RMS) level of the noise-vocoded stimulus was normalized to match that of the original speech signal.

2.2.2 Experimental Conditions

In total, 12 short sentences (6 natural and 6 noise-vocoded) were presented without any acoustic gap between them in each trial. To avoid any potential artefact from the switching of acoustic conditions at the individual sentence level, every two sentences of the same acoustic condition were grouped together and arranged in a way which the acoustic condition alternates at the group level (2 sentences) within a trial (during presentation). The linguistic content between neighbouring groups could be either matching or mismatching and the relative position of the sentence groups of different acoustic conditions also varied. This produced four different experimental conditions in total. A schematic plot of the hierarchical linguistic structure embedded in the isochronously-presented syllable streams across all conditions is depicted in **Figure 13**. In an outlier trial, 4 consecutive words from a random position were replaced by four random words so that any meaningful sentence structure is abolished.
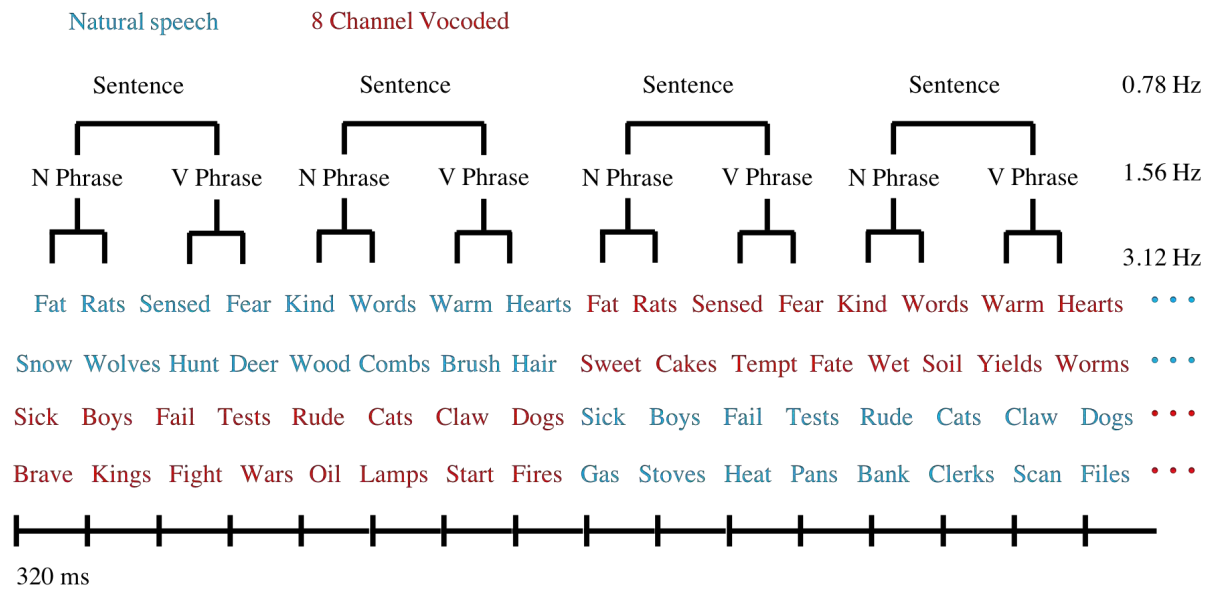
Figure 13: Sequences of monosyllabic English words were presented isochronously, forming hierarchically structured sentence pairs alternating between natural and vocoded acoustic conditions. Sentence pairs were followed by either the same two sentences or a different pair. N and V representt noun and verb, respectively. The four example text rows indicate the four different contextual conditions.

2.2.3 Stimulus Characterization

The slow varying temporal envelope which reflects sound intensity fluctuations of a speech signal largely determines its acoustic properties. To demonstrate the acoustic characteristics of our speech stimuli, we calculated the mean power spectrums of the temporal envelopes across all trials within each condition. The amplitude envelope of each individual trial was first extracted using a half-wave rectification and then frequency transformed with Fast Fourier Transform (FFT) before averaging. The mean power spectra are plotted in **Figure 14**, as the results show, there was only one common peak in the spectra at the frequency that corresponds to the onset rate of syllables/words (~ 3.12 Hz).
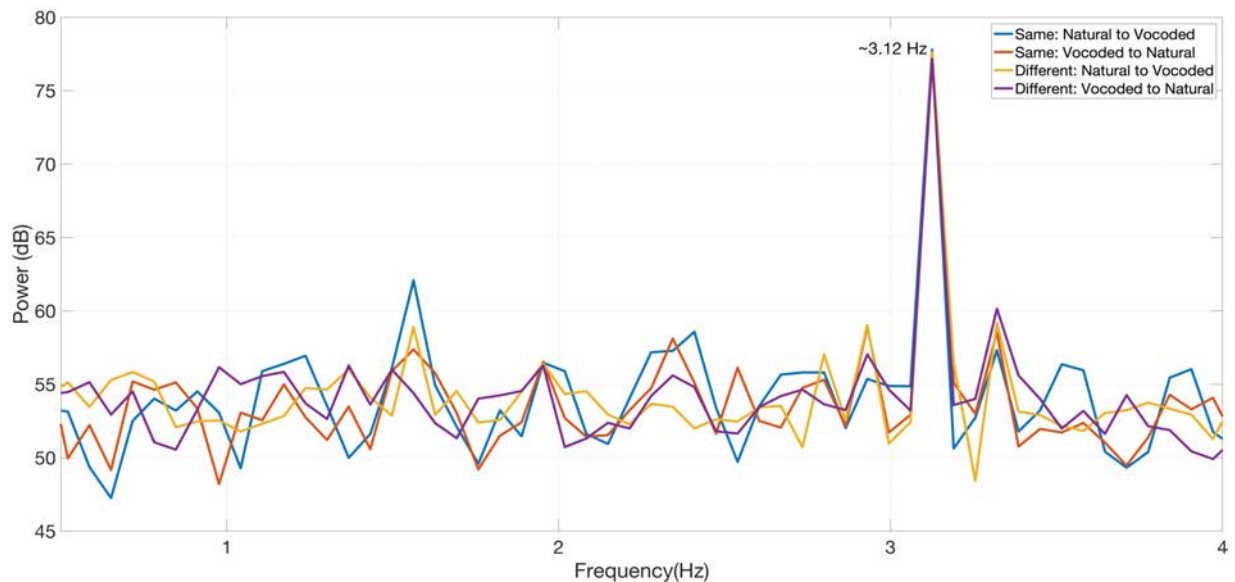
Figure 14: Mean power spectrum of the speech stimuli from different conditions. Stimulus power was strongly modulated at syllable/word rate (~3.12 Hz) but not at phrase (~1.56 Hz) or sentence rates (~0.78 Hz) (see Figure 6).

2.3 Experimental Procedure

Speech sentences were presented at 75dB SPL using a pair of insert earphones. A sample of sentences from each condition was played to the participants prior to the experiment to get them familiarised with the speech presentation style. Trials from all conditions were intermixed and evenly distributed into 4 experimental blocks with a short break assigned in between. Participants were instructed to indicate whether it was a normal trial or an outlier trial (i.e., there was at least one ungrammatical sentence they heard within the sentence stream) via button press at the end of each trial while they fixed their gaze on a frontal central cross that was projected to a ceiling screen. The button press also initiates presentation of next trial with a randomized delay at either 1.2 s, 1.4s or 1.6 s. Each block had 24 normal trials and 6 outlier trials and the trials within each block were presented in a random order. Only MEG recordings to normal trials were analysed. A technical error resulted in 2 normal trials from each condition incorrectly marked as outlier trials for one participant and one normal trial from a single condition (vocoded to natural, different sentences) was not recorded for another participant.

Analysis was carried out with 22 trials across all conditions and 23 trials for that particular condition for these two participants respectively.

2.4 MEG & MRI Data Collection

Prior to MEG recordings, marker coil positions and head shape were measured with a pen digitizer (Polhemus Fastrack, Colchester, VT). Brain activity to speech streams under different contextual conditions was recorded continuously using the KIT-Macquarie MEG160 (Model PQ1160R-N2, KIT, Kanazawa, Japan), a whole-head MEG system consisting of 160 first-order axial gradiometers with a 50-mm baseline (Kado et al., 1999; Uehara et al., 2003). MEG data was acquired with the analog filter settings as 0.03 Hz high-pass, 200 Hz low-pass, power line noise pass through and A/D convertor settings as 1000 Hz sampling rate and 16-bit quantization precision. The measurements were carried out with participants in a supine position in a magnetically shielded room (Fujihara Co. Ltd., Tokyo, Japan) and the total duration of the experiment was about 45 minutes.

Magnetic resonance images (MRI) of the head were acquired for all 18 participants at the Macquarie University Hospital, Sydney, using a 3 Tesla Siemens Magnetom Verio scanner with a 12-channel head coil. Images were acquired using an MP-RAGE sequence (208 axial slices, TR = 2000 ms, TE = 3.94 s, FOV = 240 mm, voxel size= 0.9 mm3, TI = 900, flip angle = 9°).

2.5 MEG Data Analysis

MEG data analysis was performed using the open-source FieldTrip-20160515 toolbox (Oostenveld, Fries, Maris, & Schoffelen, 2011) and custom Matlab scripts. Offline MEG data were first filtered with a high-pass filter (0.1Hz), a low-pass filter (30Hz) and a notch filter (50Hz, 100Hz, 150Hz) and then segmented into epochs according trial definition. To avoid excessive onset evoked responses, only the data between start of the second sentence and the end of each trial

were analysed further. All data trials were down-sampled to 200Hz prior to independent component analysis (Makeig, Bell, Jung, & Sejnowski, 1996) to remove eye-blinks, eye-movements, heartbeat-related artefacts and magnetic jumps. Components corresponding to those artefacts were identified as by their spectral, topographical and time course characteristics. After ICA artefact rejection, all 22 normal trials of MEG data with an epoch length of 14.8-second were averaged in the time domain.

2.5.1 Sensor Level Analysis

MEG data were analysed in the frequency domain to reveal brain activity tracking the hierarchical linguistic structure presented at multiple constant rates. After the time domain averaging, ICA-cleaned MEG data were smoothed by a Hanning window and transformed into frequency domain via the FFT (~ 0.071 Hz frequency resolution).

Motivated by a recent study from Zhang and Ding (Zhang & Ding, 2017) which demonstrated that neural tracking of hierarchical linguistic units emerges at the beginning of the stimulus onset in the form of slow fluctuations, we also calculated the magnitude-squared coherence between the MEG recordings and a slow varying composite signal. This composite signal as shown in **Figure 15** was generated as a linear superposition of 3 sinusoidal signals whose frequency corresponds to the presentation rate of syllables/words, phrases and sentences in our speech stimuli respectively and with zero initial phase. Magnitude-squared coherence or coherence is a frequency-domain measure of phase consistency between two signals across multiple measurements, with a normalized value lying between 0 and 1 at distinct frequency points. Therefore, phase relationship between these sinewaves in the composite signal can be arbitrary. By calculating the coherence between MEG recordings and this composite signal, the extent of neural tracking to hierarchical linguistic structure can then be quantified. MEG data after ICA artefact component rejection together with the composite signal introduced as an external

channel were segmented into short frames of 1.28-second in length and transformed into frequency domain via the FFT using a sliding Hanning window (50% overlap, 21 frames/trial, ~ 0.78 Hz frequency resolution). Coherences in MEG sensor space were then estimated across all frequency transformed data frames, using the power spectral density from each MEG channel and the cross-spectral density between each MEG channel and the composite signal.
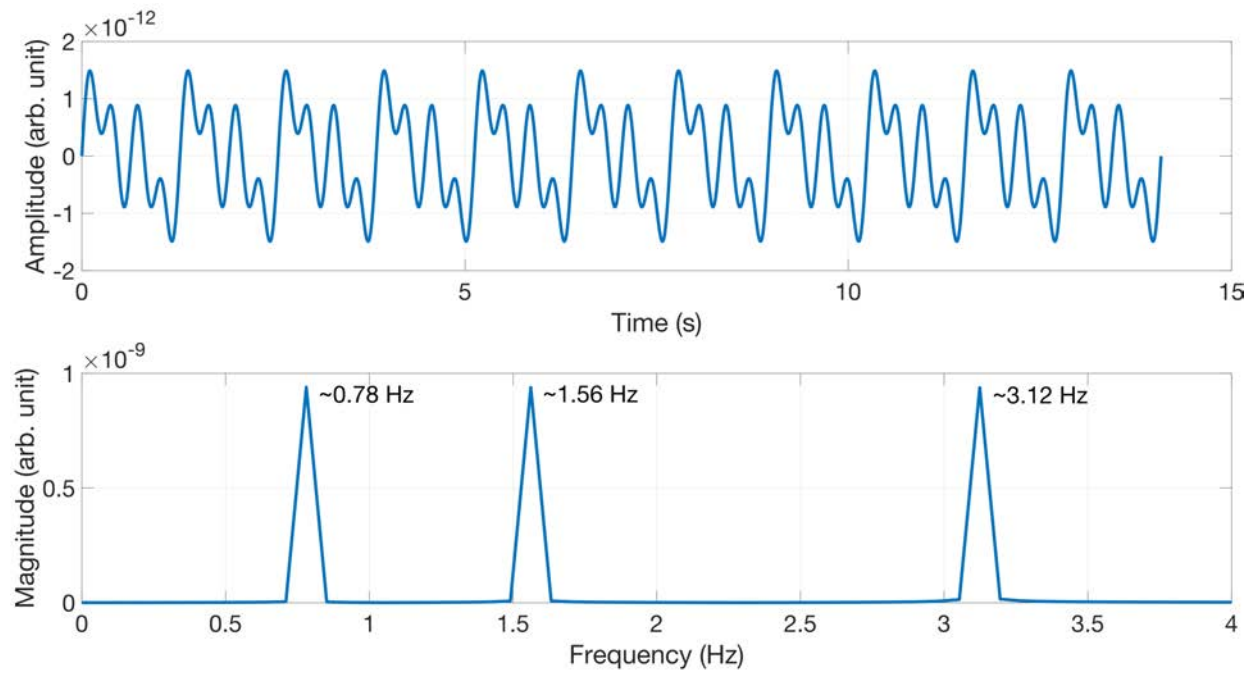

Figure 15: The composite signal used for coherence calculation. Top: time series of the composite signal with the length equals to 11 short sentences. Bottom: Frequency domain representation of the composite signal exhibiting three distinct peaks at sentence rate (~0.78Hz), phrase rate (~1.56Hz) and syllable rate (~3.12Hz) respectively.

2.5.2 Source Level Analysis

To source localize the cortical areas coherent to different levels of linguistic structure, we conducted a whole-brain beamforming analysis using Dynamic Imaging of Coherent Sources (DICS) (Gross et al., 2001), a frequency domain based linearly constrained minimum variance beamformer (Veen, Drongelen, Yuchtman, & Suzuki, 1997). For all participants source models were constructed based on their individual MRI scan obtained as described in the methods section. Cortical reconstruction (white-grey matter boundary) and segmentation was performed with the Freesurfer image analysis suite (Fischl, 2012), which is documented and freely available

for download online (http://surfer.nmr.mgh.harvard.edu/). Cortical mesh decimation (ld factor 10 resulting in 1002 vertices per hemisphere) and surface-based alignment was performed with SUMA - AFNI Surface Mapper (Saad & Reynolds, 2012), which is a program that adds cortical surface-based functional imaging analysis to the AFNI suite of programs. A single shell volume conduction model (Nolte, 2003) was adopted and the 2004 cortical surface vertices were used as MEG sources for the leadfield calculation. For more details of the source head modelling procedure, see (Li Hegner et al., 2018).

DICS was applied to the FFT-transformed MEG data frames used for sensor level analysis at the corresponding frequency of each linguistic unit across all conditions, without trial rejection. Coefficients characterizing the beamformer were computed from the cross-spectral density matrix and leadfield matrix at the dominant orientation. Source level coherence images were generated by calculating coherence values between neural activity at each vertex (source point) and the composite signal using the resulting beamformer coefficients. Source level coherence images were generated by calculating coherence between neural activity at each vertex (source point) and the composite signal. Random coherence image was produced by averaging source space coherence values calculated with the composite signal being randomly shuffled 100 times (Peelle et al., 2013). Cortical level group analyses were performed using cluster-based permutation test to correct for multiple comparisons (Maris & Oostenveld, 2007) with a typical critical alpha value of 0.05/0.01 and 1000 random permutations. Each coherence image was contrasted with the corresponding random coherence image to show its significance and the effect of immediate prior perceptual experience was evaluated by contrasting coherence images across contextual conditions.

3 Results

3.1 Behavioural Results

Error rates and accuracies for the behavioural task (**orthogonal** design to ensure maintained vigilance) are summarised in Table 4. Error rates/accuracies were calculated by averaging the miss rate/hit rate and the false alarm rate under each contextual condition. Error rates for matching (same) or mismatching (different) speech prior to noise vocoded speech were not significantly different (p =0.98, paired two-sided *t* test). In contrast, when vocoded speech was presented first, errors were significantly greater when the subsequent speech was different than when it was the same (p = 0.002), reflecting the greater difficulty of the "vocoded to natural & mismatching" condition.

Table 4:Behavioural performance for all experimental conditions (error rate mean $\pm$ SEM)

Natural to Vocoded (Same Speech)	Natural to Vocoded (Different Speech)	Vocoded to Natural (Same Speech)	Vocoded to Natural (Different Speech)
44.4 $\pm$ 3.1%	44.5 $\pm$ 1.9%	41.6 $\pm$ 2.3%	50.5 $\pm$ 1.7%
55.6 $\pm$ 3.1%	55.5 $\pm$ 1.9%	58.4 $\pm$ 2.3%	49.5 $\pm$ 1.7%

3.2 Phase-Locked Responses to Hierarchical Linguistic Structures

The frequency responses and coherences to the composite signal were calculated under each condition, averaged across all MEG channels and plotted in **Figure 16**. Both frequency response and coherence plots (not very evident under the coarse frequency resolution due to the short frame length) exhibited magnitude peaks at frequencies corresponding to the syllable rate (~3.12 Hz), phrase rate (~1.56 Hz) and sentence rate (~0.78 Hz).

The mean effect of prior perceptual experience was evident for sentence level responses: both the frequency and coherence plots showed larger mean magnitudes for the "natural to vocoded, same" condition than for any of the other conditions. Higher mean coherence was also seen for this condition at the phrase level.
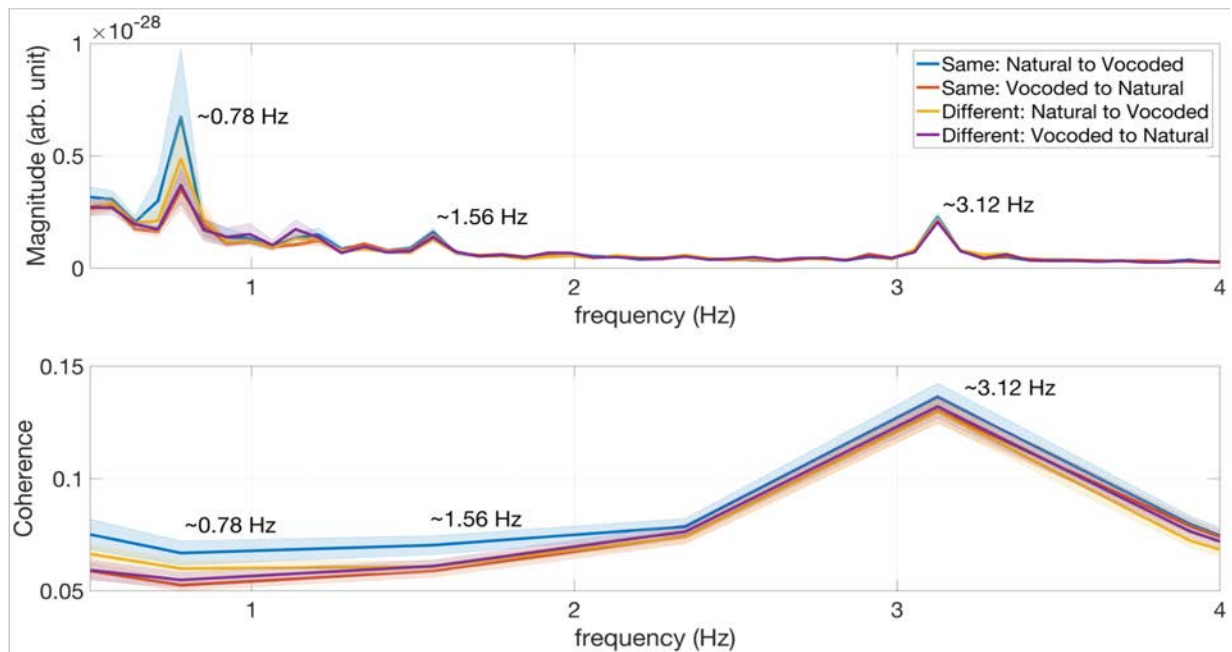
Figure 16: MEG tracking differs under different contextual conditions. Top: Averaged MEG sensor level frequency responses (160 channels)) exhibited different tracking activity to the hierarchical linguistic information (syllable, phrase and sentence). Bottom: Averaged MEG sensor level coherence between each MEG channel and the composite signal. The shaded area indicates 2 S.E.M.

3.3 Cortical Sources Coherent to Hierarchical Linguistic Structures

The DICS source localization results were quantified as coherence values and overlaid on the cortical mesh of each individual participant. For visualization purposes, source level results were grand-averaged and plotted on a common brain mesh generated using a template brain (an average of 40 brains and provided by FreeSurfer). This template brain was segmented and processed following the same procedure as described in the Data Analysis section.

Figure 17 shows grand mean source coherence results for each experimental condition and linguistic unit. Compared to sensor level results, these source coherence values are smaller due to the mapping from MEG sensors (160 channels) to cortical mesh (2004 vertices). Several features are worth noting in the grand means, prior to statistical analyses. First, mean coherence at the syllable level was bilateral and similar in magnitude, in both hemispheres, across all experimental conditions. Second, mean coherence was also relatively bilateral at the phrase and

sentence levels, but varied in magnitude across experimental conditions. At the sentence level

mean coherence was greatest for the "same: natural to vocoded condition".
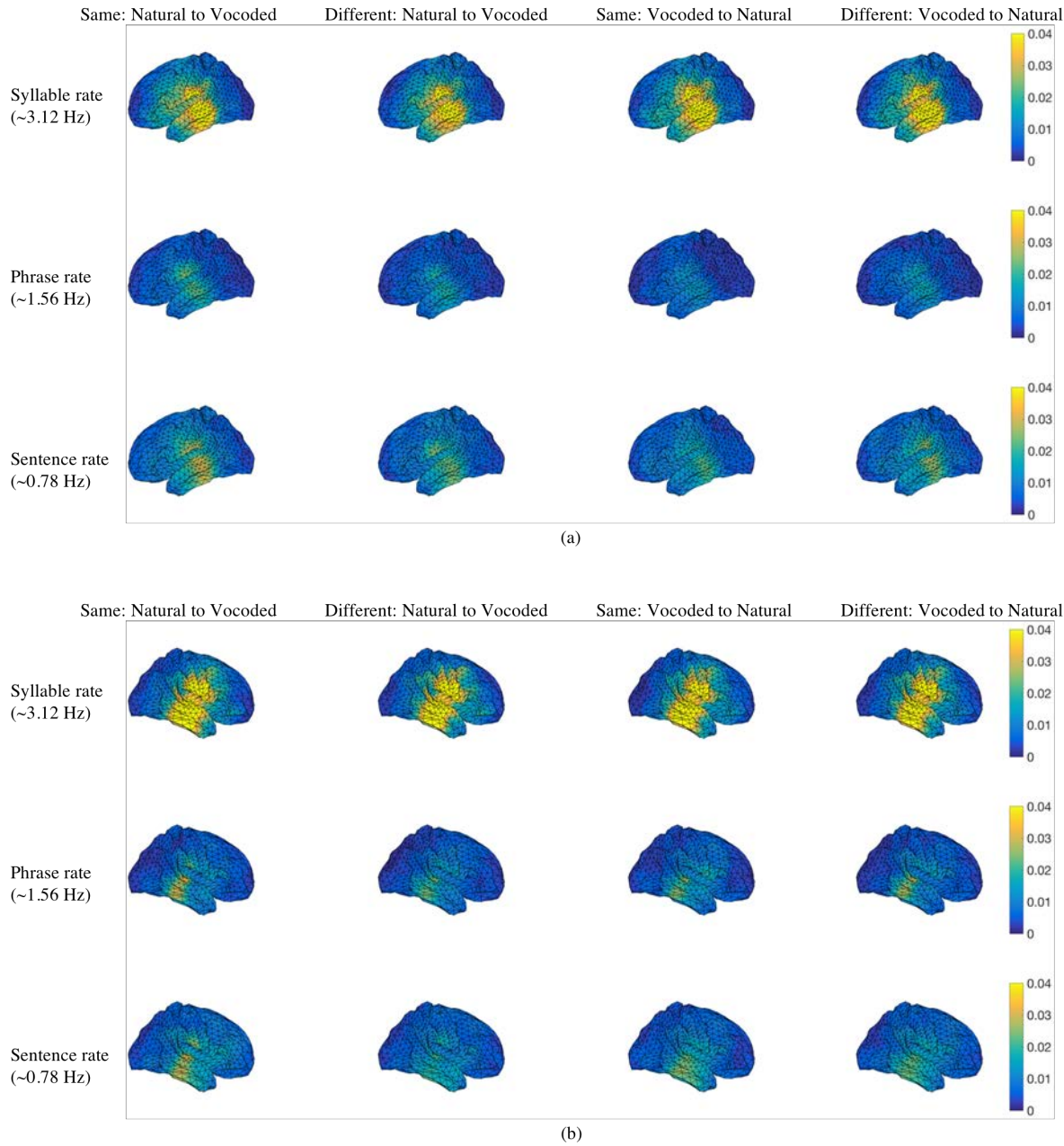

Figure 17: Grand-average of DICS source localization results across all 18 participants plotted on a template cortical mesh. (a): Left view of the grand averaged coherence values at frequencies corresponding to hierarchical linguistic structure and across all intelligibility conditions. (b): Right view of the grand averaged coherence values at frequencies corresponding to hierarchical linguistic structure and across all intelligibility conditions. Colour bars indicate coherence values.

3.3.1 Statistical mapping: Contrast with random composite signals

To test the significance of the cortical sources coherent to hierarchical embedded linguistic units

under different contextual conditions, we conducted a whole-brain analysis on the source

localized data to see whether these coherence values were significantly greater than that seen in the averaged random coherence calculated with randomly shuffled composite signals. Results are shown in **Figure 18** using one-tailed t tests with a sample-wise threshold of $p < 0.01$ and a whole-brain cluster extent threshold of $p < 0.01$ for the multiple comparison correction.
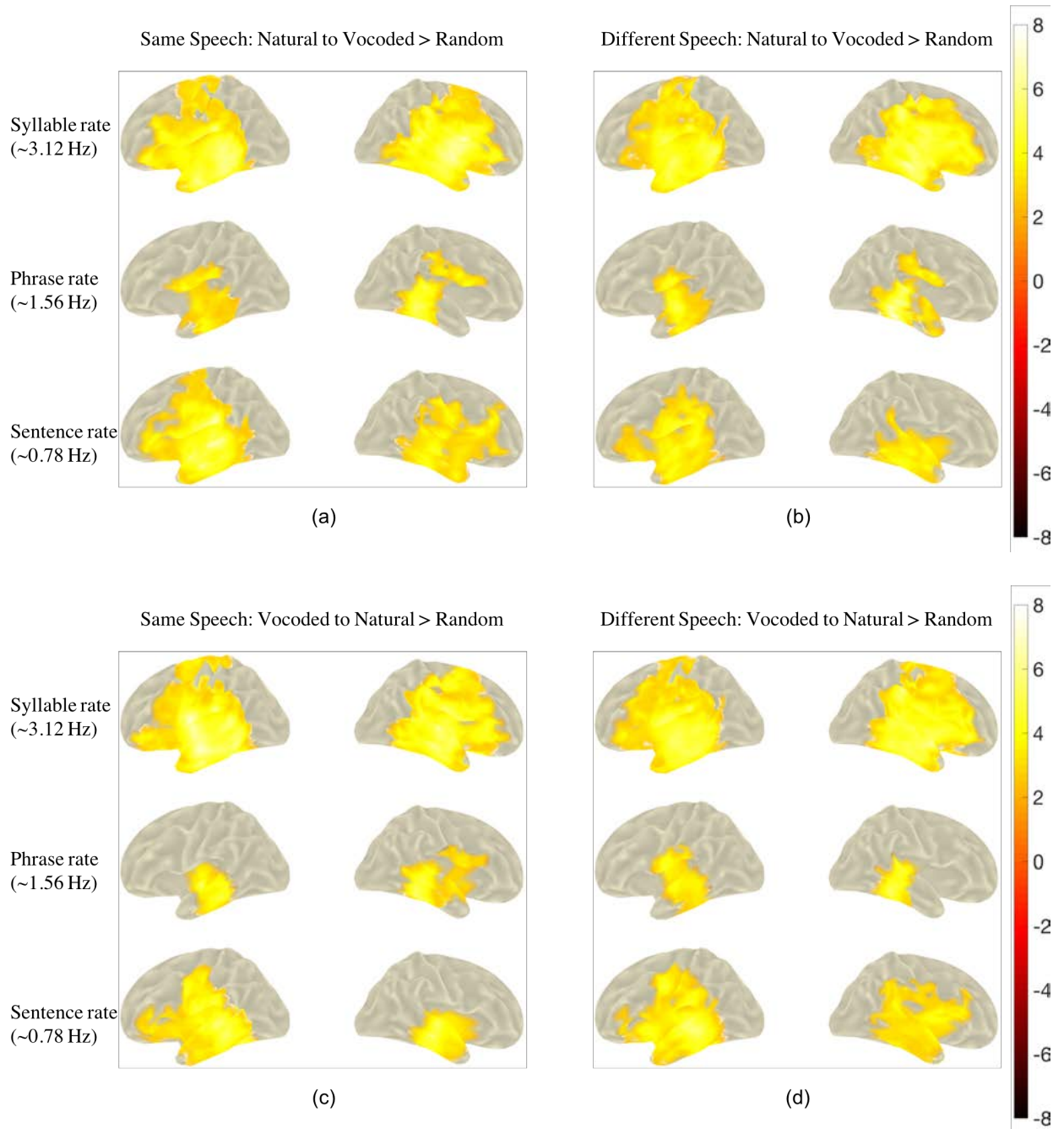

Figure 18: Contrasting source localized coherence tracking hierarchical linguistic structures under different contextual conditions with random coherence. (a) Same speech, natural speech presented prior to vocoded speech. (b) Different speech, natural speech presented prior to vocoded speech. (c) Same speech, vocoded speech presented prior to natural speech. (d) Different speech, vocoded speech presented prior to natural speech. colour bar indicates t values without thresholding.

The results showed significantly higher coherence to all levels of linguistic structure in bilateral peri-Sylvian cortices across all contextual conditions (relative to coherence to randomly shuffled composite signals).

3.3.2 Statistical mapping: Contrasts between experimental conditions

To examine the effect brought about by previous experience with the acoustic and linguistic information on cortical tracking activity, we conducted a whole-brain search for regions in which the coherence value was higher for the matching condition than the mismatching condition when the noise vocoded speech was presented either prior to or after the natural speech. As shown in **Figure 19**, a significant cluster was found when the matching noise vocoded speech was presented after natural speech using a vertex-wise threshold of $p < 0.05$ and whole-brain cluster extent correction for multiple comparison at $p < 0.05$. The enhancement in coherence compared to the mismatching condition was right hemisphere lateralized at the sentence level. No significant differences were found between the matching condition and mismatching condition when the noise vocoded speech was presented prior to the natural speech. Coherence values at syllable and phrase levels were not significantly different between matching and mismatching conditions in either order of presentation.
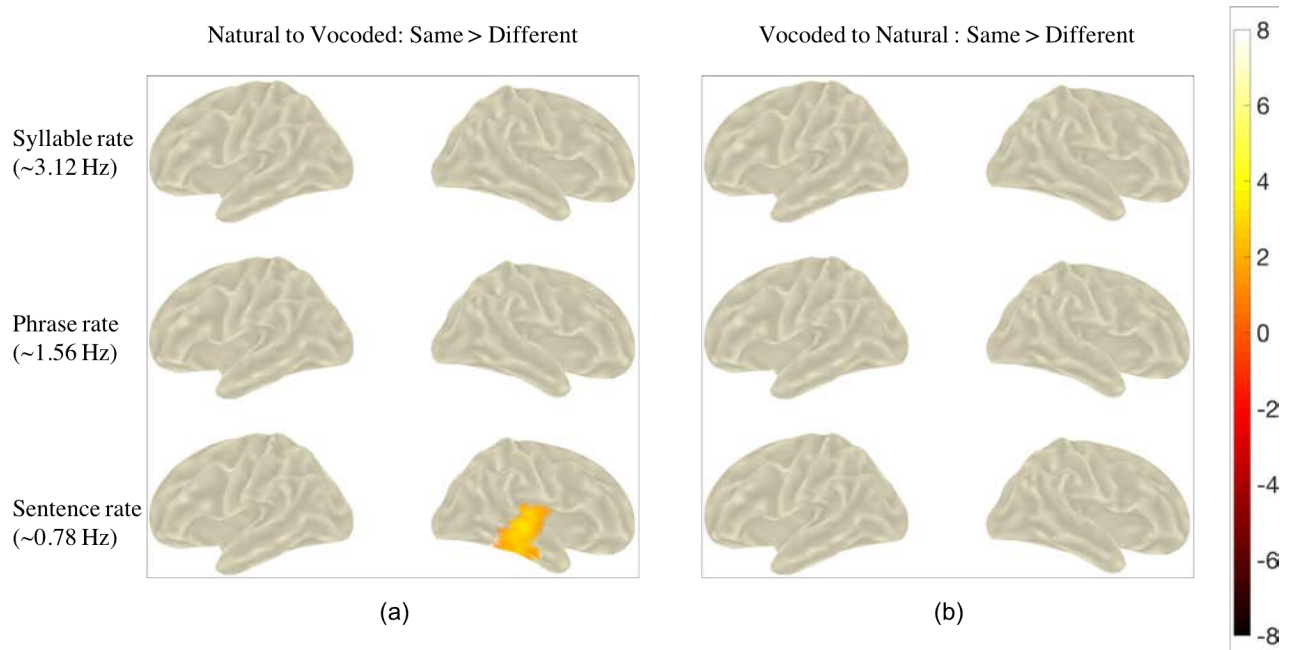
Figure 19: Contrasting source localized coherence tracking hierarchical linguistic structure across different contextual conditions. (a) Cortical regions showing enhanced coherence under natural speech condition compared to the shuffled speech condition. (b) Cortical regions showing enhanced coherence under 8 channel vocoded speech condition compared to the shuffled speech condition. colour bar indicates t values without thresholding.

4 Discussion

As shown in the ECoG study of Holdgraf et al. (Holdgraf et al., 2016), previous perceptual experience increases sensory sensitivity and enhances extraction of spectro-temporal features from degraded speech. The present results showed that when speech intelligibility was enhanced by perceptual experience with matching acoustic and linguistic information, a corresponding enhancement was obtained in MEG brain responses to linguistic structures in speech, an effect that was particularly evident for the sentence level structure. Statistical analyses at the source level revealed a region of greater coherence in the right temporal cortex to sentence level structure. When contextual information was abolished by presenting the noise-vocoded speech prior to the natural speech, no perceptual "pop-out" was achieved and there were also no differences in the corresponding MEG responses.

Our finding of no significant effect at the syllable level is consistent with the results of previous investigations of the perceptual "pop-out" effect (Millman et al., 2015), showing no effects on

the MEG phase-locking to the speech envelope (which reflects modulations at the syllable rate). As with the results of the previous Chapter 3, the lack of effect on the syllable-level responses is likely to be at least partly attributable to the fact that this response is driven largely by physical regularities present in the speech stream and is consequently less susceptible to top-down influences like that of prior experience.

The ubiquitous oscillatory neural activities in the brain have been argued to provide a potential brain mechanism deciphering perceived speech signal (Giraud & Poeppel, 2012; Hickok & Poeppel, 2007). Many neuroimaging studies examined the low frequency entrainment to slow varying speech envelope in auditory cortex, as the putative brain process segregating linguistic units at syllable scale, however results have been controversial (Ding & Simon, 2014; Peelle & Davis, 2012; Zoefel & VanRullen, 2015). The neural response to hierarchical linguistic structures (Ding et al., 2016) provides a plausible mechanism for information integration over time (Buzsáki, 2010; Schroeder, Lakatos, Kajikawa, Partan, & Puce, 2008) and facilitation of structure building operations (Bastiaansen, Magyari, & Hagoort, 2009) via coupling with higher frequency neural oscillations (Canolty et al., 2006; Lakatos et al., 2005; Sirota, Csicsvari, Buhl, & Buzsáki, 2003). Therefore, examining this hierarchy of neural processing may provide insights into the delineating process of those controversial results from speech envelope tracking measurement, e.g. the perceptual "pop-out" effect facilitated by prior experience and top-down integration.

Our statistical maps indicated that the experience-dependent enhancement of the tracking of sentence-level responses is associated with activity in the right cerebral hemisphere. This result is in contrast to those of previous neuroimaging studies of the perceptual "pop-out" phenomenon (Dehaene-Lambertz et al., 2005; Liebenthal et al., 2003; Millman et al., 2015; Sohoglu et al., 2012; Liberto, Crosse, & Lalor, 2018; Di Liberto, Lalor, & Millman, 2018) which have reported left hemisphere activation (Dehaene-Lambertz et al., 2005; Sohoglu et al., 2012;

Di Liberto et al., 2018), bilateral activation (Liebenthal, Binder, Piorkowski, & Remez, 2003), or no effect (Millman et al., 2015; Liberto et al., 2018). However, one fMRI study (Giraud et al., 2004) did report right hemisphere activation (right anterior superior temporal sulcus) when participants listened to noise vocoded sentences (without comprehension), and again after training (with comprehension).

The issue of hemispheric specialisations for speech analysis is complex (Poeppel, Emmorey, Hickok, & Pylkkänen, 2012, p. 201). However, the role of the right hemisphere in perceptual enhancement by prior experience is consistent with the model proposed by Zatorre (Zatorre, 1997) in which the left hemisphere is specialised for temporal processing while the right hemisphere is specialised for spectral processing (see also Poeppel, 2003 for a complementary model conceptualised in the time domain). Ding and colleagues (Ding et al., 2014) reported that spectral detail (not just the temporal envelope) is necessary for a robust representation of speech, since cortical tracking of the speech envelope is severely impaired by noise vocoding.

Our finding that MEG responses reflect increased intelligibility induced by prior experience have clear implications for biomedical applications including cochlear implants, since achieving intelligibility of speech is the major objective of such interventions. Our results suggest that MEG speech tracking responses can serve as a useful and objective neural marker of speech perception and speech intelligibility in cochlear implant recipients.

5 Acknowledgements

6. Author Contributions

Q.M., Y.L.H., I.G., C.M and B.J. conceived and designed the experiment. Q.M. performed the MEG experiments. QM, Y.L.H and B.J wrote the paper. All of the authors discussed the results and edited the manuscript.

References

Ahissar, E., Nagarajan, S., Ahissar, M., Protopapas, A., Mahncke, H., & Merzenich, M. M. (2001).
Speech comprehension is correlated with temporal response patterns recorded from
auditory cortex. *Proceedings of the National Academy of Sciences*, *98*(23), 13367–13372.
https://doi.org/10.1073/pnas.201400998

Bastiaansen, M., Magyari, L., & Hagoort, P. (2009). Syntactic Unification Operations Are
Reflected in Oscillatory Dynamics during On-line Sentence Comprehension. *Journal of
Cognitive Neuroscience*, *22*(7), 1333–1347. https://doi.org/10.1162/jocn.2009.21283

Buzsáki, G. (2010). Neural Syntax: Cell Assemblies, Synapsembles, and Readers. *Neuron*, *68*(3),
362–385. https://doi.org/10.1016/j.neuron.2010.09.023

Canolty, R. T., Edwards, E., Dalal, S. S., Soltani, M., Nagarajan, S. S., Kirsch, H. E., … Knight, R. T.
(2006). High Gamma Power Is Phase-Locked to Theta Oscillations in Human Neocortex.
Science, *313*(5793), 1626–1628. https://doi.org/10.1126/science.1128115

Davis, M. H., Johnsrude, I. S., Hervais-Adelman, A., Taylor, K., & McGettigan, C. (2005). Lexical
information drives perceptual learning of distorted speech: evidence from the
comprehension of noise-vocoded sentences. *Journal of Experimental Psychology:
General*, *134*(2), 222.

Dehaene-Lambertz, G., Pallier, C., Serniclaes, W., Sprenger-Charolles, L., Jobert, A., & Dehaene,
S. (2005). Neural correlates of switching from auditory to speech perception.
NeuroImage, *24*(1), 21–33. https://doi.org/10.1016/j.neuroimage.2004.09.039

Di Liberto, G. M., Lalor, E. C., & Millman, R. E. (2018). Causal cortical dynamics of a predictive

enhancement of speech intelligibility. *NeuroImage*, *166*, 247–258.

https://doi.org/10.1016/j.neuroimage.2017.10.066

Ding, N., Chatterjee, M., & Simon, J. Z. (2014). Robust cortical entrainment to the speech

envelope relies on the spectro-temporal fine structure. *Neuroimage*, *88*, 41–46.

Ding, N., Melloni, L., Zhang, H., Tian, X., & Poeppel, D. (2016). Cortical tracking of hierarchical

linguistic structures in connected speech. *Nature Neuroscience*, *19*(1), 158.

https://doi.org/10.1038/nn.4186

Ding, N., & Simon, J. Z. (2012). Emergence of neural encoding of auditory objects while listening

to competing speakers. *Proceedings of the National Academy of Sciences*, *109*(29),

11854–11859. https://doi.org/10.1073/pnas.1205381109

Ding, N., & Simon, J. Z. (2014). Cortical entrainment to continuous speech: functional roles and

interpretations. *Frontiers in Human Neuroscience*, *8*.

https://doi.org/10.3389/fnhum.2014.00311

Doelling, K. B., Arnal, L. H., Ghitza, O., & Poeppel, D. (2014). Acoustic landmarks drive delta–

theta oscillations to enable speech comprehension by facilitating perceptual parsing.

NeuroImage, *85*, 761–768. https://doi.org/10.1016/j.neuroimage.2013.06.035

Drullman, R., Festen, J. M., & Plomp, R. (1994). Effect of reducing slow temporal modulations

on speech reception. *The Journal of the Acoustical Society of America*, *95*(5 Pt 1), 2670–

2680.

Fischl, B. (2012). FreeSurfer. *NeuroImage*, *62*(2), 774–781.

https://doi.org/10.1016/j.neuroimage.2012.01.021

Giraud, A. L., Kell, C., Thierfelder, C., Sterzer, P., Russ, M. O., Preibisch, C., & Kleinschmidt, A. (2004). Contributions of sensory input, auditory search and verbal comprehension to cortical activity during speech processing. *Cerebral Cortex (New York, N.Y.: 1991)*, *14*(3), 247–255.

Giraud, A.-L., & Poeppel, D. (2012). Cortical oscillations and speech processing: emerging computational principles and operations. *Nature Neuroscience*, *15*(4), 511–517.

Gross, J., Kujala, J., Hämäläinen, M., Timmermann, L., Schnitzler, A., & Salmelin, R. (2001). Dynamic imaging of coherent sources: Studying neural interactions in the human brain. *Proceedings of the National Academy of Sciences*, *98*(2), 694–699. https://doi.org/10.1073/pnas.98.2.694

Hickok, G., & Poeppel, D. (2007). The cortical organization of speech processing. *Nature Reviews Neuroscience*, *8*(5), 393–402. https://doi.org/10.1038/nrn2113

Holdgraf, C. R., Heer, W. de, Pasley, B., Rieger, J., Crone, N., Lin, J. J., … Theunissen, F. E. (2016). Rapid tuning shifts in human auditory cortex enhance speech intelligibility. *Nature Communications*, *7*, 13654. https://doi.org/10.1038/ncomms13654

Howard, M. F., & Poeppel, D. (2010). Discrimination of Speech Stimuli Based on Neuronal Response Phase Patterns Depends on Acoustics But Not Comprehension. *Journal of Neurophysiology*, *104*(5), 2500–2511. https://doi.org/10.1152/jn.00251.2010

Kado, H., Higuchi, M., Shimogawara, M., Haruta, Y., Adachi, Y., Kawai, J., … Uehara, G. (1999). Magnetoencephalogram systems developed at KIT. *IEEE Transactions on Applied Superconductivity*, *9*(2), 4057–4062. https://doi.org/10.1109/77.783918

Kayser, S. J., Ince, R. A. A., Gross, J., & Kayser, C. (2015). Irregular Speech Rate Dissociates

    Auditory Cortical Entrainment, Evoked Responses, and Frontal Alpha. *Journal of*

    Neuroscience, *35*(44), 14691–14701. https://doi.org/10.1523/JNEUROSCI.2243-15.2015

Lakatos, P., Shah, A. S., Knuth, K. H., Ulbert, I., Karmos, G., & Schroeder, C. E. (2005). An

    Oscillatory Hierarchy Controlling Neuronal Excitability and Stimulus Processing in the

    Auditory Cortex. *Journal of Neurophysiology*, *94*(3), 1904–1911.

    https://doi.org/10.1152/jn.00263.2005

Li Hegner, Y., Marquetand, J., Elshahabi, A., Klamer, S., Lerche, H., Braun, C., & Focke, N. K.

    (2018). Increased Functional MEG Connectivity as a Hallmark of MRI-Negative Focal and

    Generalized Epilepsy. *Brain Topography*, 1–12. https://doi.org/10.1007/s10548-018-

    0649-4

Liberto, G. M. D., Crosse, M. J., & Lalor, E. C. (2018). Cortical Measures of Phoneme-Level

    Speech Encoding Correlate with the Perceived Clarity of Natural Speech. *ENeuro*,

    ENEURO.0084-18.2018. https://doi.org/10.1523/ENEURO.0084-18.2018

Liebenthal, E., Binder, J. R., Piorkowski, R. L., & Remez, R. E. (2003). Short-Term Reorganization

    of Auditory Analysis Induced by Phonetic Experience. *Journal of Cognitive Neuroscience*,

    15(4), 549–558. https://doi.org/10.1162/089892903321662930

Luo, H., & Poeppel, D. (2007). Phase Patterns of Neuronal Responses Reliably Discriminate

    Speech in Human Auditory Cortex. *Neuron*, *54*(6), 1001–1010.

    https://doi.org/10.1016/j.neuron.2007.06.004

Makeig, S., Bell, A. J., Jung, T.-P., & Sejnowski, T. J. (1996). Independent Component Analysis of

    Electroencephalographic Data. In D. S. Touretzky, M. C. Mozer, & M. E. Hasselmo (Eds.),

Advances in Neural Information Processing Systems 8 (pp. 145–151). MIT Press.

Retrieved from http://papers.nips.cc/paper/1091-independent-component-analysis-of-

electroencephalographic-data.pdf

Maris, E., & Oostenveld, R. (2007). Nonparametric statistical testing of EEG- and MEG-data.

Journal of Neuroscience Methods, *164*(1), 177–190.

https://doi.org/10.1016/j.jneumeth.2007.03.024

Millman, R. E., Johnson, S. R., & Prendergast, G. (2015). The role of phase-locking to the

temporal envelope of speech in auditory perception and speech intelligibility. *Journal of*

Cognitive Neuroscience, *27*(3), 533–545. https://doi.org/10.1162/jocn_a_00719

Nolte, G. (2003). The magnetic lead field theorem in the quasi-static approximation and its use

for magnetoencephalography forward calculation in realistic volume conductors.

Physics in Medicine and Biology, *48*(22), 3637–3652.

Nourski, K. V., Reale, R. A., Oya, H., Kawasaki, H., Kovach, C. K., Chen, H., … Brugge, J. F. (2009).

Temporal Envelope of Time-Compressed Speech Represented in the Human Auditory

Cortex. *Journal of Neuroscience*, *29*(49), 15564–15574.

https://doi.org/10.1523/JNEUROSCI.3065-09.2009

Oostenveld, R., Fries, P., Maris, E., & Schoffelen, J.-M. (2011). FieldTrip: Open Source Software

for Advanced Analysis of MEG, EEG, and Invasive Electrophysiological Data [Research

article]. https://doi.org/10.1155/2011/156869

Peelle, J. E., & Davis, M. H. (2012). Neural Oscillations Carry Speech Rhythm through to

Comprehension. *Frontiers in Psychology*, *3*. https://doi.org/10.3389/fpsyg.2012.00320

Peelle, J. E., Gross, J., & Davis, M. H. (2013). Phase-locked responses to speech in human auditory cortex are enhanced during comprehension. *Cerebral Cortex (New York, N.Y.: 1991), 23*(6), 1378–1387. https://doi.org/10.1093/cercor/bhs118

Rimmele, J. M., Zion Golumbic, E., Schröger, E., & Poeppel, D. (2015). The effects of selective attention and speech acoustics on neural speech-tracking in a multi-talker scene. *Cortex, 68*, 144–154. https://doi.org/10.1016/j.cortex.2014.12.014

Saad, Z. S., & Reynolds, R. C. (2012). SUMA. *Neuroimage, 62*(2), 768–773. https://doi.org/10.1016/j.neuroimage.2011.09.016

Schroeder, C. E., Lakatos, P., Kajikawa, Y., Partan, S., & Puce, A. (2008). Neuronal oscillations and visual amplification of speech. *Trends in Cognitive Sciences, 12*(3), 106–113. https://doi.org/10.1016/j.tics.2008.01.002

Shannon, R. V., Zeng, F.-G., Kamath, V., Wygonski, J., & Ekelid, M. (1995). Speech Recognition with Primarily Temporal Cues. *Science, 270*(5234), 303–304. https://doi.org/10.1126/science.270.5234.303

Sirota, A., Csicsvari, J., Buhl, D., & Buzsáki, G. (2003). Communication between neocortex and hippocampus during sleep in rodents. *Proceedings of the National Academy of Sciences, 100*(4), 2065–2069. https://doi.org/10.1073/pnas.0437938100

Smith, Z. M., Delgutte, B., & Oxenham, A. J. (2002). Chimaeric sounds reveal dichotomies in auditory perception. *Nature, 416*(6876), 87–90. https://doi.org/10.1038/416087a

Sohoglu, E., Peelle, J. E., Carlyon, R. P., & Davis, M. H. (2012). Predictive Top-Down Integration of Prior Knowledge during Speech Perception. *Journal of Neuroscience, 32*(25), 8443–8453. https://doi.org/10.1523/JNEUROSCI.5069-11.2012

Uehara, G., Adachi, Y., Kawai, J., Shimogawara, M., Higuchi, M., Haruta, Y., … Kado, H. (2003). Multi-Channel SQUID Systems for Biomagnetic Measurement. *IEICE TRANSACTIONS on Electronics*, *E86-C*(1), 43–54.

Veen, B. D. V., Drongelen, W. V., Yuchtman, M., & Suzuki, A. (1997). Localization of brain electrical activity via linearly constrained minimum variance spatial filtering. *IEEE Transactions on Biomedical Engineering*, *44*(9), 867–880. https://doi.org/10.1109/10.623056

Zhang, W., & Ding, N. (2017). Time-domain analysis of neural tracking of hierarchical linguistic structures. *NeuroImage*, *146*, 333–340. https://doi.org/10.1016/j.neuroimage.2016.11.016

Zion Golumbic, E. M., Ding, N., Bickel, S., Lakatos, P., Schevon, C. A., McKhann, G. M., … Schroeder, C. E. (2013). Mechanisms Underlying Selective Neuronal Tracking of Attended Speech at a "Cocktail Party." *Neuron*, *77*(5), 980–991. https://doi.org/10.1016/j.neuron.2012.12.037

Zoefel, B., & VanRullen, R. (2015). The Role of High-Level Processes for Oscillatory Phase Entrainment to Speech Sound. *Frontiers in Human Neuroscience*, *9*. https://doi.org/10.3389/fnhum.2015.00651

Appendix 1. Sentence stimuli

Fat rats sensed fear	Kind words warm hearts	Young kids close gates
Stacked shelves hold cans	Long fights cause hate	Flax threads hang plates
Big men drive trucks	Dead sharks spout blood	Their store sold jeeps
Bright flares shine light	Shrewd dogs dig holes	Wise cubs sip milk
Dry fur rubs skin	Lean girls like jeans	Four farms found cows
Sly fox stole eggs	Sick boys fail tests	Sharp knives cut cheese
Top chefs buy beef	Rear gates stop draughts	Soap suds cleanse toes
Our boss made deals	Firm palms make bread	Loud sounds scare moms
Two groups plant shrubs	Bad smells fill town	Weird clowns wear hats
All moms love kids	His aunt tied shoes	Her sons paint walls
New plans give hope	Quiet lambs graze grass	Giant bears walk trails
Large ants built nests	Soft forks spill rice	Drunk dudes sang tunes
Teen apes chase bugs	Tree frogs stalk flies	Small chicks catch grubs
Rude cats claw dogs	Black skies show stars	Brown bags take space
Rich cooks brew tea	Tall guys flee camp	Hot grills cook steaks
Fun games waste hours	Grey sheep seek hills	Big rocks clog roads

Pink toys please girls	Iced beer costs bucks	Storm floods ruin farms
Great waves wreck ships	Brave kings fight wars	Warm ground melts snow
Vain ears hear talk	Sore eyes shed tears	Keen blades slash tires
Close friends swap gifts	Harsh trails sprain joints	Posh wives pay bills
Horse hooves crush rocks	Mad dogs bite tails	Good shops pour drinks
Red lights stall cars	Fine gifts please hosts	Some pets climb trees
House maids scrub floors	Fierce flames sear steak	Snow limbs lift weights
Oil lamps start fires	Snow wolves hunt deer	Chrome tanks leak gas
Wood combs brush hair	Sheer noise hurts ears	Smart girls read books
Cold storms harm plants	John's wife bakes cakes	South lane leads home
Bowled balls strike pins	Blunt sticks smash glass	Parched fields need help
Three teams lost games	Smooth eggs hatch chicks	Steep hills slow bikes
Gas stoves heat pans	Cute birds build nests	Deep trust bonds friends
Cheap baits halt slugs	Sour food draws breath	Low planes dust crops
Weak sun heats rooms	Tight fists knock doors	Cruel hooks catch fish
Bee stings prick arms	Rough walks tax legs	Thick fog blocks views
Straw hats stop sun	Chopped logs choke creeks	Fire doors seal smoke

Farm aids swing bats	Tough spades crack slabs	Bald men ride trains
Old pumps lack grease	Spare keys lock halls	Plump wool coats sheep
Stretched arms seize balls	Iron spoon knocked floor	Wall clocks tell time
Round box stores coins	Bank clerks scan files	Square nets grab prawns
Dried fruit tastes good	Deep breaths save life	Mild rain wets ground
Gold rings cause fights	Small hands knead dough	Slim hips twirl hoops
Shoe tread stops slips	Thin ice risks lives	Brick walls guard homes
Fried chips burn tongues	Dark nights veil owls	Dear friends send mail
Open sports draw crowds	North winds bring joy	Sweet cakes tempt fate
Tall trees lose leaves	Lost goats scale cliffs	Grown men miss youth
Cracked plates spoil food	Wild pines drop cones	Spiked pins pierce rags
Chilled sheets help sleep	Bored dads drink beer	Wet soil yields worms
Bleak seas hide crabs	Bar soap cleans paws	Flat screws fix lights
Back teeth hurt jaws	Cool rooms keep meat	Calm swells raise yachts
Huge bull jumps fence	Bus tours tire guests	Tight belts hold pants
Race cars dodge oil	White sand covers boats	Road bikes skip holes
King crabs eat shrimp	Clay mugs store pens	Short talks blow minds

Wine grapes have seeds	Aged trains use coal	Hedge plants block paths
Quick gales break kites	Hard falls hurt knees	Spring buds prize soil
Rose tea stains pots	Used bricks fill yards	Toy spoons stir cups
Hot baths treat flu	Green plants feed birds	Bush snakes kill mice
Axe strokes trim rope	Strong light fades cloth	Wide trucks move trash
Nice guys give seats	Silk scarves ease throats	Eight ducks cross fields
Brass clips grip notes	Blue pens write words	Long waits bore boys
Salt lakes ooze slime	Trust funds hoard wealth	Stiff brooms sweep stones
Fresh staff like work	Flight crews serve lunch	Steel whisks whip cream
Sun glare burns eyes	Clear tape seals splits	High racks hold coats

Chapter 5: Evaluation of a MEG system for Unilateral Cochlear Implant Recipients

Qingqing Meng[1,2,4]
Yiwen Li Hegner[1,2]
Catherine McMahon[1,3,4,5]
Blake W Johnson[1,2,4]

[1]HEARing Co-operative Research Centre, Melbourne, Victoria, Australia
[2]Macquarie University, Department of Cognitive Science, Sydney, New South Wales, Australia
[3]Macquarie University, Department of Linguistics, Sydney, New South Wales, Australia
[4]ARC Centre of Excellence in Cognition and its Disorders, Macquarie University, Sydney, New South Wales, Australia
[5]Centre for Implementation of Hearing Research, Macquarie University, New South Wales, Australia

Abstract

The success in application of cochlear prosthetic devices introduces new scientific opportunities for basic and biomedical research into the effects of sensory deprivation on the central auditory system and for investigations of functional plasticity after restoration of hearing. To date, however, investigations in humans have been limited due to the incompatibility of cochlear implant (CI) systems with functional neuroimaging techniques, such as functional magnetic resonance imaging (fMRI) and magnetoencephalography (MEG), in particular, due to the ferromagnetic components implanted within the skull. Here we describe the development and evaluation of a prototype, custom-engineered MEG system for unilateral CI recipients. It has been designed to cope with the inherent CI electromagnetic artefacts with higher-order gradiometers while measuring auditory responses from the cortical hemisphere contralateral to the implant. We evaluated this MEG system with both normal hearing participants and CI recipients. Under the current design, auditory evoked responses can be reliably recorded from normal hearing listeners with an external CI emulator positioned below the side of the head further away from the MEG sensor array. Noise levels in the actual CI recipients were also strongly attenuated but remained in the picoTesla range, likely due to motion of the internal magnet caused by cardiac pulsations of the head.

1 Introduction

Cochlear implants (CI) have been developed with the aim of restoring a sense of sound to profoundly deaf people by electrically stimulating the residual afferent neurons in the cochlea, the peripheral auditory end organ (Zeng, 2004). Modern CI systems have achieved a remarkable success and have been regarded as the most widely used neural prosthetic devices by far. Despite of the very limited and crude input, high performing CI recipients can often understand speech well in quiet environments (Tyler, Lowder, Parkinson, Woodworth, & Gantz, 1995). However, clinical results have demonstrated stark variations in speech perception performance among individual CI recipients (Shannon, Zeng, Kamath, Wygonski, & Ekelid, 1995). This variation may, in part, be due to varying degrees of auditory pathway degradation from sensory deprivation, differences in cognition, or the interactions between both (Wong & Ryan, 2015; Peelle & Wingfield, 2016). In particular, alterations in the central auditory system caused by deafness are not necessarily reversible, even when sensory input is restored (Moore & Shannon, 2009). The effects of hearing deprivation on central auditory system and brain plasticity after hearing restoration are thus, unique research opportunities in auditory neuroscience provided by CI. Furthermore, results from these basic and biomedical researches may be of benefit in pre-implantation evaluation and post-implantation rehabilitation, and ultimately aid in developing better CI systems. Therefore, there is an increasing interest in measuring high-level auditory brain function in cochlear implant recipients.

Owing to its high temporal resolution and quiet operation, magnetoencephalography (MEG) has long been a valuable tool for the study of central auditory system and speech processing with normal hearing population (Baillet, 2017; Cheyne & Papanicolaou, 2017). It has much higher temporal resolution than hemodynamic monitoring techniques such as functional magnetic resonance imaging (fMRI) (Stamatakis, Orfanidou, & Papanicolaou, 2017), and in practice has

better spatial resolution than electroencephalography (EEG) (Baillet, Mosher, & Leahy, 2001). It is well suited for studying the developing brain, i.e., investigating auditory brain function with preschool children aged 3-5 years (Johnson, Crain, Thornton, Tesan, & Reid, 2010). Driven by the neuroscientific development that hearing researchers and clinicians shifted from a focus on the auditory periphery to a greater appreciation of higher-level brain functions in hearing (Wilson & Dorman, 2008), MEG has also found applications in investigating auditory brain function among patients with auditory impairments, such as hearing loss (presbyacusis) and subjective tinnitus (Adjamian, 2014; Alain, Roye, & Salloum, 2014). The prominence of MEG in recent years in the context of hearing research has also been attributed to the veritable paradigm shift in neuroscience, from an emphasis on simple "evoked" or "event-related" brain responses to well-defined experimental manipulations, recognition of the importance of ongoing, intrinsic brain activity (Raichle, 2009). Compared to other techniques, MEG is particularly efficacious for measuring these electromagnetic brain oscillations.

However, due to the inherent interference caused by the electronic and magnetic components in CI system to the Superconducting Quantum Interference Devices (SQUIDs) used in conventional MEG systems (Fagaly, 2006), measurements of brain responses in CI recipients have generally not been possible. As outlined in **Figure 20**, the artefacts are produced by: 1. the electronic components of the sound processor which captures and processes the incoming acoustic signal; 2. the internal coil magnet which aligns the internal receiving coil with the external transmitting coil; 3. the radio-frequency (RF) signal which is transmitted between the external and internal coils as an encoding of the acoustic signal and 4. the electric currents produced by the electrode array that stimulates the auditory nerve.
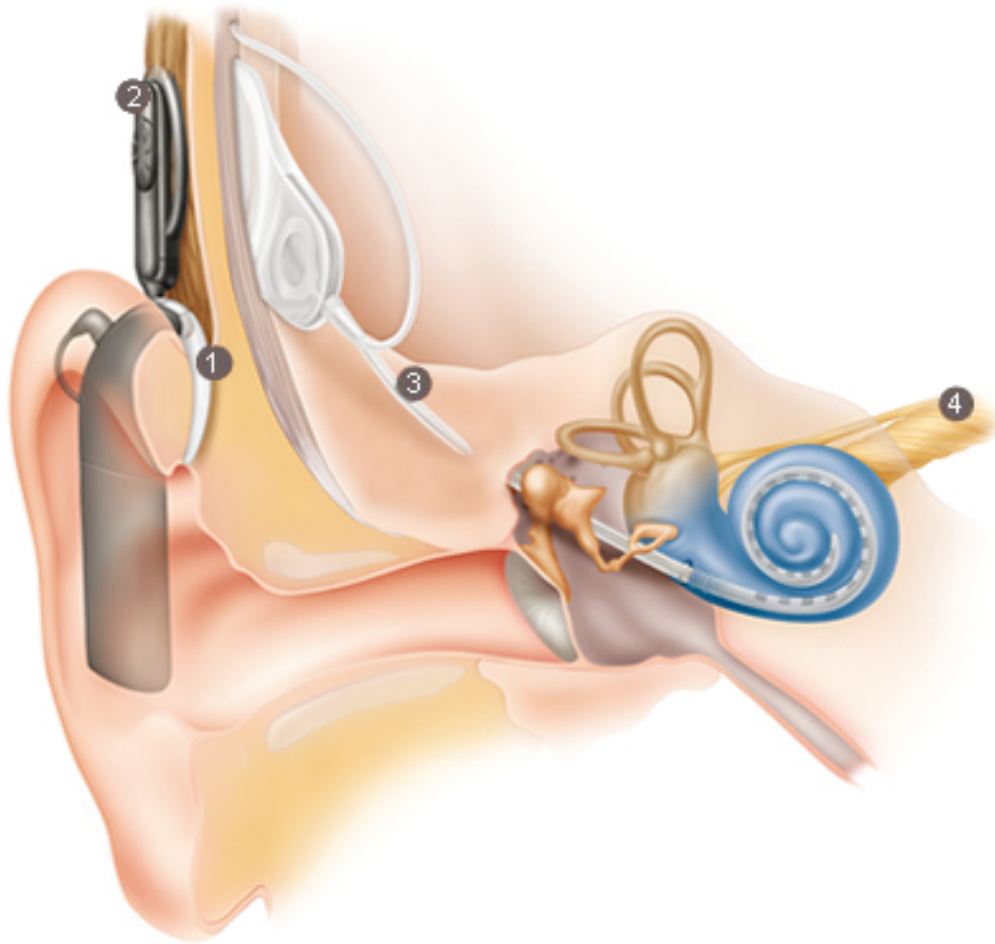
Figure 20: Cochlear implant system. 1: sound processor worn behind the ear. 2: transmitting coil aligned with the receiving coil placed under the scalp via a pair of magnets. 3: internal part of the implant with electrode array inserted in the cochlear. 4: hearing nerve which sends the electric pulses to the brain. Figure adapted with permission from (http://www.cochlear.com/wps/wcm/connect/au/home/understand/hearing-and-hl/hl-treatments/cochlear-implant)

Several MEG studies have been conducted under unique set-ups and their results showed the possibility of measuring auditory evoked fields (AEFs) from unilateral CI recipients who received magnet-free implants (Pelizzone, Hari, Mäkelä, Kaukoranta, & Montandon, 1986; Hari, Pelizzone, Mäkelä, Huttunen, & Kuuutila, 1988; Hoke, Pantev, Lütkenhöner, Lehnertz, & Sürth, 1989). In a more recent longitudinal experiment (Pantev, Dinnesen, Ross, Wollbrink, & Knief, 2006), AEFs were acquired from two unilateral CI recipients at 10 consecutive time instants over a 2-year period. Compared with a group of normal hearing participants, AEFs with almost normal component configuration were observed at the last MEG measurement and were source localized to the contralateral auditory cortex which demonstrated the adequacy of CI

137

stimulation. The evolving trajectory of AEF source waveforms exhibited similar temporal dynamics with the word intelligibility test results, demonstrating its sensitivity to index the plasticity of human auditory system after CI implantation. Nevertheless, this study was again conducted with magnet-free CI recipients.

With an aim to accommodate recipients using conventional CI devices with magnets, engineers at Kanazawa Institute of Technology (KIT), Nonoichi Ishikawa, Japan have developed a prototype, custom-engineered MEG system designed to cope with the electromagnetic artefacts caused by CI systems. A general principle of the prototype MEG system is to employ two functionally distinct sensor arrays to capture the cortical responses and the artefacts caused by CI systems separately. Higher-order gradiometers that are sensitive only to near-field sources would serve well as measuring sensors to detect the brain responses directly underneath, while magnetometers that are also sensitive to distant noise sources would be used as reference sensors to measure the environmental noise (Vrba & Robinson, 2001).

2 The Prototype MEG System

2.1 Overview of the Initial Prototype

The initial setup of the prototype MEG system as shown in **Figure 21a** was contained in a cylindrical dewar. With a flat tail of approximately 20 cm outer diameter, it covered one side of a participant's head. During an experiment, participants were instructed to lie down on the bed on the side with the CI so that the brain activity from the contralateral side could be measured by the MEG (**Figure 21b**). The height of the headrest was adjustable so that the participant's head was always positioned directly below and with a good contact with the dewar tail.

Figure 21: The custom-engineered MEG system for cochlear implant recipients. Left: Appearance of the system. Right: Demonstration of the experimental setup with a normal hearing person and a CI emulator box by the side of his head (figure for display only, during the actual experiment MEG sensor plane touched the side of participant's head and the CI emulator was placed underneath the other side of the head).

2.1.1 MEG Sensor Configuration and Characteristics

A schematic plot of sensors employed in this prototype MEG system is shown in **Figure 22**.

According to the layout, 20 axial second-order gradiometers (0 to 19) with 50 mm symmetric

baseline were configured to a plane towards the bottom of the dewar tail. These higher-order

gradiometers were used as measuring sensors to detect brain activities from the near-field

(mainly temporal area). Another set of 12 magnetometers (R0 to R11) were configured to

another plane 90 mm above a subset of the measuring sensors. They were intended to operate

as reference sensors and were mainly responsible for capturing electromagnetic noises created

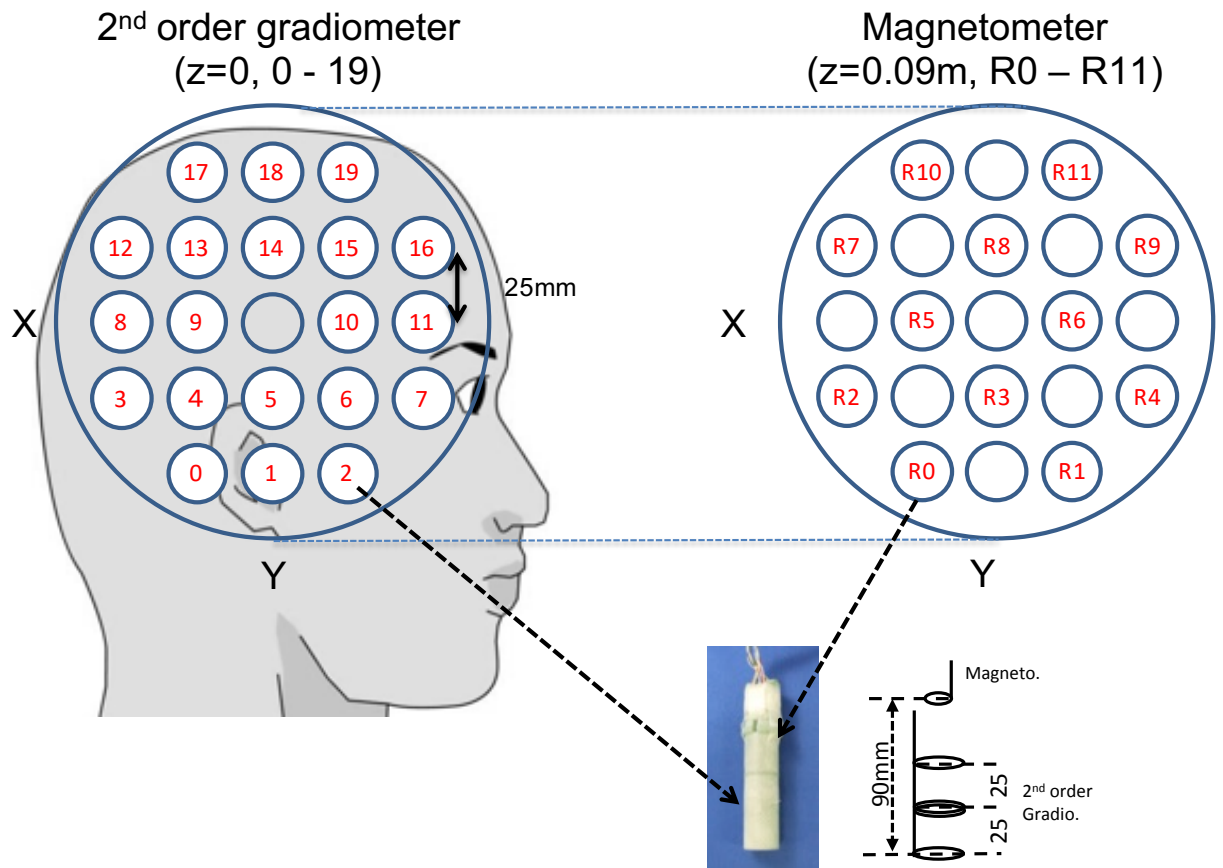by the CI system and other general environmental artefacts.

Figure 22: Diagram of the layout of measuring sensors and reference sensors employed in the prototype MEG system (courtesy of M. Higuchi, KIT)

The characteristics of both kinds of MEG sensors employed are illustrated in **Figure 23**. As the "response versus distance" curves indicate, the output amplitude of the symmetric baseline second-order gradiometer (green) decayed quickly as the distance to the magnetic source increased. The gradiometers behave like spatial high-pass filters (Vrba, Fife, Burbank, Weinberg, & Brickett, 1982) so that they should be less affected by the CI system located further away, while remaining sensitive to the neuromagnetic signals generated from the cortical area directly underneath. On the other hand, output amplitude from the magnetometer (black) changed more slowly with distance. In this way, the strong artefacts created by the CI system could still be effectively measured by the magnetometers even though they were further away. For comparison, the performance curve for first-order gradiometer that is usually employed by conventional MEG systems as primary sensor is also plotted in **Figure 23** (magenta).
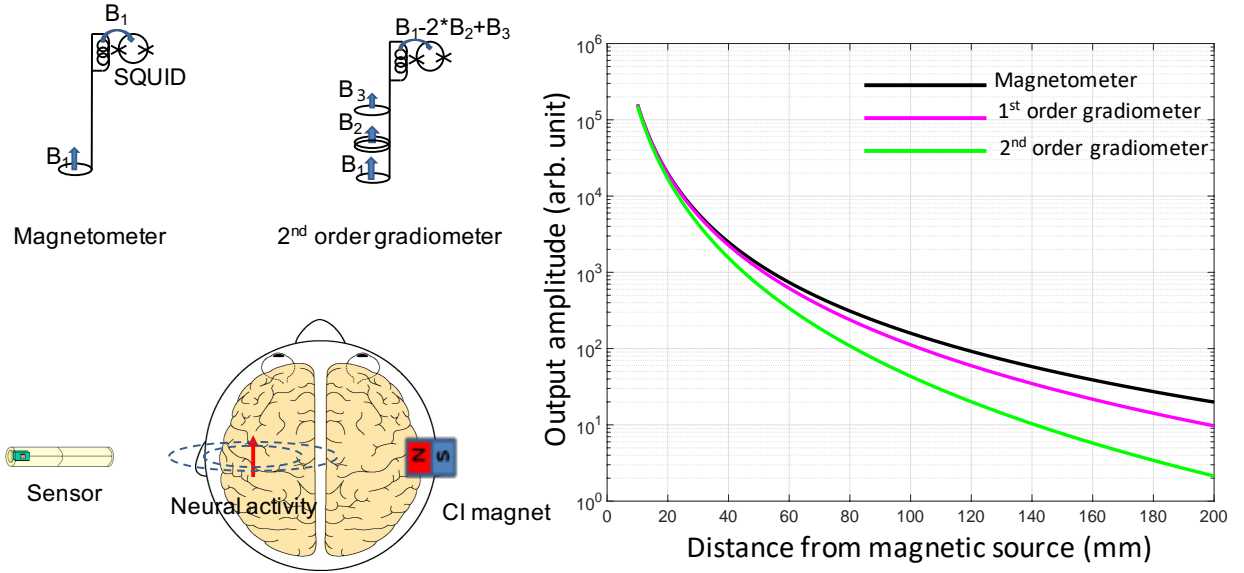
Figure 23: MEG sensor performance characterised by the output amplitude versus distance from magnetic source plot (courtesy of M. Higuchi, KIT)

2.1.2 Tests with Normal Hearing Participants and a CI Emulator

Performance of the prototype MEG system was first evaluated with 20 normal hearing participants using a simple auditory paradigm that measures the AEFs. 100 pure tones (1kHz, 0.2s duration) were presented at a sound pressure level (SPL) of 70dB with an Inter-Stimulus-Interval (ISI) randomly assigned between 0.85s and 1.25s. Sound stimuli were delivered to the left ear via an insert earphone (Model ER-30, Etymotic Research Inc., Elk Grove Village, IL) while participants were instructed to listen passively with their gaze fixed on a cross marked on the wall. MEG recordings were acquired with the analog filter parameters set to 0.3 Hz high-pass, 200 Hz low-pass and power line noise pass through. Within the data acquisition software MEG160 (Yokogawa Electric Corp., Eagle Technology Corp., KIT), raw MEG data were first segmented into trials of 0.7s (0.2s baseline) in length and then averaged in the time domain. The time averaged data were smoothed by a moving average window (32 ms) and then baseline corrected. Because there was no head-localization system installed with this prototype system and due to the head positioning difference across participants, it was not meaningful to average across their sensor-level data. Thus, only the AEF from one representative participant is shown here in **Figure 24**.

141

However, similar results with the clear pattern of magnetic sink and source were obtained from all other participants. These AEF results suggested that the existing sensor array had a proper coverage to unilateral auditory cortex and was capable of measuring brain responses in the absence of electromagnetic artefacts caused by the CI system.
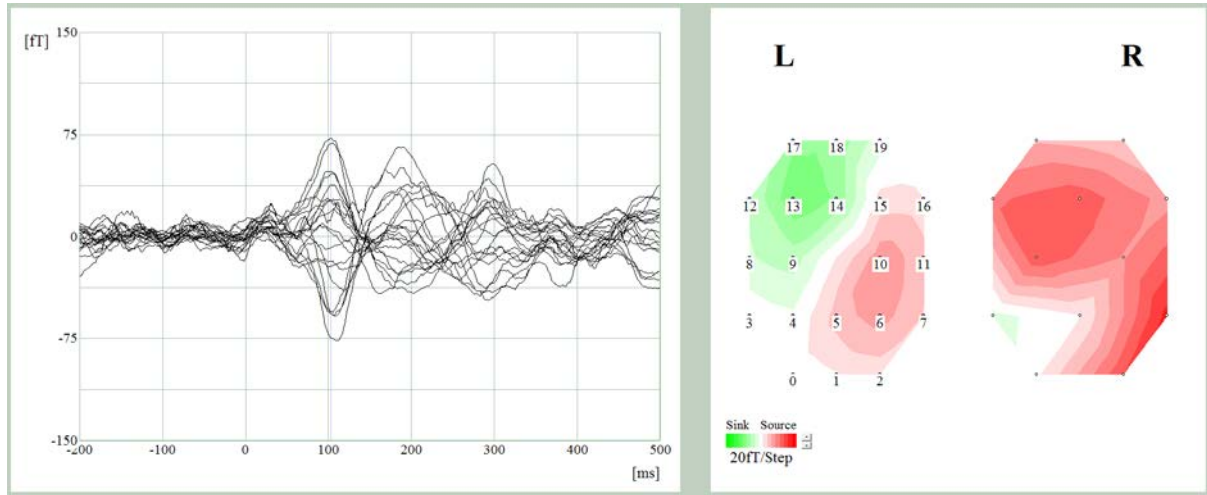

Figure 24: MEG measured AEF from a representative normal hearing participant. Left: Time courses of the measured AEF with deflections occur around 100 ms after stimulus onset (0 s) and within femtoTesla range (10^{-14} T). Right: Topographical view of the measuring sensor configuration (0-19, L), the reference sensor configuration (20-32, R) and the distribution of the measured magnetic fields.

Next, we evaluated the effectiveness of the noise reduction operation facilitated by the reference sensor array. A CI emulator was placed 14cm below the center of the dewar tail to produce, as close as possible, the electromagnetic artefacts that would be present when an actual CI user would be tested. This emulator is a standard clinical CI system with the internal part enclosed in a plastic box and electrodes output to a 25-pin D-sub connector. The same experimental paradigm described above with normal hearing participants was employed while the pure tones were fed into the CI sound processor via an audio accessory cable. The sound processor encodes incoming acoustic signals and then transmits them to the CI emulator box as radio frequency signals through a pair of coils. To reduce unnecessary magnetic artefacts, the external coil magnet was taken off and the external coil was taped onto the emulator box at the position that was aligned with the internal coil. MEG recordings were acquired under the same settings and went through the

same processing steps except for an additional noise reduction process after the time domain average. This noise reduction operation used data from the reference sensor array and an algorithm named Continuously Adjusted Least-squares Method or CALM (Adachi, Shimogawara, Higuchi, Haruta, & Ochiai, 2001). For comparison, frequency responses of the time-averaged MEG data before and after the noise reduction operation are plotted in **Figure 25**, together with the frequency response of an empty room recording of the same length. Although the CI emulator-induced artefact was significantly reduced (especially at low frequency region, ~ 10 times smaller up to 40Hz) with the application of CALM, it is evident that the amplitude of the residual artefacts remained well above the level of the empty room recording. Results of the measurement with the CI emulator suggested this initial MEG prototype was not effective to capture cortical responses (typically in the range of 10^{-14} Tesla) in the presence of strong electromagnetic noise because strong residual artefacts still remained after the noise reduction operation. These results showed that the best achievable results of the initial prototype MEG system across the frequency spectrum were still well above the noise levels that would be required for measurement of brain signals (less than 100 fT).
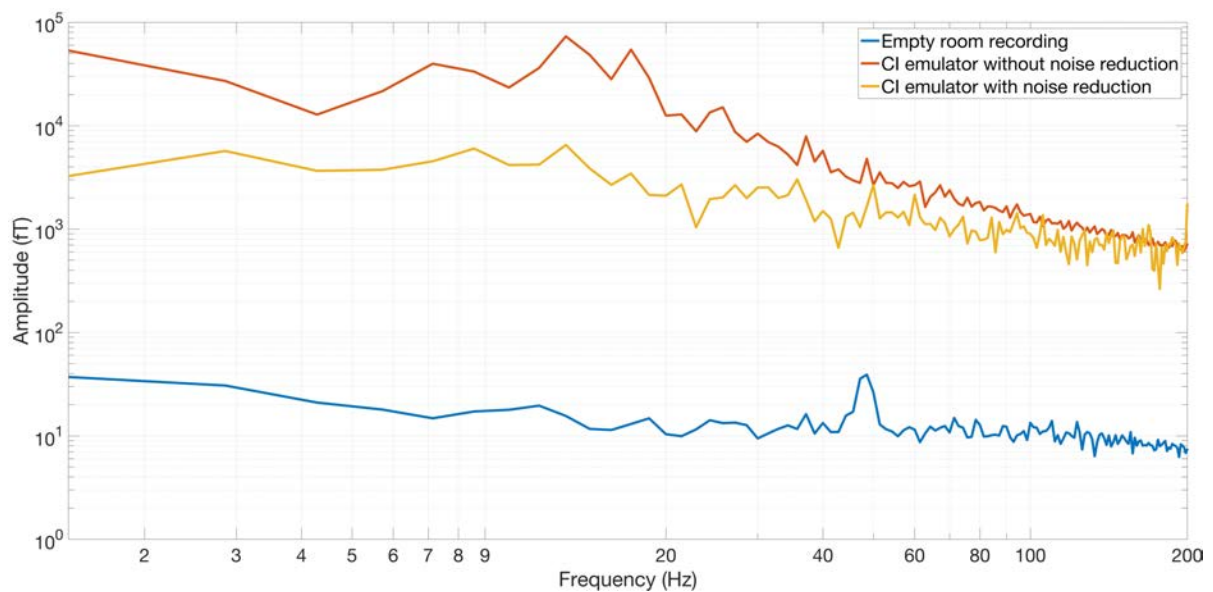
2.2 An Upgraded MEG System

To further improve the noise reduction performance and to increase the sensitivity to brain responses, a hardware upgrade was implemented. Two groups of novel irregular baseline second-order gradiometers replaced the regular baseline second-order gradiometers and magnetometers setup. As is shown in **Figure 26**, these new sensor arrays were configured in a larger sized cylindrical dewar with the flat tail of the same diameter.

Figure 26: The upgraded MEG system with two types of irregular baseline second-order gradiometers

2.2.1 Irregular Baseline MEG Sensors

Layout of the upgraded MEG sensor arrays is shown in **Figure 27**. 20 type B irregular baseline (9 mm versus 41 mm) second-order gradiometers were installed and 12 type A irregular baseline

(16 mm versus 34 mm) second-order gradiometers were configured concentrically with a subgroup of type B sensors. Compared with conventional MEG sensors, this irregular baseline setup was characterized by a unique deep trough in the "response versus distance" curve as shown in **Figure 28**. The distance of this near-null responsiveness could be determined by manipulating the ratio of the baseline part *a* and part *b* length. The 20 type B sensors were used as measuring sensors as they were not designed to be sensitive to the magnetic sources at a distance correspond to the location of a CI (~110 mm), while the 12 type A sensors were used as reference sensors due to the near-null responsiveness to magnetic sources at locations corresponding to the auditory cortex (~40mm) directly underneath. Therefore, in the ideal situation, subtraction of the CI artefact signals captured by the type A reference sensors from the signals measured by the type B sensors would reveal clean cortical signals.
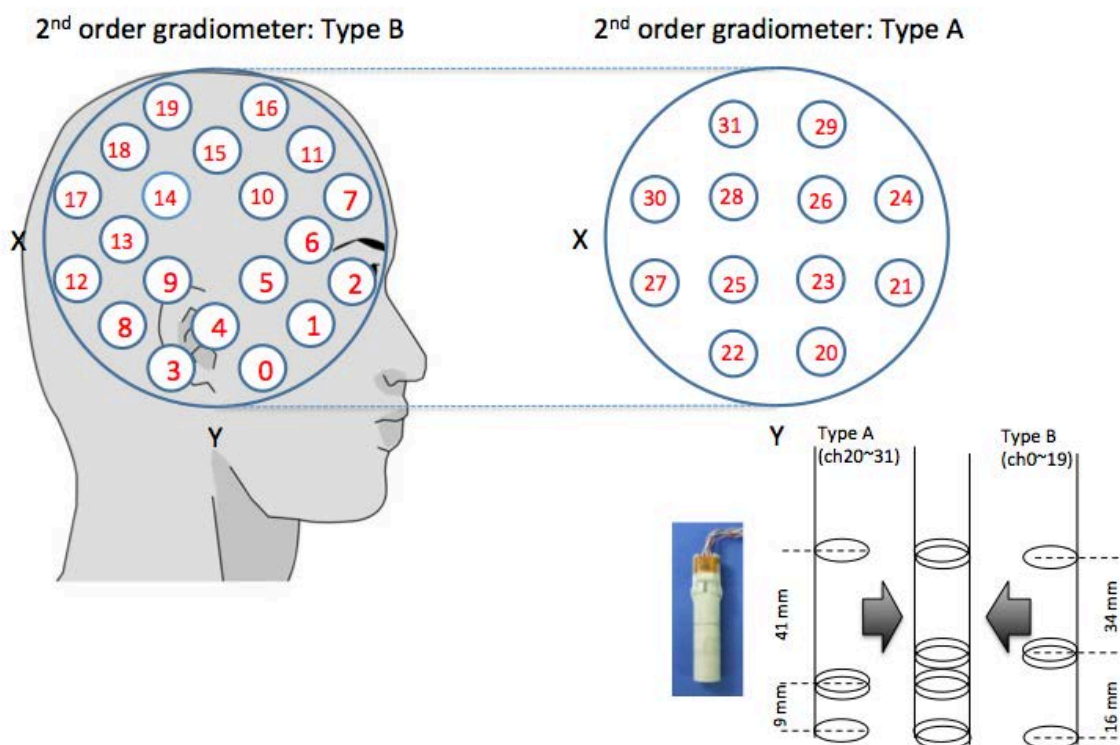

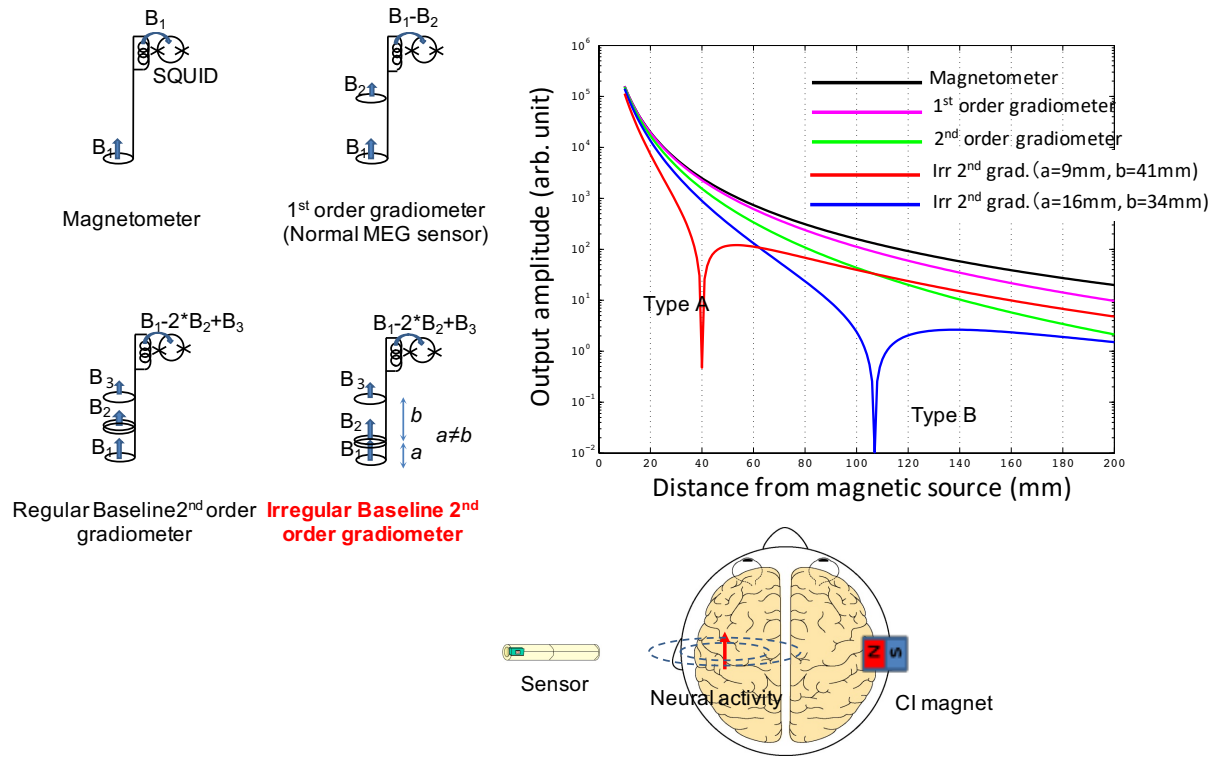*Figure 27: Sensor array layout of the upgraded MEG system (courtesy of M. Higuchi, KIT)*

Figure 28: Characteristics of the upgraded MEG sensors using irregular baselines (courtesy of M. Higuchi, KIT)

Frequency responses of the time averaged MEG data before and after CALM noise reduction operation are shown in **Figure 29**, together with an empty room recording. As shown, the novel irregular baseline MEG measuring sensors exhibited a much lower response to the artefacts caused by the CI emulator. Furthermore, the amplitude level of residual artefacts after CALM noise reduction closely matched with the level of the empty room recording which suggested the feasibility of concurrently measuring brain responses with the presence of a CI emulator.
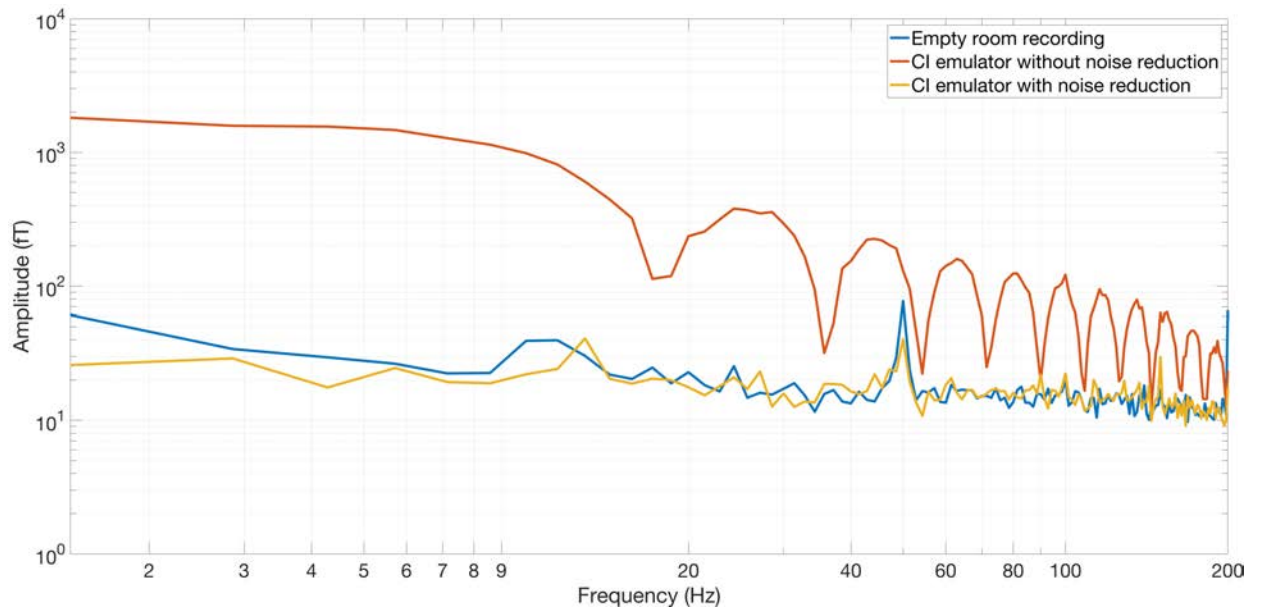
146

Figure 29: Frequency responses of time averaged MEG data measured with the upgraded prototype MEG system using the AEF paradigm. Blue: Frequency response of an empty room recording. Orange: Frequency response measured with a CI emulator, without any noise reduction. Yellow: Frequency response measured with a CI emulator, with the CALM noise reduction.
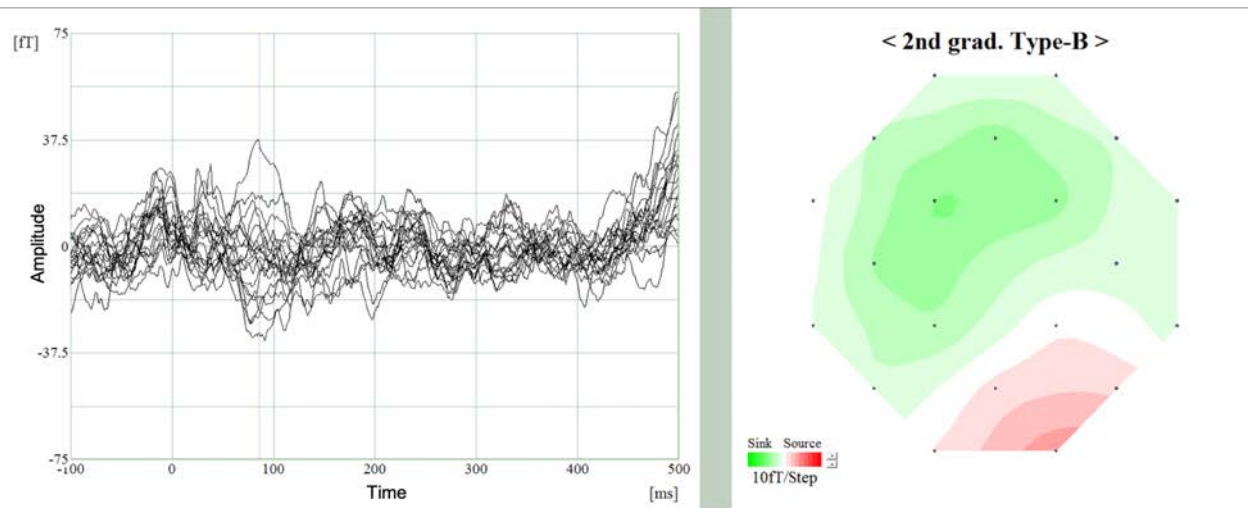
2.2.2 AEFs in normal hearing participants

We next measured eight normal hearing participants together with the CI emulator, using the same simple AEF paradigm. 100 pure tones (1kHz, 50ms duration) with an ISI randomized between 0.85s and 1.25s were presented to the left ear of the participant at 70dB SPL using insert earphones (Model ER-30, Etymotic Research Inc., Elk Grove Village, IL). During the test, participants were instructed to lie down on their left side with their head rested close to the joined side of a U-shaped travel pillow. A customised tube with a diameter of 15cm was attached to the open side of the pillow near the occipital area so that the CI emulator box could be placed directly underneath the left side of the participant's head with minimum head movement. MEG recordings were acquired first with participants receiving only monaural sound stimulation, and then a separate recording was conducted together with the CI emulator placed directly below the participant's ear receiving concurrent sound stimulation. The CI emulator was stimulated by exactly the same acoustic signal via an audio accessory cable. The same data analysis procedure was carried out in the acquisition software MEG160, noise reduction (CALM) was applied to the MEG data acquired with the CI emulator. Time averaged AEFs from a representative participant

are plotted in **Figure 30**. As can be seen, comparable auditory evoked fields were obtained with or without the CI emulator. This was a significant improvement over the initial prototype and evidenced the capability of the current sensor array setup using two kinds of novel irregular-baseline second-order gradiometers. By rejecting excessive artefacts characterized by the reference sensor array from signals of the measuring sensor array, now the amplitude of time-averaged AEFs fell into the amplitude scale of common brain responses (50 – 100 fT) and exhibited comparable components configuration and topographical distribution with the cortical responses measured without the CI emulator.
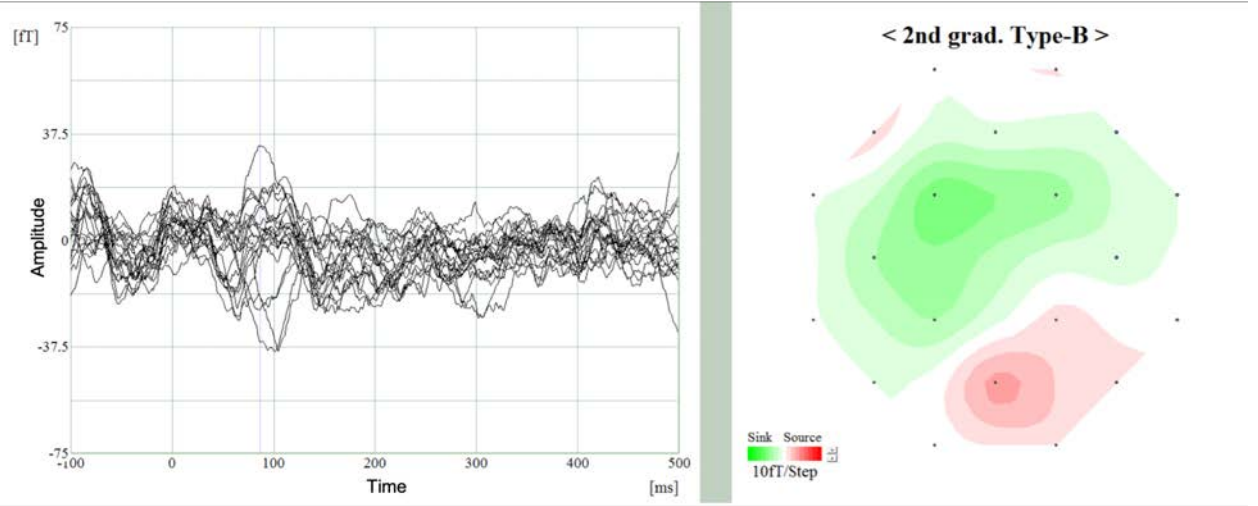
(a)

(b)

Figure 30: Auditory evoked fields measured with the upgraded prototype MEG system. (a): AEF measured from a representative normal hearing participant. (b): AEF measured from the same normal hearing participant with a cochlear implant emulator (noise reduction algorithm applied).

2.2.3 Phantom tests

In the upgraded system, a set of head position localization system with five MEG compatible coils was installed to enable the cortical source localization analysis. In conventional whole-head MEG systems, the number of measuring sensors normally exceeds 100 and the sensor arrays are configured on a sphere that gives a good coverage to a participant's head. Thus, source localization accuracy using this prototype MEG system may be compromised due to the limited number of measuring sensors (20 channels) and a flat array configuration. The most basic

149

evaluation for MEG measurements is to localize a single dipole. We therefore conducted single dipole localization tests with a single wire set adopted from a dry phantom head for MEG (Oyama, Adachi, Yumoto, Hashimoto, & Uehara, 2015). MEG phantom heads are normally used to imitate equivalent current dipoles (ECDs) that are assumed to represent the neural activity in the human brain. As shown in **Figure 31 (c)**, this single wire set entails two individual conducting wires (0.16 mm diameter) orthogonally wound as two isosceles triangles through four triangular holes in a quadrangular pyramid resin bobbin. Sinusoidal signal of 11Hz and 0.2V generated from a function generator was sent to each individual wire to produce a single current source at the base of each isosceles triangle. The positions of the current sources (ECDs) were estimated from MEG recordings using dipole-fitting. To get the designed position of the ECDs, four MEG compatible localization coils were attached to the corners of the frame on the bobbin to serve as markers and their positions were estimated with the prototype MEG system. The goodness-of-fit for ECDs estimation and marker-coil measurement all exceeded 99%. The designed positions of ECDs were then numerically calculated using the geometry information of the single bobbin and the estimated marker-coil positions. Compared to the designed positions, displacement of the estimated ECD positions were all below 5 mm. The phantom test result demonstrated the capability of this prototype MEG system in accurately localizing a single dipole source. However, further investigations were needed when strong electromagnetic CI artefacts were present with CI recipients.
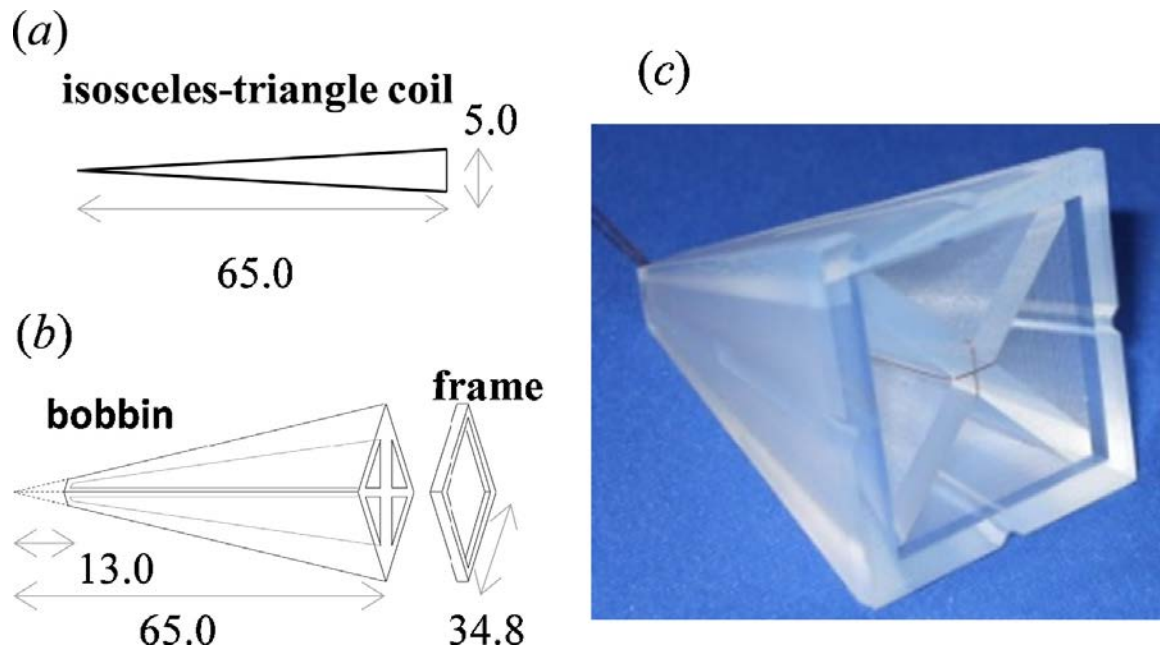
Figure 31: Wire-set for a MEG phantom. (a) Isosceles-triangle model with a finite base. (b) A quadrangular-pyramid bobbin with a frame. (c) A photograph of fabricated wire set. Two orthogonally oriented isosceles triangle wires were wound through four triangular holes in the bobbin. Figure adapted with permission from (Oyama et al., 2015)

3 Normal hearing participants and CI emulator: Concurrent EEG/MEG recordings and source analysis

3.1 Materials & methods

From our previous observations, there were strong CI artefacts time-locked to the acoustic signal presentation in the measured MEG signals. The residual artefacts corresponding to the onset and offset of the auditory stimulation were dominant even after noise reduction operations were applied. These stimulation-time-locked CI artefacts have been hypothesized to be caused by the stimulus excitation within CI sound processor and the transmission of RF signals between the external and internal coils (Wagner, Maurits, Maat, Başkent, & Wagner, 2018). To further reduce the on- and off-stimulation related CI artefact, a modified paradigm that presents continuous white noise in the background during 50ms 1kHz pure tone presentations was employed in the tests with CI recipients. The rationale was that white noise would cause rapid amplitude fluctuating artefacts which ultimately yields an output with flat amplitude that corresponds to the temporal envelope of the noise at the SQUIDs. This is consistent with the observation in EEG

recordings with a CI artificial brain that broadband auditory stimulation, such as speech, caused less CI EEG artefacts than with simpler auditory stimulation that involved the activation of fewer CI electrodes with well-defined amplitude envelope (Wagner et al., 2018). We assumed that when the white noise amplitude is above a certain threshold, there would not be any further amplitude change corresponding to the onset and offset of other signals embedded in the background noise. This modified paradigm was first tested with pure tone signals (1kHz, 50ms, 1-2 sec ISI) embedded in white noise using the CI emulator. The level of background white noise was empirically manipulated and the time-averaged results are shown in **Figure 32**. As the results demonstrated, when the white background noise reached a certain level, the time-locked CI artefacts associated with pure tone presentation could be effectively supressed.
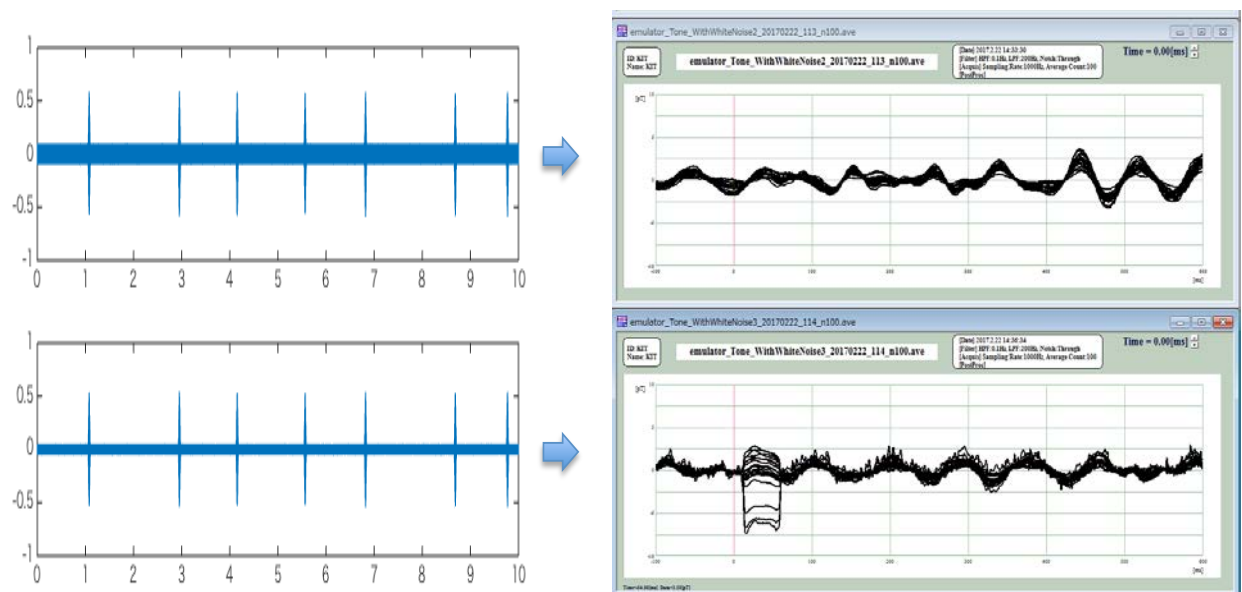

Figure 32: Demonstration of the tone-in-noise stimuli (courtesy of M. Higuchi, KIT). Left: snippets of the time course of pure tones embedded in white noise (two different noise levels). Right: Time averaged MEG recordings corresponding to different signal-to-noise ratios demonstrating effect of background noise when presented at an adequate level.

3.1.1 Participants

Four adults (3 females, ages 25-39 years) with normal hearing and no history of neurological, psychiatric, or developmental disorders participated in this study. All participants were right-handed and gave written informed consent under the process approved by the Human Subjects

152

Ethics Committee of Macquarie University. As reimbursement for their participation, all subjects received payment.

3.1.2 Stimuli

1 kHz pure tones with a duration of 50ms were filtered with a Hanning window and then mixed with continuous background white noise (~ 5 dB SNR). In total, 300 pure tones were presented at 70 dB SPL with an ISI randomly assigned between 1 to 2 s.

3.1.3 Procedure

All participants received monaural stimulation and listened passively while fixing their gaze on a frontal central cross that was marked on the wall inside of the testing room. Instructed to lie down on their left side, pure tone signals embedded in white noise were delivered to participants' left ear using the same insert earphone as was used in the previous test measurements. The CI emulator received exactly and concurrently the same auditory stimuli from an audio accessory cable connected to the sound processor and was placed directly below the left ear to mimic the experiment scenario with CI recipients. The external coil magnet was taken off and the external coil was taped onto the emulator box at the position that was aligned with the internal coil. To ensure monaural auditory stimulation, the non-stimulated ear was blocked using an ear plug.

3.1.4 MEG, EEG & MRI Data Collection

Brain activities from the contralateral side of the acoustic stimulation were recorded using the upgraded prototype MEG system described in the previous sections with the analog filter settings at 0.3 Hz high-pass, 200 Hz low-pass, power line noise pass through. Concurrent EEG recordings were also acquired using a 64-electrode, MEG-compatible system (BrainProducts GmbH, Gilching, Germany). Both the MEG and EEG measurements were obtained while the participant

was lying down in a magnetically shielded room (MSR) (Fujihara Co. Ltd., Tokyo, Japan) with a sampling frequency of 1kHz. Prior to the concurrent MEG & EEG recordings, marker coil positions, electrode positions, and detailed head shape were recorded with a pen digitizer (Polhemus Fastrack, Colchester, VT).

Magnetic resonance images (MRI) were acquired at the Macquarie University Hospital, Sydney, using a 3 Tesla Siemens Magnetom Verio scanner with a 12-channel head coil. Images were acquired using an MP-RAGE sequence (208 axial slices, TR = 2000 ms, TE = 3.94 s, FOV = 240 mm, voxel size= 0.9 mm3, TI = 900, flip angle = 9°).

3.1.5 Data Analysis

MEG and EEG data were analysed using the Fieldtrip-20160515 toolbox (Oostenveld, Fries, Maris, & Schoffelen, 2011) and custom Matlab (MathWorks) scripts. Offline continuous raw MEG data were first filtered with a notch filter (50Hz, 100Hz, 150Hz) and then went through the noise reduction process using CALM (10s time window). The filtered MEG data were segmented into short epochs (trials) of 1.5 seconds (0.5 s before and 1 s after the tone stimulus onset). Trials that showed large variance were rejected (due to inter-individual differences, a maximum of 150 trials were rejected) and then subjected to the independent component analysis (ICA; runica; Makeig, Bell, Jung, & Sejnowski, 1996). ICA was applied to remove eye-blinks, eye-movements, heartbeat-related artefacts and artefacts caused by the CI system. Independent components corresponded to those artefacts were identified as by their spectral, topographical and time course characteristics. MEG data that went through ICA artefact component rejection were then baseline-corrected (-0.3 s to stimulus onset) and averaged in the time domain to yield the AEFs. Offline continuous EEG data (DC mode) were first 1Hz high-pass filtered (4th order Butterworth) and cut into 1.5 s trials (0.5 s before and 1 s after the tone stimulus onset). Similar to the pre-processing procedure with the concurrent MEG data, trials with large variances were rejected

and then the rest of the trials went through ICA data cleaning. The ICA components corresponded to eye movements, heart beat and CI-related artefact were removed from the data. The cleaned EEG data were then re-referenced using average reference and event-related averaged across trials (baseline window -0.3 to 0 s at stimulus onset).

Individual MRI based cortical reconstruction (white-grey matter boundary) and segmentation was performed with the Freesurfer image analysis suite (Fischl, 2012), which is documented and freely available for download online (http://surfer.nmr.mgh.harvard.edu/). Cortical mesh decimation (ld factor 10 resulting in 1002 vertices per hemisphere) and surface-based alignment was performed with open source SUMA - AFNI Surface Mapper (Saad & Reynolds, 2012). For more details of this procedure, please refer to the method section of (Li Hegner et al., 2018). The 2004 cortical surface vertices were used as MEG/EEG sources for the leadfield calculation. Single shell volume conduction model was used for the MEG head model (Nolte, 2003). A boundary element model 'dipoli' (Oostendorp & van Oosterom, 1989) was used for the EEG head model with three layers (brain, skull and scalp with default conductivities corresponding to 0.33, 0.0041 and 0.33). Source localization was then implemented separately for MEG and EEG data using Minimum-Norm Estimation (MNE; Hämäläinen & Ilmoniemi, 1994). The baseline window (-0.3 to 0 s) was selected as covariance time window with a scaling factor (λ) equals to 3. However, for comparability, the same time windows were selected for the auditory source localization of both the MEG and the EEG data.
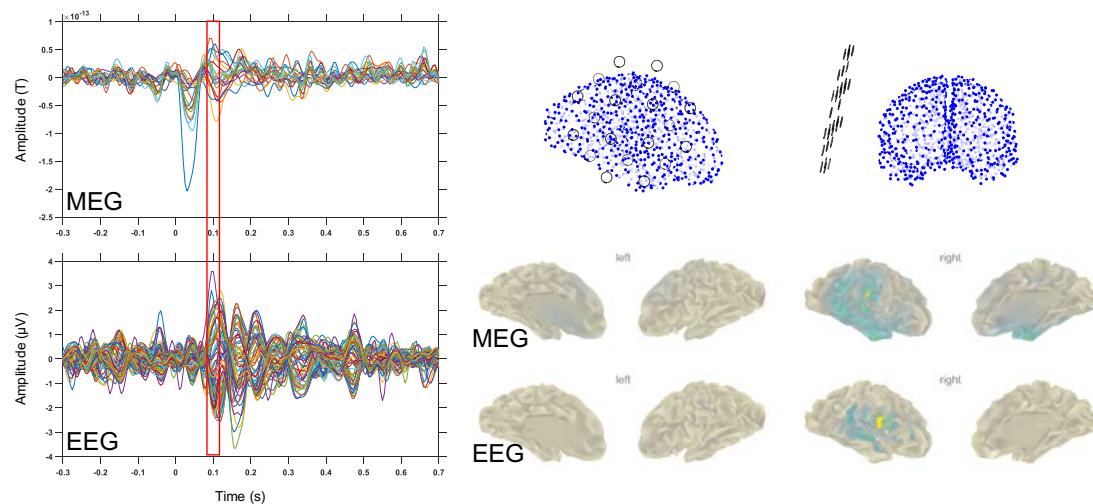
3.2 Results

Time domain averaged AEPs and AEFs measured from normal hearing participants with CI emulator are plotted in **Figure 33 (a-d left)**. The individual cortical sheet source models are displayed as blue dots as well as their relative position to the MEG sensors (**Figure 33, a-d, upper right**). The time windows (window size 20 ms) selected for the individual MNE source localization

were according to the time of the N100m peak in the concurrent EEG data, marked as red rectangle (**Figure 33**, **a-d, left**). Prominent auditory evoked responses could be observed from all measurements around 100ms after stimulus onset, although transient residual artefacts remained in AEFs after noise reduction operation. MNE source localization results for both MEG and EEG data are overlaid on individual cortical sheet (**Figure 33, a-d, bottom right**). In general, the N100m peak timing and the auditory cortical source localization performance were comparable between the concurrent MEG and EEG data. Compared to the EEG results, source localization from MEG measurements showed a bit more focal activation in the primary auditory area on the right hemisphere, which is contralateral to the ear received acoustic stimulation.
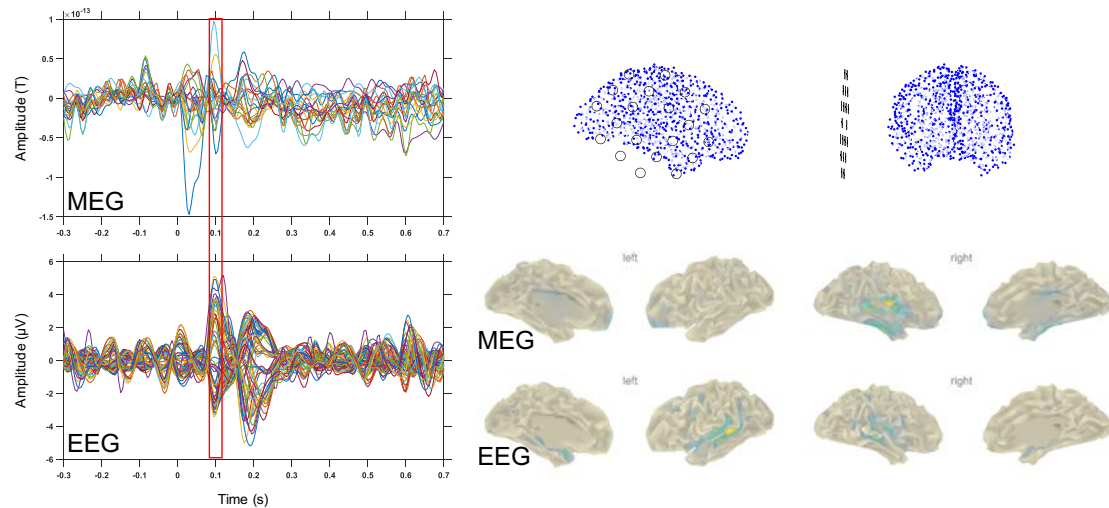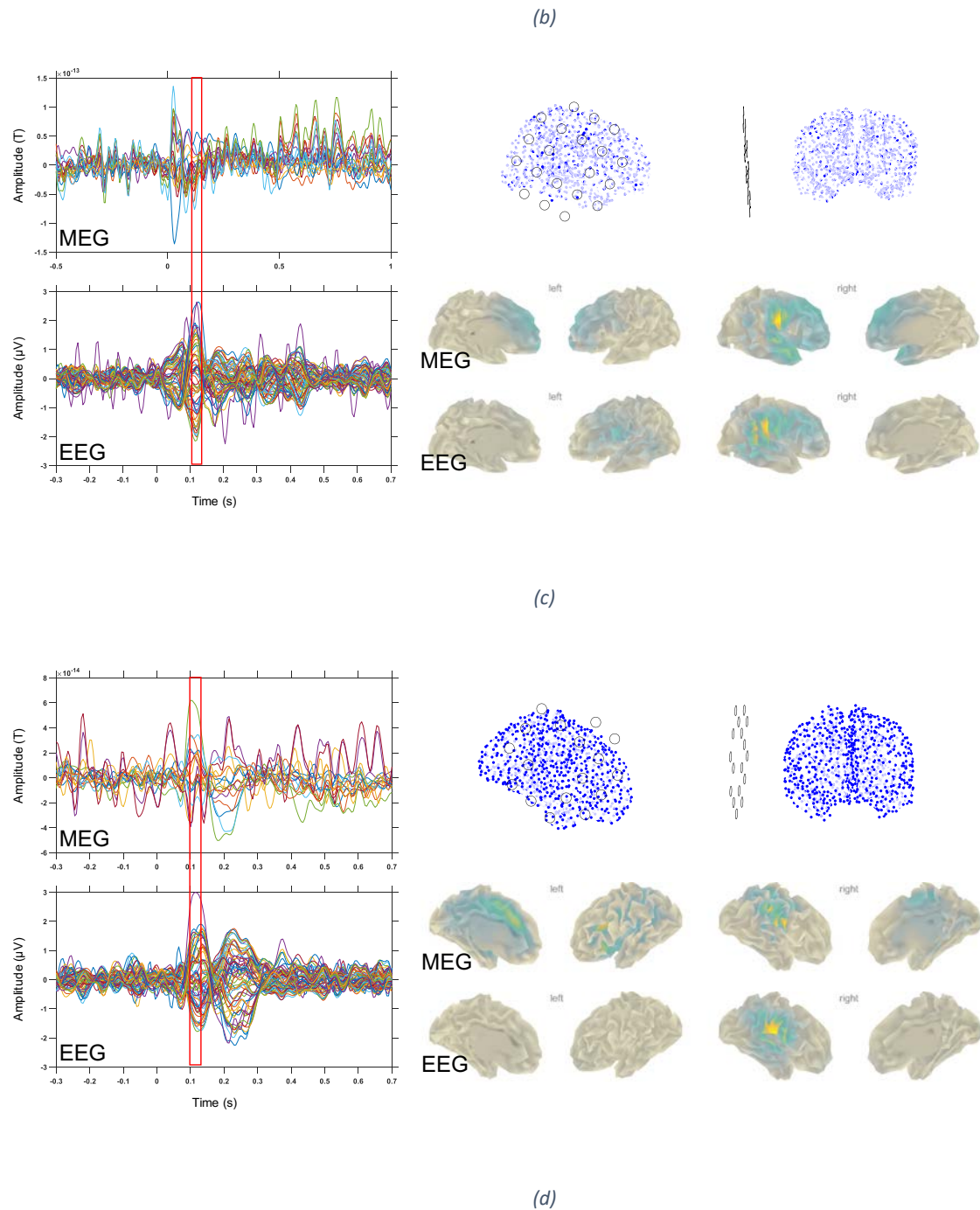

(a)

Figure 33: Time domain averaged AEPs and AEFs measured from four (a - d) normal hearing participants with CI emulator. Left: Time course of measured AEFs and AEPs, time windows selected for MNE source analysis are marked as red rectangles. Upper right: Individual cortical sheet source models relative to the MEG sensor array position during measurement. Bottom right: MNE source localization results from MEG and EEG overlaid on individual cortical sheet (individually scaled between the minimum and maximum).

4 Tests with Cochlear Implant Recipients

4.1 Materials & methods

Four post-lingually deaf experienced unilateral CI recipients (Cochlear™, 2 females, 1 right-ear implanted) aged between 61 and 70 years old participated in this study. Although with a varying

hearing ability, hearing aids were all fitted in the contralateral ears. All participants were financially-compensated for their time and provided written informed consent approved by the Macquarie University Human Research Ethics Committee. All methods and procedures were identical to those described above for normal hearing participants except the following:

Stimulus delivery: Acoustic signals calibrated at 70 dB SPL at the insert earphone were fed directly into the CI sound processor via an audio accessory cable.

External magnet: The external magnet was removed and the external CI coil was manually aligned with the internal CI coil and taped to the participants scalp.

Head model: It was not possible to obtain MRI images for the CI participants. Head shapes of CI recipients were digitized in detail. This head shape was used to customize a template brain to produce a "close to individual" three-layer head model. A common brain mesh was first extracted from the segmented fsaverge template brain (an average of 40 brains and provided by FreeSurfer) that went through the same SUMA procedure as described above for the individual cortical mesh of the normal hearing participants, and was then manually warped to match the individually digitized head shape with individual landmarks (nasion, left and right preauricular).

4.2 Results

Figure 34 shows the frequency spectra of averaged MEG data obtained from two CI recipients, superimposed on the plots described above using the CI emulator. These results showed that (1) before noise reduction, noise levels in the two CI recipients were substantially higher, across the frequency spectrum, than those observed with the CI emulator; and (2) noise levels were strongly attenuated after noise reduction operation but remained substantially higher (in the picoTesla range) than those achieved with noise reduction in the CI emulator tests (in the femtoTesla range).
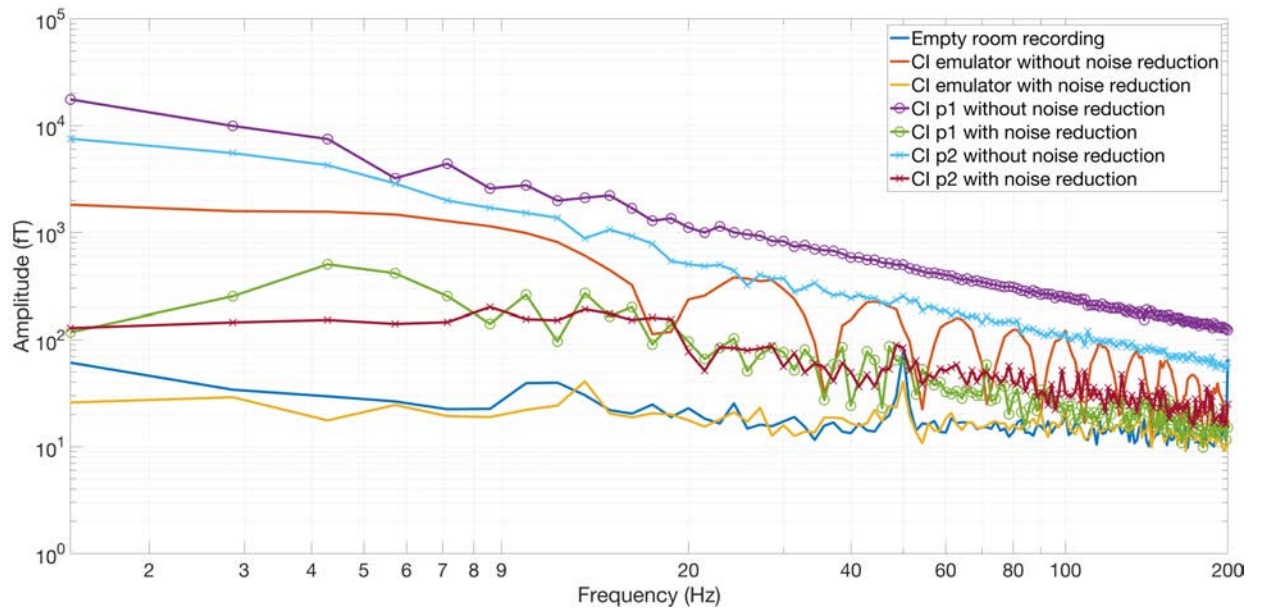
Figure 34: Frequency responses of time averaged MEG data measured with the upgraded prototype MEG system using the AEF paradigm. Blue: Frequency response of an empty room recording. Orange: Frequency response measured with a CI emulator, without any noise reduction. Yellow: Frequency response measured with a CI emulator, with the CALM noise reduction. Purple (with marker "o") Frequency response measured with CI recipient 1, without any noise reduction. Green (with marker "o") Frequency response measured with CI recipient 1, with the CALM noise reduction. Light blue (with marker "x") Frequency response measured with CI recipient 2, without any noise reduction. Red (with marker "x") Frequency response measured with CI recipient 2, with the CALM noise reduction,

The higher noise levels in the MEG data with the CI recipients were evident in the time domain averaged AEPs and AEFs **Figure 35 (a-d, left)**. The individually adjusted cortical source models and their relative position to the MEG sensors, as well as the auditory source localization results from the CI recipients are shown in **Figure 35 (a-d, right)**. Residual CI artefact (specially related to the onset and offset of the tone stimulus) could be observed in the EEG data. However, this artefact could be mostly temporally separated from the N100m peak since the tone stimulus was of 50 ms duration. On the other hand, MEG data acquired from the CI recipients were heavily dominated by the CI artefact despite the exhaustive approaches of noise reduction. As is shown in **Figure 35**, normal AEF components could not be observed from the time domain averaged MEG data. In addition, the amplitude of the MEG event-related responses were 10-100 times larger than that of the normal hearing participants with CI emulator (with the exception of one CI user, after discarding three noisy sensors, see **Figure 35 c**).
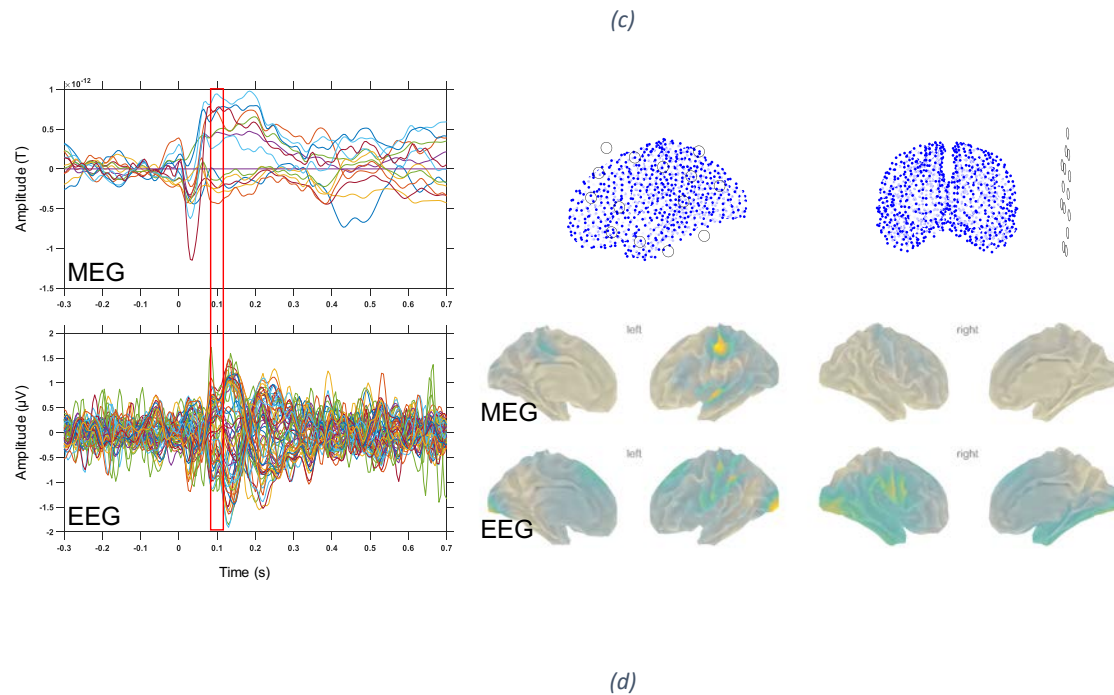
(a)

(b)

160
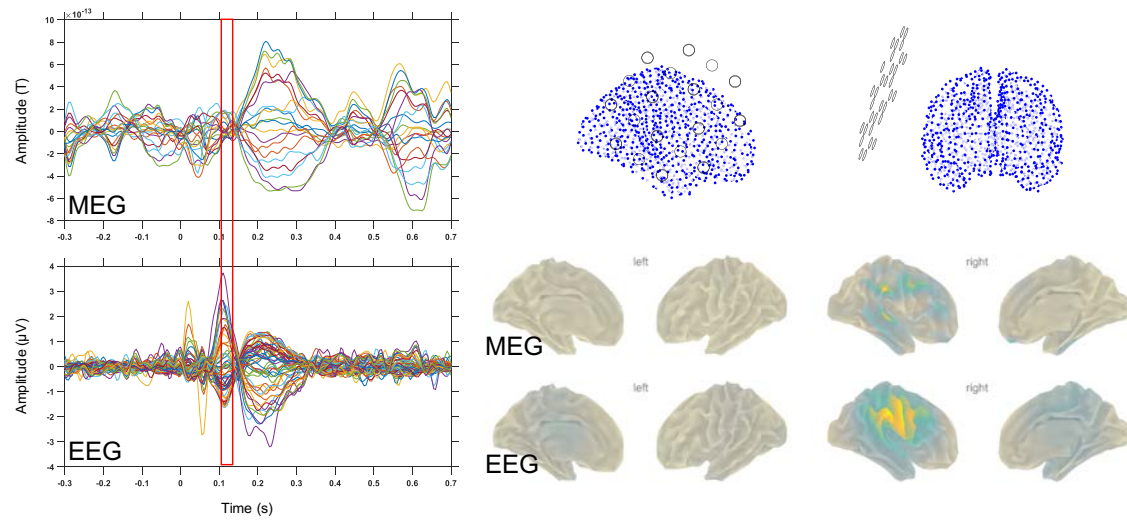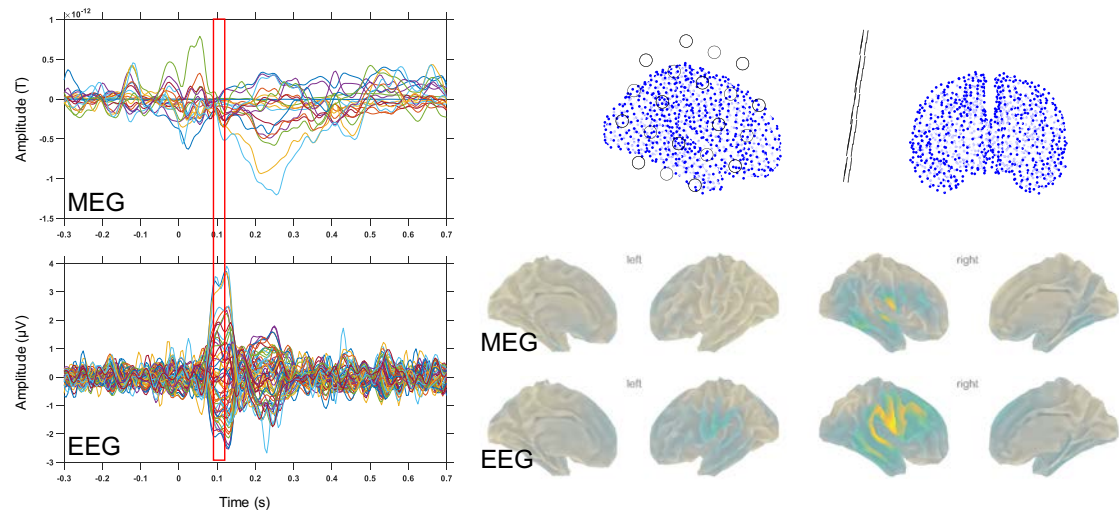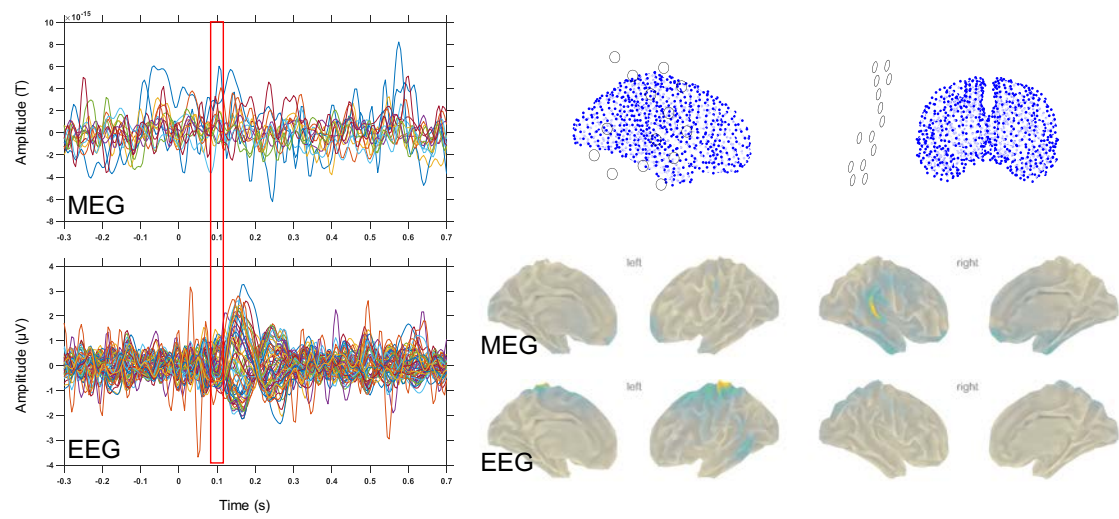
Figure 35: Time domain averaged AEPs and AEFs measured from four (a - d) CI recipients. Left: Time course of measured AEFs and AEPs, time windows selected for MNE source analysis are marked as red rectangles. Upper right: Individual cortical sheet source models relative to the MEG sensor array position during measurement. Bottom right: MNE source localization results from MEG and EEG overlaid on individually-warped template cortical sheet.

5 Discussion

Cochlear implants as the most successfully and widely used neural prosthetic devices have been employed to restore hearing of profoundly deaf people for almost 40 years. The changes in brain after receiving CI and the role of plasticity within central nervous system on auditory restoration, however, still remain largely unexplored. Of the currently available non-invasive whole-head functional imaging techniques, both MEG and EEG are silent and have a uniquely high temporal resolution down to milliseconds, which make them well suitable to study auditory brain function. However, cortical neural source localization appears to be more accurate in MEG than EEG since the neuromagnetic signals can pass through different head tissues without distortion (Baillet et al., 2001). The big challenge is that due to the magnet implanted with the CI inside the skull of the recipient as well as the electromagnetic disturbances during the CI operation, it is so far not feasible to record whole-head MEG of a common CI recipient without damaging the MEG sensors. It is because the magnet of a conventional CI has a magnetic strength of 340 Gauss,

which is equivalent to 0.034 Tesla. The measurable brain MEG signal is in the range of 10^{-14} Tesla, so theoretically the CI-related artefact could be one billion times larger than the brain signal. Even for EEG, the CI-related electric artefact remains a big issue and could be several orders of magnitude stronger than the brain signal (Gilley et al., 2006; Martin, 2007; Wagner et al., 2018).

In the current study, we reported and evaluated the development of a custom-engineered MEG system which was designed to measure cortical auditory responses in unilateral CI recipients from the side contralateral to their CI devices (not restricted to 'magnet-free' CIs). This unique MEG system has undergone the second iteration of its design phase. Testing results with normal hearing participants (with or without a CI emulator) have demonstrated that this system can detect and source localize brain responses in the presence of strong electromagnetic artefacts caused by CI system outside the head.

The higher noise levels in the actual CI recipients relative to the CI emulator can be attributed to the small movements of the internal magnet in the head, primarily motions induced by the cardiac pulsation. While the MEG system coped extremely well with the static field of the magnetic in the CI emulator (which was not attached to the head), dynamic fields caused even by very tiny movements of the magnet are evidently much more problematic. Compared to artefacts caused by static magnetic sources (CI emulator placed below participants' head), the moving magnetic artefacts are much higher in field strength across the entire frequency spectrum.

Future directions with this prototype MEG system could take into consideration of the following points: Potential differences in brain responses between participants receives acoustic and electric stimulation; Accuracy of source localization without individual structural MRI scan from CI recipients; Upgrade to the existing sensor array to improve the noise reduction performance.

6. Author Contributions

Q.M., Y.L.H., C.M and B.J. conceived and designed the experiment. Y.L.H and Q.M. performed the MEG experiments. QM, Y.L.H and B.J wrote the paper. All of the authors discussed the results and edited the manuscript.

References

Adachi, Y., Shimogawara, M., Higuchi, M., Haruta, Y., & Ochiai, M. (2001). Reduction of non-
periodic environmental magnetic noise in MEG measurement by continuously adjusted
least squares method. *IEEE Transactions on Applied Superconductivity*, *11*(1), 669–672.
https://doi.org/10.1109/77.919433

Adjamian, P. (2014). The application of electro- and magneto-encephalography in tinnitus
research - methods and interpretations. *Frontiers in Neurology*, *5*, 228.
https://doi.org/10.3389/fneur.2014.00228

Alain, C., Roye, A., & Salloum, C. (2014). Effects of age-related hearing loss and background
noise on neuromagnetic activity from auditory cortex.

Baillet, S. (2017). Magnetoencephalography for brain electrophysiology and imaging. *Nature
Neuroscience*, *20*(3), 327–339.

Baillet, S., Mosher, J. C., & Leahy, R. M. (2001). Electromagnetic brain mapping. *IEEE Signal
Processing Magazine*, *18*(6), 14–30.

Cheyne, D. O., & Papanicolaou, A. C. (2017). Magnetoencephalography and magnetic source
imaging. *Oxford Handb. Funct. Brain Imaging Neuropsychol. Cogn. Neurosci.*, 13–42.

Fagaly, R. (2006). Superconducting quantum interference device instruments and applications.
Review of Scientific Instruments, *77*(10), 101101.

Fischl, B. (2012). FreeSurfer. *NeuroImage*, *62*(2), 774–781.
https://doi.org/10.1016/j.neuroimage.2012.01.021

Hämäläinen, M. S., & Ilmoniemi, R. J. (1994). Interpreting magnetic fields of the brain: minimum

norm estimates. *Medical & Biological Engineering & Computing*, *32*(1), 35–42.

https://doi.org/10.1007/BF02512476

Hari, R., Pelizzone, M., Mäkelä, J., Huttunen, J., & Kuuutila, J. (1988). Neuromagnetic Responses

from a Deaf Subject to Stimuli Presented through a Multichannel Cochlear Prosthesis*.

Ear and Hearing, *9*(3), 148–152.

Hoke, M., Pantev, C., Lütkenhöner, B., Lehnertz, K., & Sürth, W. (1989). Magnetic fields from

the auditory cortex of a deaf human individual occurring spontaneously or evoked by

stimulation through a cochlear prosthesis. *Audiology*, *28*(3), 152–170.

Johnson, B. W., Crain, S., Thornton, R., Tesan, G., & Reid, M. (2010). Measurement of brain

function in pre-school children using a custom sized whole-head MEG sensor array.

Clinical Neurophysiology, *121*(3), 340–349.

Johnson, B. W., & Hautus, M. J. (2010). Processing of binaural spatial information in human

auditory cortex: neuromagnetic responses to interaural timing and level differences.

Neuropsychologia, *48*(9), 2610–2619.

https://doi.org/10.1016/j.neuropsychologia.2010.05.008

Li Hegner, Y., Marquetand, J., Elshahabi, A., Klamer, S., Lerche, H., Braun, C., & Focke, N. K.

(2018). Increased Functional MEG Connectivity as a Hallmark of MRI-Negative Focal and

Generalized Epilepsy. *Brain Topography*, 1–12. https://doi.org/10.1007/s10548-018-

0649-4

Makeig, S., Bell, A. J., Jung, T.-P., & Sejnowski, T. J. (1996). Independent Component Analysis of

Electroencephalographic Data. In D. S. Touretzky, M. C. Mozer, & M. E. Hasselmo (Eds.),

Advances in Neural Information Processing Systems 8 (pp. 145–151). MIT Press.

Retrieved from http://papers.nips.cc/paper/1091-independent-component-analysis-of-

electroencephalographic-data.pdf

Moore, D. R., & Shannon, R. V. (2009). Beyond cochlear implants: awakening the deafened

brain. *Nature Neuroscience*, *12*(6), 686–691. https://doi.org/10.1038/nn.2326

Oostenveld, R., Fries, P., Maris, E., & Schoffelen, J.-M. (2011). FieldTrip: Open Source Software

for Advanced Analysis of MEG, EEG, and Invasive Electrophysiological Data [Research

article]. https://doi.org/10.1155/2011/156869

Oyama, D., Adachi, Y., Yumoto, M., Hashimoto, I., & Uehara, G. (2015). Dry phantom for

magnetoencephalography —Configuration, calibration, and contribution. *Journal of*

Neuroscience Methods, *251*, 24–36. https://doi.org/10.1016/j.jneumeth.2015.05.004

Pantev, C., Dinnesen, A., Ross, B., Wollbrink, A., & Knief, A. (2006). Dynamics of auditory

plasticity after cochlear implantation: a longitudinal study. *Cerebral Cortex*, *16*(1), 31–

36.

Peelle, J. E., & Wingfield, A. (2016). The neural consequences of age-related hearing loss.

Trends in Neurosciences, *39*(7), 486–497. https://doi.org/10.1016/j.tins.2016.05.001

Pelizzone, M., Hari, R., Mäkelä, J., Kaukoranta, E., & Montandon, P. (1986). Activation of the

auditory cortex by cochlear stimulation in a deaf patient. *Neuroscience Letters*, *68*(2),

192–196. https://doi.org/10.1016/0304-3940(86)90140-0

Raichle, M. E. (2009). A paradigm shift in functional brain imaging. *Journal of Neuroscience*,

29(41), 12729–12734.

Saad, Z. S., & Reynolds, R. C. (2012). SUMA. *Neuroimage*, *62*(2), 768–773. https://doi.org/10.1016/j.neuroimage.2011.09.016

Shannon, R. V., Zeng, F.-G., Kamath, V., Wygonski, J., & Ekelid, M. (1995). Speech Recognition with Primarily Temporal Cues. *Science*, *270*(5234), 303–304. https://doi.org/10.1126/science.270.5234.303

Stamatakis, E. A., Orfanidou, E., & Papanicolaou, A. C. (2017). Functional Magnetic Resonance Imaging. *The Oxford Handbook of Functional Brain Imaging in Neuropsychology and Cognitive Neurosciences*, 43.

Tyler, R., Lowder, M. W., Parkinson, A. J., Woodworth, G. G., & Gantz, B. J. (1995). Performance of adult ineraid and nucleus cochlear implant patients after 3.5 years of use. *Audiology*, *34*(3), 135–144.

Vrba, J., Fife, A. A., Burbank, M. B., Weinberg, H., & Brickett, P. A. (1982). Spatial discrimination in SQUID gradiometers and 3rd order gradiometer performance. *Canadian Journal of Physics*, *60*(7), 1060–1073. https://doi.org/10.1139/p82-144

Vrba, J., & Robinson, S. E. (2001). Signal processing in magnetoencephalography. *Methods (San Diego, Calif.)*, *25*(2), 249–271. https://doi.org/10.1006/meth.2001.1238

Wagner, L., Maurits, N., Maat, B., Başkent, D., & Wagner, A. E. (2018). The Cochlear Implant EEG Artifact Recorded From an Artificial Brain for Complex Acoustic Stimuli. *IEEE Transactions on Neural Systems and Rehabilitation Engineering*, *26*(2), 392–399. https://doi.org/10.1109/TNSRE.2018.2789780

Wilson, B. S., & Dorman, M. F. (2008). Cochlear implants: a remarkable past and a brilliant future. *Hearing Research*, *242*(1), 3–21.

Wong, A. C. Y., & Ryan, A. F. (2015). Mechanisms of sensorineural cell damage, death and

survival in the cochlea. *Frontiers in Aging Neuroscience*, *7*.

https://doi.org/10.3389/fnagi.2015.00058

Zeng, F.-G. (2004). Auditory Prostheses: Past, Present, and Future. In *Cochlear Implants:*

Auditory Prostheses and Electric Hearing (pp. 1–13). Springer, New York, NY.

https://doi.org/10.1007/978-0-387-22585-2_1

General Discussion

1 Summary of results

The most salient results of the present thesis are the following:

1. Our results (chapters 3 and 4) replicate those reported by Ding and colleagues (Ding, Melloni, Zhang, Tian, & Poeppel, 2016) and demonstrate that the human brain is sensitive to abstract linguistic structures.

2. The results of Experiment 1 (chapter 3) show that brain responses to syllable-level linguistic units are hemispherically bilateral and sustained across different levels of intelligibility.

3. In contrast, the brain responses to larger linguistic structures were modulated by the intelligibility of the speech stream. Specifically, the magnitudes of the phrase- and sentence-level responses declined, and lateralisation to the left hemisphere increased, as a function of reduced intelligibility.

4. The results of Experiment 2 (chapter 4) showed that prior experience with matching intelligible speech enhances the brain responses to sentence-level (the most abstract) linguistic structure but had no significant effect on syllable- and phrase-level brain responses.

5. The results of Experiment 2 also show that the effect of prior experience was lateralised to the right cerebral hemisphere.

6. Our evaluation of the prototype MEG system showed that the effects of a cochlear implant on MEG measurements are severe. We have demonstrated that the prototype system is capable of measuring auditory evoked responses under ideal conditions in the presence of a cochlear implant emulator. However, further technical and methodological

development are required for the system to allow brain measurements with actual cochlear implant users.

2. Significance

2.1 Replication of Ding et al.

Our experiments are, to our knowledge, the first replications of the MEG work originally reported by Ding et al. (2016; note however this group (Ding et al., 2017) has reported a replication of their results using EEG). The results confirm that cortical activity associated with hierarchical linguistic structures in connected speech can be measured non-invasively with MEG. These high-level linguistic regularities that facilitate parsing of the speech stream are not physically present in the acoustic stimulus and therefore must be imposed by high-level linguistic processed during comprehension in the brain itself (Ding, Melloni, Zhang, Tian, & Poeppel, 2016). As such, these neural responses reflect and indicate (i.e. are neural markers of) a crucial component of linguistic processing. An objective neural marker of high-level speech processing is highly significant for both basic science (neurolinguistics); and for applications such as cochlear implants and hearing aids, where speech comprehension is the primary and most important objective of intervention (Cosetti & Waltzman, 2011). The successful replication of the result of the Ding et al. (2016) experimental paradigm sets the stage for the following parametric investigations of the effects of speech intelligibility on this brain response.

2.2 Effects of intelligibility

The results of Experiment 1 show that brain responses to different linguistic units are differentially modulated by speech intelligibility. The syllable level response was not significantly affected by changes in intelligibility. On the other hand, phrase- and sentence-level responses (Chapter 3 **Figure 9**) decreased systematically with reduced intelligibility. The lack of effect on

syllable-level responses can be attributed to the fact that these are associated with a temporal regularity that is physically present within the speech stream (i.e. the syllable rate). The speech envelope was faithfully preserved across all intelligibility conditions with our noise-vocoding operation.

The differential modulation of brain responses to different linguistic units obtained in the present study may have relevance to the contradictory results obtained in previous studies examining the effects of speech intelligibility on neural entrainment to the speech envelope. While several studies have reported significant effects (Ding, Chatterjee, & Simon, 2014; Peelle, Gross, & Davis, 2013), others have obtained null results (Howard & Poeppel, 2010). Our syllable rate response, which was not sensitive to intelligibility, corresponds to the speech envelope response measured in all four of the studies cited above. This indicates that the speech envelope response may not be particularly sensitive to intelligibility since it seems to be largely driven by the acoustic regularities that are physically present in the speech stream (see also Doelling et al. (Doelling, Arnal, Ghitza, & Poeppel, 2014), who reported that delta-theta brain oscillations are driven by acoustic landmarks). The present results indicate that brain tracking of speech is more sensitive to intelligibility when the physical and linguistic regularities are dissociated (phrase and sentence level) than when they are confounded (syllable level).

Furthermore, our source analysis reveals a bilateral activation of brain response to syllable level linguistic structure and a left-hemisphere lateralisation of cortical activity to phrase and sentence level linguistic units. Our results (contrasting natural speech and shuffled speech) are entirely consistent with the conclusions of Peelle (Peelle, 2012). In this review of fMRI studies of spoken language processing, Peelle concluded that cortical lateralisation depends in a graded fashion on the level of acoustic and linguistic processing required (**Figure 36**). Processing related to non-speech signals (amplitude modulated noise) is bilateral. As the requirements for linguistic

analysis and integration increase (AM sounds, phonemes, words, phrases and sentences), neural processing became increasingly left-lateralised.
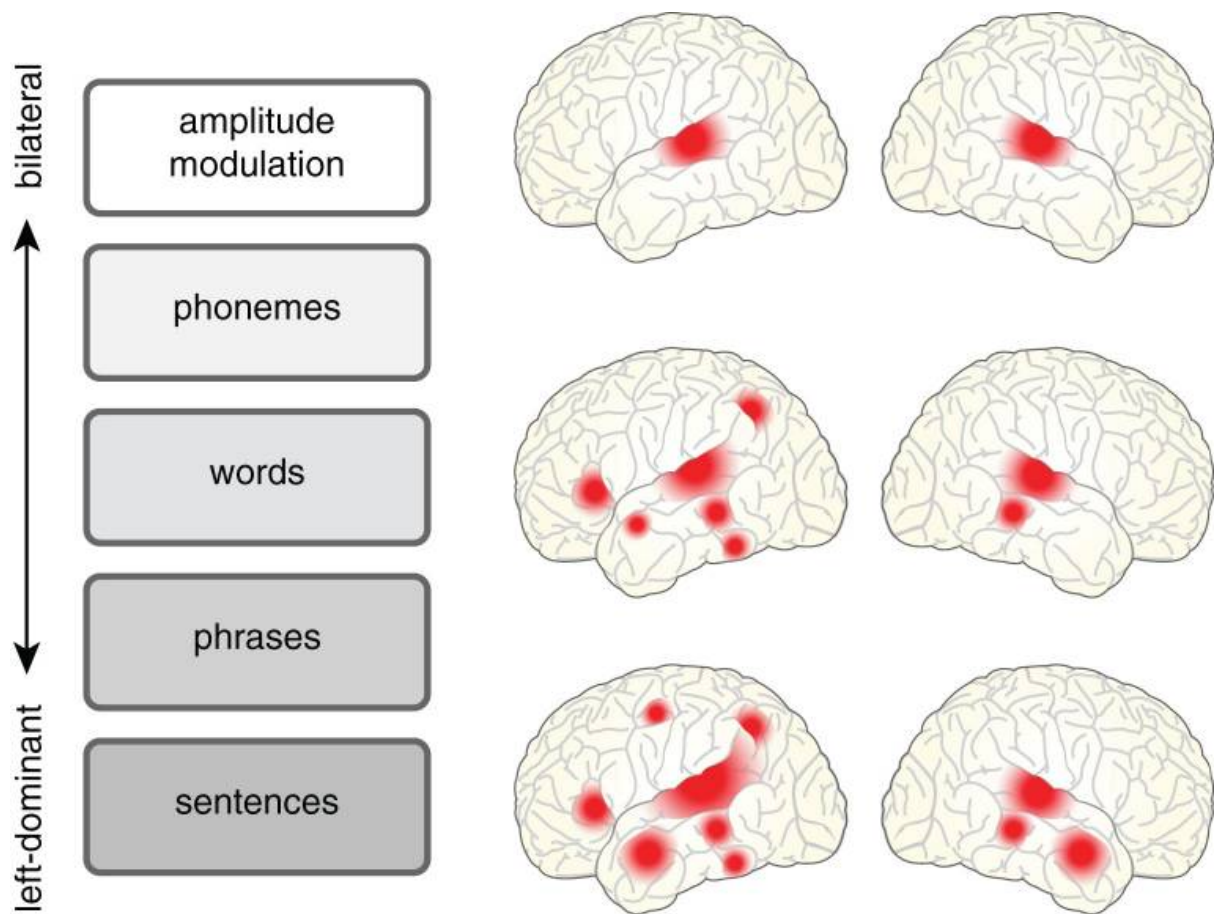

Figure 36: The cortical regions involved in processing spoken language depend in a graded fashion on the level of acoustic and linguistic processing required. Processing related to amplitude modulated noise is bilateral (e.g., Giraudetal.,2000), shown at top. However, as the requirements for linguistic analysis and integration increase, neural processing shows a concomitant increase in its reliance on left hemisphere regions for words [see meta-analysis in Davis and Gaskell (2009)] and sentences [see meta-analysis in Adank (2012)]. Figure adapted with permission from (Peelle, 2012).

2.3 Effects of Immediate Prior Experience

Results from Experiment 2 (Chapter 4) showed that the brain response tracking hierarchical linguistic structures is also modulated by prior experience with intelligible speech. While syllable- and phrase-level brain responses to degraded speech were not significantly affected by prior experience with intact speech, sentence-level responses were slightly but significantly enhanced (Chapter 4, **Figure 4**). As with intelligibility, the lack of effect on the syllable-level response could be attributed to the fact that this peak is driven largely by the low-level, physical regularity of the

speech stream (i.e. the syllable rate), since that the temporal envelope which reflects sound amplitude fluctuation is preserved with noise-vocoding.

Our results showing experience-dependent effects for sentence level-brain responses stand in contrast to those obtained in several previous electrophysiological studies. Millman et al. (Millman, Johnson, & Prendergast, 2015) found no effect on MEG phase-locking to the speech temporal envelope of tone-vocoded speech after training with intact speech, even though the training produced a robust perceptual "pop-out" effect. Their speech tracking measures effectively correspond to our syllable-level response (because they used single sentences, which cannot generate the phrase and sentence responses produced with our isochronous sentence streams) and agree with our results showing no effect of prior experience on the syllable-level response. Similarly the ECoG study of Holdgraf et al. (Holdgraf et al., 2016) used non-isochronous sentences and found no effect on phase entrainment to the envelope of filtered speech utterance before and after experience with the unfiltered speech, although an increase of high-gamma activity was reported. On the other hand, in the present study, our sentence-level brain responses were independent of and dissociated from any physical characteristics of the stimuli, i.e. they could not have been driven by any physical feature of the stimuli and must have been generated by the brain itself. In other words, the present experiment provides a clear separation between bottom-up and top-down neurophysiological processes.

Our results provide good evidence for a rapid effect of perceptual experience (a single exposure to clear speech) on cortical tracking activity to sentence-level linguistic structure. The lack of a significant effect at the phrase level is more difficult to interpret. In principle there is no reason to believe that phrase parsing should be less susceptible to prior experience than sentence parsing and it is unclear whether the lack of effect is real or just due to the relatively low sensitivity of the measurements. Assuming that it is real, one interpretation could be that prior

exposure to speech has most effect on larger linguistic units that require integration over longer stretches of time. That is, prior experience with speech has most effect on fairly abstract representations of speech content and less effect on more veridical representations of spectral-temporal structure.

Our source analyses further suggest that the enhancement in the tracking of sentence-level linguistic units seems to be importantly mediated by the right hemisphere. This result stands in contrast to a number of previous neuroimaging studies of the perceptual "pop-out" phenomenon (Dehaene-Lambertz et al., 2005; Liebenthal et al., 2004; Millman et al., 2015; Sohoglu et al., 2012) which have reported either left hemisphere activation (Dehaene-Lambertz et al., 2005; Sohoglu, Peelle, Carlyon, & Davis, 2012), bilateral activation (Liebenthal, Binder, Piorkowski, & Remez, 2003), or no effect on neurophysiological measures (Millman et al., 2016). One fMRI study however has reported results consonant with ours. Giraud et al. (2004) required participants to listen to noise vocoded sentences (without comprehension), and again after training (with comprehension). Comprehension was found to activate bilateral middle and inferior temporal gyri, and the anterior superior temporal sulcus in the right hemisphere.

The issue of hemispheric specialisations for speech analysis is a complex topic and one that is currently in flux (Poeppel, Emmorey, Hickok, & Pylkkänen, 2012, p. 201). However, the role of the right hemisphere in perceptual enhancement by prior experience is readily encompassed within a model proposed by Zatorre (Zatorre, 1997) which posits that the left hemisphere is specialised for temporal processing while the right hemisphere is specialised for spectral processing (for a complementary conceptualisation, see (Poeppel, 2003)). Ding and colleagues (Ding et al., 2014) reported that spectral detail (not just the temporal envelope) is necessary for a robust representation of speech, since cortical tracking of the speech envelope is severely impaired by noise vocoding when there is background noise presented at a certain level. In

addition, the ECoG study by Holdgraf et al. (Holdgraf et al., 2016) has shown that the neuronal retuning induced by prior experience reflects enhanced extraction of spectro-temporal detail from the degraded speech.

2.4 MEG prototype

Our evaluation work on the prototype MEG system quantitively demonstrated the impact of CI on MEG measurements. As shown in the frequency response plot in **Figure 6** (Chapter 5), artefacts produced by a CI emulator exhibited much higher amplitude than normal brain response across the whole frequency range of interest (0 – 200Hz). Although noise reduction can to some extend supress the CI related artefact, the level of residual artefact is still too high to permit any brain response measurement in the presence of a CI emulator. This result suggested that noise reduction via employing two functionally distinct sensor arrays is achievable in principle, however a system-level development is required based on the combination of conventional 2nd order gradiometers and magnetometers. A system upgrade with the installation of two groups of novel irregular baseline 2nd order gradiometers greatly improved the performance of the prototype MEG system. It can be seen clearly from the frequency response plot (Chapter 5, **Figure 11**) that even without any noise reduction operation the amplitude of MEG recording to a CI emulator is much lower than the noise reduced recording measured and processed with the initial prototype. On the same frequency response plot, the noise reduced response curve further demonstrated that brain response measurement can be detected even in the presence of a CI emulator as the level of residual artefact is now lower than typical brain responses.

Our results from tests with CI users however are much worse than the evaluations results with the CI emulator. As indicated in **Figure 16** (Chapter 5), MEG data were heavily dominated by CI artefacts despite of many approaches to noise reduction. This severe deterioration of

performance in tests with CI users could be due to but are not limited to the following factors depicted in **Figure 37**: firstly, distance from the magnet (~0.034 T) included in typical CI systems to the MEG sensor array is shorter in the testing scenario of actual CI users which fail to accommodate the optimal performance parameter defined by the existing sensor arrays; secondly this magnet is implanted below the scalp together with the CI systems, therefore inevitably head movements associated with physiological activities such as breathing or heartbeat would cause strong artefacts across all frequencies; lastly, the electromagnetic disturbances during the CI operation is not completely simulated with the CI emulator. The electric currents that stimulate hearing nerve fibre through the implanted electrodes could also introduce further artefacts.

Although source analysis using the noisy MEG data measured with CI users seemed to indicate a valid region of cortical sources which is even more focal than the result calculated with current EEG recordings, this result needs to be further validated for a proper interpretation. Testing a MEG phantom with an integrated cochlear implant system could potentially be a good validation method. In the meanwhile, further system level hardware upgrades in conjunction with more sophisticated noise reduction algorithm are required to allow definite measurement with CI recipients.

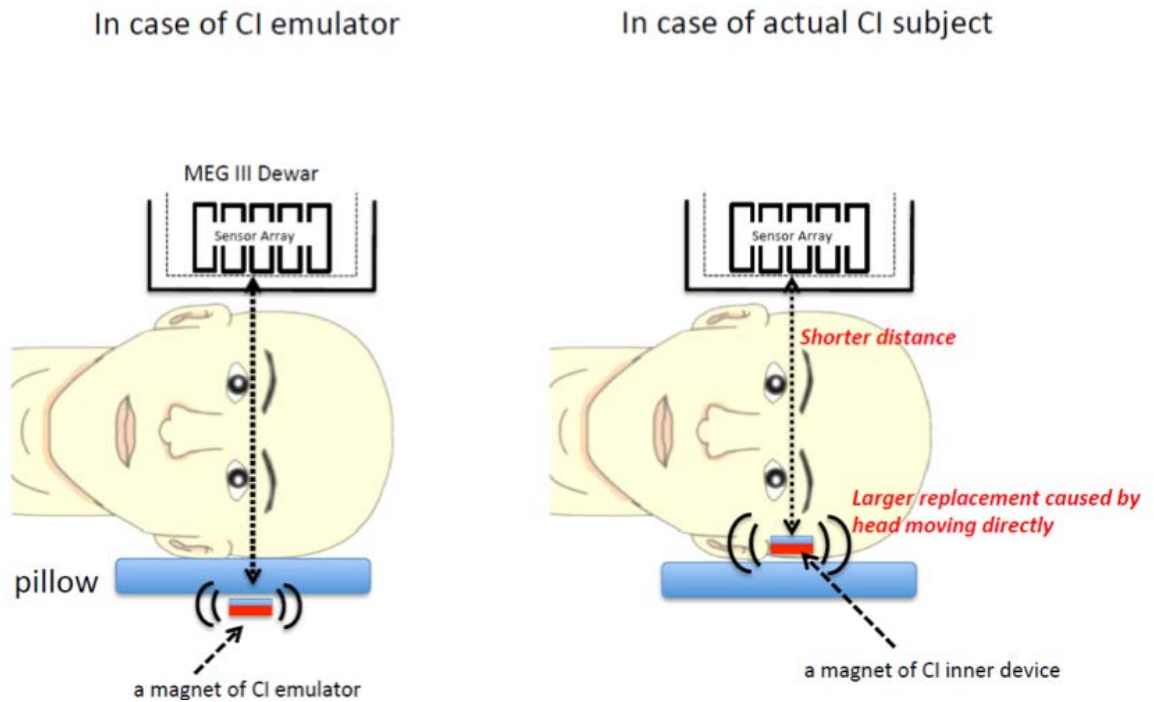In case of CI emulator   In case of actual CI subject

Figure 37: Testing setup with the prototype MEG system. Left: Testing scenario with a CI emulator. Right: Testing scenario with actual CI users (courtesy of M. Higuchi, KIT).

3 Future Directions

3.1 Measuring Cochlear Implant Users and Potential Applications

As our experiment results demonstrated, the brain response tracking high-level linguistic structures (especially at sentence level) is highly sensitive to speech intelligibility associated with changes in speech acoustics and in the meantime exhibits a fast plasticity driven by prior perceptual experience with intelligible speech. This neural tracking activity nicely characterizes the dominant factors involved in linguistic processing, from both the bottom-up and top-down process perspectives. It therefore can serve well as an objective neural marker of high-level speech processing which will greatly benefit research works in basic science (neurolinguistics) and also provide clinical significance in hearing impairment interventions, e.g. trajectory of brain changes after CI implantation could be measured through longitudinal studies.

In the meanwhile, a possible methodological improvement to the existing prototype MEG system may be achieved by implementing this hierarchical tracking paradigm described in Experiment 1

and 2 (Chapter 3 and 4). Since the cortical tracking activity to high-level linguistic structure is dissociated from encoding acoustic cues, spectrally it is separable from responses to stimulus onset (low-level linguistic structure) which is overwhelmed by CI related artefacts. Cortical response tracking larger linguistic units could thus potentially be captured from CI users using the prototype MEG system in conjunction with proper noise reduction operation.

To verify the possibility of measuring the demonstrated cortical activity tracking hierarchical linguistic structures in CI recipients, a preliminary EEG test was carried out. One of the unilateral CI recipients (female, left-ear implanted, 61 years old) who participated in previous tests evaluating the prototype MEG system was recruited again. As all incoming speech signal will be process by the CI sound processor which introduces spectral degradation, the synthesized syllables were adjusted to 500 ms and only natural and shuffled speech conditions were used for this test. The participant was familiarised with the speech sentences with a script given one week before the test, example sentences from each condition were also played prior to the experiment. The same experiment procedure was carried out as detailed in the first experiment with normal hearing participants (Chapter 3).

The same EEG system (BrainProducts GmbH, Gilching, Germany) employed for previous evaluation work of the prototype MEG system was used again as it is less prone to CI artefacts. Information and results from this preliminary test are described as below.

EEG electrodes that are directly above the external coil of the CI system were not connected to the scalp and were further discarded during offline data analysis (fewer than 3 electrodes). Prior to EEG recordings, marker coil positions, electrode positions, and detailed head shape were recorded with a pen digitizer (Polhemus Fastrack, Colchester, VT). The magnet of the external CI

coil was taken out and the external coil was manually aligned with the internal CI coil and taped to the participant's scalp.

Offline EEG data was analyzed following the procedure descried in Chapter 3 and Chapter 6. Frequency response and coherence with the composite signal calculated for both "Natural" and "Shuffled" conditions were averaged across all EEG channels and plotted in **Figure 38**.
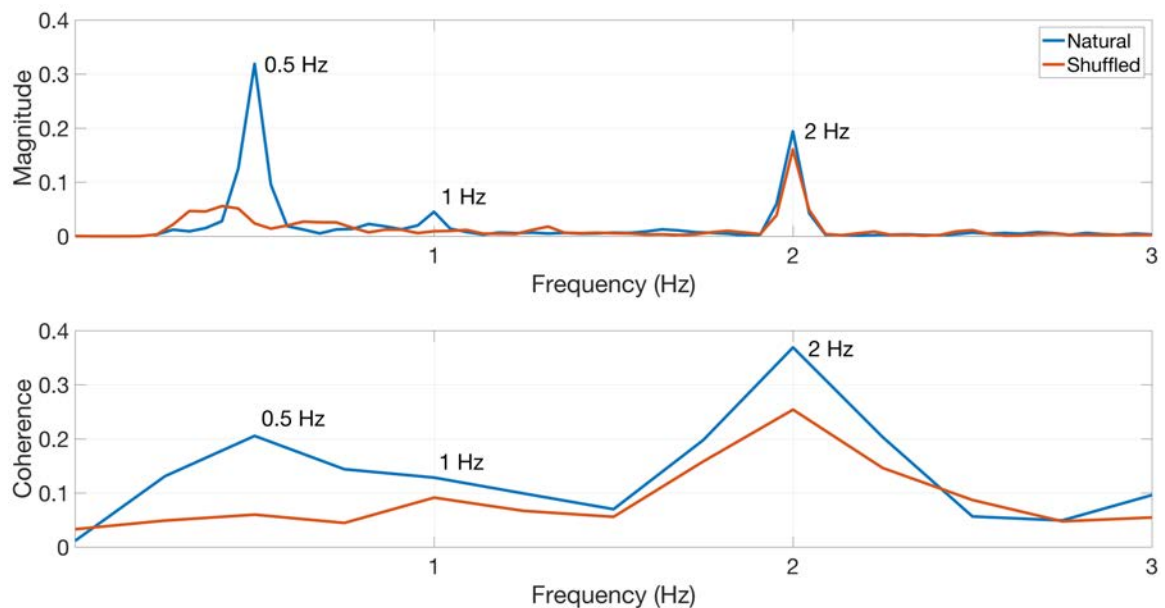

Figure 38: EEG measurement of a unilateral CI recipient showing brain tracking activity. Top: Averaged EEG sensor level frequency responses (60 channels) exhibited different tracking activity to the hierarchical linguistic information (syllable, phrase and sentence). Bottom: Averaged EEG sensor level coherence between each EEG channel and the composite signal (59 channels).

It is evident that both frequency response and coherence show peaks (limited by frequency resolution) corresponding to the phrase rate (1 Hz) and sentence rate (0.5 Hz) in additions to the syllable frequency (2 Hz) response under the "Natural speech" condition. Under the "Shuffled speech" condition, however no clear response to phrase and sentence level linguistic structures can be observed.

Nevertheless, application of this brain tracking measurement is not restricted to listeners with hearing impairments. Language processing in developing population (young children) and

difficult-to-test population (autism spectrum disorder) can also be effectively and objectively assessed.

3.2 Development of the Prototype MEG System

The unique prototype MEG system has undergone two iterations of its design phase. As discussed in previous sections, the employment of novel irregular baseline 2nd order gradiometers greatly improved the performance in noise suppression. However, measurements with actual CI recipients still exhibited very high level residual artefacts. A potential improvement in sensory array design may be achieved by employing more diversified irregular baseline 2nd order gradiometers for the measuring sensor array and reference sensor array respectively. Compared to the current system using two types of sensors with null or near null responsiveness at two distinct distance points, this new sensor array comprised of several sub-arrays with different baseline ratios according to their locations to measurement object can essentially enable this unique measurement characteristic within two sets of different distance range. In this way, the distance displacement problem during test actual CI recipients compared to the emulator and even variations in head-size across different CI recipients could be better accommodated and eventually lead to a greater noise reduction.

4 Conclusions

The present work was motivated by an emerging consensus that much of the observed variability in cochlear implant performance may be attributable to changes in how the brain processes speech, as a result of the profound sensory deprivation imposed by deafness (Wilson & Dorman, 2008); and a current lack of knowledge about such effects in the human brain. The results of this thesis contribute to this body of knowledge by showing that brain responses to hierarchical linguistic structures provide objective markers of speech processing that are demonstrably sensitive to manipulations of intelligibility and may therefore be useful and objective markers of

180

the nature of the "compromised auditory brains" of cochlear implant recipients. As such this is an early step toward the goal of a 'top-down', cognitive neuroscience-based approach to better understanding how the CI and the human brain interact. This more comprehensive approach to CI research has important implications for both clinical rehabilitation and basic cognitive science and is highly likely to have translational benefits for other disorders of language, reading, and cognition.

Functional neuroimaging studies of cochlear implant recipients will reveal how the brain interprets and responds to information provided by an artificial sensory input device and will reveal how these interpretations resemble and how they differ from those derived from natural inputs. A central challenge of 21st Century biomedical neuroscience will be to determine how the human brain can communicate directly with prosthetic devices, and the constraints and limitations on these communications. Therefore, these studies will be also highly pertinent to and will inform subsequent research on the bionic eye, the hippocampal prosthesis, and brain computer interfaces to mechanical output devices. However, cochlear implants present important challenges to existing neuroimaging techniques, and it will be important to develop new types of instrumentation that can measure brain signals from cochlear implant recipients and are also capable of rejecting the large artefacts that are generated by the implants themselves.

Studying the central consequences of profound deafness in humans will fill a clear and significant gap in the current neuroimaging literature; advance our understanding of central auditory processing disorders due to hearing loss; contribute to further development of hearing aid and implant technologies; and provide objective neurophysiological targets for improving training strategies for cochlear implant recipients.

References

Cosetti, M. K., & Waltzman, S. B. (2011). Cochlear implants: current status and future potential. *Expert Review of Medical Devices*, *8*(3), 389–401. https://doi.org/10.1586/erd.11.12

Dehaene-Lambertz, G., Pallier, C., Serniclaes, W., Sprenger-Charolles, L., Jobert, A., & Dehaene, S. (2005). Neural correlates of switching from auditory to speech perception. *NeuroImage*, *24*(1), 21–33. https://doi.org/10.1016/j.neuroimage.2004.09.039

Ding, N., Chatterjee, M., & Simon, J. Z. (2014). Robust cortical entrainment to the speech envelope relies on the spectro-temporal fine structure. *Neuroimage*, *88*, 41–46.

Ding, N., Melloni, L., Yang, A., Wang, Y., Zhang, W., & Poeppel, D. (2017). Characterizing Neural Entrainment to Hierarchical Linguistic Units using Electroencephalography (EEG). *Frontiers in Human Neuroscience*, *11*. https://doi.org/10.3389/fnhum.2017.00481

Ding, N., Melloni, L., Zhang, H., Tian, X., & Poeppel, D. (2016). Cortical tracking of hierarchical linguistic structures in connected speech. *Nature Neuroscience*, *19*(1), 158. https://doi.org/10.1038/nn.4186

Doelling, K. B., Arnal, L. H., Ghitza, O., & Poeppel, D. (2014). Acoustic landmarks drive delta–theta oscillations to enable speech comprehension by facilitating perceptual parsing. *NeuroImage*, *85*, 761–768. https://doi.org/10.1016/j.neuroimage.2013.06.035

Holdgraf, C. R., Heer, W. de, Pasley, B., Rieger, J., Crone, N., Lin, J. J., … Theunissen, F. E. (2016). Rapid tuning shifts in human auditory cortex enhance speech intelligibility. *Nature Communications*, *7*, 13654. https://doi.org/10.1038/ncomms13654

Howard, M. F., & Poeppel, D. (2010). Discrimination of Speech Stimuli Based on Neuronal

   Response Phase Patterns Depends on Acoustics But Not Comprehension. *Journal of*

   Neurophysiology, *104*(5), 2500–2511. https://doi.org/10.1152/jn.00251.2010

Liebenthal, E., Binder, J. R., Piorkowski, R. L., & Remez, R. E. (2003). Short-Term Reorganization

   of Auditory Analysis Induced by Phonetic Experience. *Journal of Cognitive Neuroscience*,

   15(4), 549–558. https://doi.org/10.1162/089892903321662930

Millman, R. E., Johnson, S. R., & Prendergast, G. (2015). The role of phase-locking to the

   temporal envelope of speech in auditory perception and speech intelligibility. *Journal of*

   Cognitive Neuroscience, *27*(3), 533–545. https://doi.org/10.1162/jocn_a_00719

Peelle, J. E. (2012). The hemispheric lateralization of speech processing depends on what

   "speech" is: a hierarchical perspective. *Frontiers in Human Neuroscience*, *6*.

   https://doi.org/10.3389/fnhum.2012.00309

Peelle, J. E., Gross, J., & Davis, M. H. (2013). Phase-locked responses to speech in human

   auditory cortex are enhanced during comprehension. *Cerebral Cortex (New York, N.Y.:*

   1991), *23*(6), 1378–1387. https://doi.org/10.1093/cercor/bhs118

Poeppel, D. (2003). The analysis of speech in different temporal integration windows: cerebral

   lateralization as 'asymmetric sampling in time.' *Speech Communication*, *41*(1), 245–255.

Poeppel, D., Emmorey, K., Hickok, G., & Pylkkänen, L. (2012). Towards a new neurobiology of

   language. *Journal of Neuroscience*, *32*(41), 14125–14131.

Sohoglu, E., Peelle, J. E., Carlyon, R. P., & Davis, M. H. (2012). Predictive Top-Down Integration

   of Prior Knowledge during Speech Perception. *Journal of Neuroscience*, *32*(25), 8443–

   8453. https://doi.org/10.1523/JNEUROSCI.5069-11.2012

Wilson, B. S., & Dorman, M. F. (2008). Cochlear implants: a remarkable past and a brilliant

future. *Hearing Research*, *242*(1), 3–21.

Zatorre, R. J. (1997). Cerebral Correlates of Human Auditory Processing. In *Acoustical Signal*

Processing in the Central Auditory System (pp. 453–468). Springer, Boston, MA.

https://doi.org/10.1007/978-1-4419-8712-9_42

Office of the Deputy Vice-Chancellor (Research)

Research Office
C5C Research HUB East, Level 3, Room 324
MACQUARIE UNIVERSITY NSW 2109 AUSTRALIA

Phone   **+61 (0)2 9850 4194**
Fax   +61 (0)2 9850 4465
Email   ethics.secretariat@mq.edu.au

17 March 2014

Associate Professor Blake Johnson
Department of Cognitive Science
Faculty of Human Sciences
Macquarie University NSW 2109

Dear Associate Professor Johnson

RE: *MEG, EEG and fMRI Studies of adult cognition* (REF: 5201300054)

Thank you for your correspondence dated 17 January 2014 submitting an amendment to the above study. The Human Research Ethics Committee (HREC) (Medical Sciences) reviewed your proposed amendment out of session.

I am pleased to advise that ethical approval of the following amendments to the above study has been granted, effective 8 March 2014:

1. The use of MEG III with cochlear implant recipients.

2. To include adults with deafness or impaired hearing and who have been implanted with a unilateral cochlear implant and/or fitted with a hearing aid (or aids) as participants in the above study. These participants have been included in order to study the cognitive and neural consequences of hearing loss and restored hearing with the MEG III system.

3. Adults with cochlear implants will be recruited via advertisements placed at Cochlear Ltd, Macquarie University Department of Audiology and the Sydney Cochlear Implant Centre.

4. The addition of Mr David Meng and Ms Julia Shibaylo as personnel on the above study.

The following documentation submitted with your amendment request has been reviewed and approved:

Documents reviewed	Version no.	Date
Macquarie University HREC Request for Amendment Form		Received 29/01/2014
Advertisement entitled *Cochlear Implant/Hearing Aid Study*		
Macquarie University Participant Information and Consent Form entitled *MEG, EEG and fMRI Studies of Adult Cognition*	2.0	08/03/2014

Please ensure that all documentation has a version number and date in future correspondence with the Committee.

The HREC (Medical Sciences) Terms of Reference and Standard Operating Procedures are available from the Research Office website at:

http://www.research.mq.edu.au/for/researchers/how_to_obtain_ethics_approval/human_research_ethics

Please do not hesitate to contact the Ethics Secretariat should you have any questions regarding your ethics application.

The HREC (Medical Sciences) wishes you every success in your research.

Yours sincerely

Professor Tony Eyers
Chair, Macquarie University Human Research Ethics Committee (Medical Sciences)

This HREC is constituted and operates in accordance with the National Health and Medical Research Council's (NHMRC) *National Statement on Ethical Conduct in Human Research* (2007) and the *CPMP/ICH Note for Guidance on Good Clinical Practice*.